THE SYNTHESIS AND BREAST CANCER INHIBITORY ACTIVITY OF CINNAMIC ACID ANALOGUES BASED ON THE HALOGENATED MONOTERPENE PHARMACOPHORE

A Thesis Submitted in Fulfillment of the Requirements for the Degree of

MASTERS OF SCIENCE (PHARMACY)

Of

RHODES UNIVERSITY

By

MAYNARD TENDAI CHIWAKATA

FEBRUARY 2012

Acknowledgements

My sincere gratitude goes to my supervisors, Dr D. Beukes and Dr A. Edkins for their guidance, assistance, patience and advice throughout my project. They have made these two years bearable, enjoyable, and have greatly contributed to my growth in the research field.

I would want to thank the following people who also contributed to the success of my work. I wouldn't have made it without them:

- Dr Marietjie Stander from Stellenbosch University for her help with ESI-MS.
- Professor John Bolton from University of Cape Town for the collection and identification of algae
- Jo-anne de la Mare and Buhle Moyo for the training and assistance in biological activity assays.
- Dr P. Kempgens for training and assistance in NMR spectroscopy
- Mr and Mrs Morley for technical support
- Dr C. Oltmann for being a wonderful tutor during my academic internship
- Pharmaceutical Chemistry lectures: Dr Samant, Dr Tandlich and Dr Goosen for advice and contributions to my work
- Ayeshah Fateemah Fauzee for the great help in putting this thesis together
- Andrew Mellon Foundation Scholarship and the National Research Foundation for funding my research

I would also like to acknowledge my G3 friends; Anthonia Afolayan, Tatenda Munedzimwe, Jameel Fakee, Mutenta Nyambe and Denzel Mubare for all the good times and laughter in the lab, and to all faculty colleagues for the wonderful memories. Special thanks to my best friends; Tendai L. Matonhodze, Eldinah Hwengwere and Safeeya Ally. Your company, support and motivation are greatly appreciated. You guys are the best.

A special mention goes to my parents (**Samson** and **Smolly Chiwakata**), and my two amazing brothers, **Marlon** and **Allen Chiwakata** for their undying love, support, encouragement and belief in me. I love you guys and thank you for always being there with me through this academic journey. Finally, to Luan Schutte, for contributing in making my dreams come true.

Abstract

Breast cancer is one of the leading causes of death, with mortality rate estimates of 465 000 deaths per annum. It is estimated that 1.3 million women are diagnosed with the disease each year especially in the developing countries. Current chemotherapy relies on the use of high doses of non-specific toxic agents that possess adverse side effects and compromise patient's compliance and adherence to treatment. Paclitaxel, one of the common drugs used in breast cancer chemotherapy results in sensory and motor neuropathy, whilst hormonal therapy e.g. Herceptin causes severe cardiovascular, gastrointestinal and cutaneous side effects. There has been a demand in developing newer cancer agents that demonstrate selective cytoxicity with minimal effect on normal body tissue.

Numerous studies have shown that marine organisms produce a wide range of halogenated compounds that possess cytotoxic properties, and hence can be a source of new drug hits or leads for cancer therapy. Halomon, a polyhalogenated monoterpene from *Portieria hornemannii*, displayed interesting activity against brain, renal and lung cancer tumours with selective/differential cytotoxicity. This inspired us to focus our project on halogenated monoterpenes isolated from the same Rhodophyta class as *P. hornemannii* but with particular attention to *Plocamium* species. Several metabolites have been isolated from *P. cornutum*, *P. corallorhiza* and *P. suhrii* that possess interesting cytotoxicities against a breast cancer cell line (MCF7) and an oesophageal cancer line (WHCO1). The aim of the project was therefore centred at isolating target compounds for preliminary structure-activity studies against a breast cancer cell line, and use this information to synthesize a series of analogues that are more stable than the natural products and yet as active using a fragment-based type approach to map out pharmacophoric elements.

Five metabolites were isolated from *P. cornutum* and five from *P. corallorhiza*. Cell-based assays were conducted using an MTT assay kit against MCF7 and MDA-MB-231 breast cancer cell lines and **(1E,3E,5S,6R)-1,5,6-trichloro-2-(dichloromethyl)-6-methylocta-1,3,7-triene,** isolated from *P. cornutum* was the most active with IC_{50} values of 3.0 µM and 6.15 µM respectively. Introduction of a terminal aromatic ring to enhance stability, together with varying substituents (H, CH_3, CF_3, Br, CN, CHO, $CHCl_2$) on position 7 of the molecule, gave rise to a series of cinnamate ester derivatives inspired by **(1E,3E,5S,6R)-1,5,6-trichloro-2-(dichloromethyl)-6-methylocta-1,3,7-triene.** The analogues were synthesized from their benzaldehyde precursors *via* Aldol condensation, esterification and Wittig

reactions. Their carboxylic acid counterparts were synthesized by hydrolysis of the parent esters in an attempt to promote water solubilities of the analogues.

Biological activity assays were then conducted with the cinnamate analogues against the MDA-MB-231 breast cancer cell line using an MTT assay kit. Ester derivatives with -CHO and -$CHCl_2$ functionalities had IC_{50} values of 43.45 µM and 100.01 µM respectively whilst the other ester derivatives were inactive. It was concluded that either an aldehyde (-CHO) or *gem*-dichlorides (-$CHCl_2$) is specifically required for cytotoxic activity to be observed. None of the carboxylic acids were active which could have been due to failure of the compounds to enter the breast cancer cells and reach the target site because of their polar nature. Compounds with -CHO and -$CHCl_2$ functionalities were therefore selected for future SARs studies.

TABLE OF CONTENTS

Acknowledgements		ii
Abstract		iii
Table of Contents		v
List of Figures		ix
List of Tables		xi
List of Schemes		xii
List of Abbreviations		xiv
Chapter One: Literature review		
1.1	Introduction	1
1.1.1	Breast cancer	1
1.1.2	Causes and symptoms	1
1.1.3	Epidemiology and risk factors	1
1.1.4	Classification of breast cancer	2
1.1.5	Current treatment (chemotherapy) and short falls	2
1.2	Natural products: Possible new drug leads	4
1.3	Examples of promising natural products as marine anti-cancer agents	6
1.3.1	Halichondrin B	6
1.3.2	Halomon	8
1.4	Halogenated compounds from marine environment	11
1.4.1	Cytotoxicity activity of halogenated compounds	11
1.4.2	Medicinal chemistry of halogens	14
1.5	Aims and objectives	16
1.6	References	17

Chapter Two: Isolation of halogenated monoterpenes from *Plocamium cornutum* and *Plocamium corallorhiza*

2.1 Introduction 22

2.1.1 Biological activity of acyclic and cyclic halogenated monoterpenes 24

2.1.2 Halogenated monoterpenes from South African *Plocamium* spp. 25

2.1.3 Chapter aims 28

2.2 Results and discussion 29

2.2.1 Effect of transit and solvents on the metabolite profiles of *P. corallorhiza* 29

2.2.2 Intra- and inter-site variation of secondary metabolites from *Plocamium* spp 31

2.2.3 Isolation and characterization of halogenated monoterpenes from *P. cornutum* 37

2.2.4 Isolation and characterization of halogenated monoterpenes from *P. corallorhiza* 44

2.2.5 Biological activity of halogenated monoterpenes 55

2.3 Conclusion 57

2.4 Experimental 58

2.4.1 General experiments 58

2.4.2 Extraction procedures 59

2.4.2.1 Small-scale ultra-sound assisted extractions 59

2.4.2.2 Isolation and purification of secondary metabolites from *P. cornutum* 59

2.4.2.3 Isolation and purification of secondary metabolites from *P. corallorhiza* 60

2.5 References 62

Chapter Three: Synthesis of halogenated monoterpene inspired inhibitors of cancer cell growth

3.1 Introduction 65

3.1.1 Lead optimization of natural products 65

3.1.2 Fragment-based drug design 67

3.1.3 Rationale 69

3.1.3 Cinnamic acid derivatives 71

3.2 Results and discussion 72

3.2.1 Synthesis of *o*-methyl cinnamate and its carboxylic aic derivative 73

3.2.2 Synthesis of *o*-bromo cinnamate and its carboxylic acid derivative 76

3.2.3 Synthesis of *o*-formyl cinnamate and its carboxylic acid derivative 76

3.2.4 Synthesis of *o*-cyano cinnamate and its carboxylic acid derivative 80

3.2.5 Synthesis of *o*-dichloromethyl cinnamate and its carboxylic acid derivative 81

3.2.6 Synthesis of *o*-trifluoromethyl cinnamate and its carboxylic acid derivative 86

3.3 Experimental 91

3.4 References 102

Chapter Four: Biological activity of halogenated monoterpene inspired inhibitors

4.1 Introduction 106

4.1.1 3-(4,5-dimethylthiazol-2-yl)-2,5-diphenyl tetrazolium bromide (MTT) reduction assays 106

4.1.2 MDA-MB-231 breast cancer cell line 108

4.2 Results and Discussion 110

4.2.1 Optimization of the cytotoxicity assay on MDA-MB-231 cells 110

4.2.2 Validation of cytotoxicity assay on MDA-MB-231 cells using Paclitaxel 112

4.2.3 Investigation into possible interaction between derivatives and cell proliferation reagent 112

4.2.4 Cytotoxicity of cinnamate ester derivatives 114

4.2.5 Cytotoxicity of cinnamic acid derivatives 118

4.3 Conclusion 120

4.4 Experimental 121

4.4.1 Cell culture 121

4.4.2 Microscopic count of viable cells 121

4.4.3 Cytotoxicity assay 122

4.5 References 123

Chapter Five: Summary and Conclusion

5.1 Summary and conclusion 125

Appendices available of CD CD

LIST OF FIGURES

Figure 1.1	General view of how a bulk group enhances binding affinities	14
Figure 2.1	Photographs of A) *P. cornutum* and B) *P. corallorhiza*	28
Figure 2.2	^{1}H NMR profiles (400 MHz, $CDCl_3$) of *P. corallorhiza* crude extracts using different solvents	30
Figure 2.3	Expansions of ^{1}H NMR profiles (600 MHz, $CDCl_3$) of crude extracts (A-E) obtained from individual *P. corallorhiza* plants from Noordhoek (Port Elizabeth, South Africa)	32
Figure 2.4	Expansions of ^{1}H NMR profiles (600 MHz, $CDCl_3$) of crude extracts (A-D) obtained from individual *P. corallorhiza* plants collected from Port Alfred, South Africa	33
Figure 2.5	Expansion of ^{1}H NMR profiles (400 MHz, $CDCl_3$) of crude extracts (A & B) obtained from individual *P. cornutum* plants at Kalk Bay, Cape Town (South Africa)	34
Figure 2.6	Expansion of ^{1}H NMR profiles (400 MHz, $CDCl_3$) of crude extracts (A-C) obtained from P. cornutum plants collected at Kenton-on-Sea (A), Kalk Bay (Cape Town) (B) and Noordhoek (Port Elizabeth) (C)	35
Figure 2.7	Crude ^{1}H NMR (400 MHz, $CDCl_3$) spectrum of *P. cornutum* collected from Kalk Bay, Cape Town (South Africa)	37
Figure 2.8	^{1}H NMR (400 MHz, $CDCl_3$) spectrum of **2.11**	39
Figure 2.9	^{1}H NMR (400 MHz, $CDCl_3$) spectrum of **2.12**	40
Figure 2.10	^{1}H NMR (400 MHz, $CDCl_3$) spectrum of **2.13**	41
Figure 2.11	^{1}H NMR (400 MHz, $CDCl_3$) spectrum of **2.14**	41
Figure 2.12	^{1}H NMR (400 MHz, $CDCl_3$) spectrum of **2.15**	42
Figure 2.13	^{1}H NMR (400 MHz, $CDCl_3$) spectrum of **2.26**	49
Figure 2.14	^{1}H NMR (400 MHz, $CDCl_3$) spectrum of **2.33**	50
Figure 2.15	^{1}H NMR (400 MHz, $CDCl_3$) spectrum of **2.34**	51
Figure 2.16	^{1}H NMR (400 MHz, $CDCl_3$) spectrum of **2.37**	52
Figure 2.17	^{1}H NMR (400 MHz, $CDCl_3$) spectrum of **2.38**	53

Figure 3.1	Summary of structure-activity information for halogenated monoterpenes from South African *Placamium* spp	69
Figure 3.2	^{1}H NMR (400 MHz, $CDCl_3$) spectrum of *o*-methyl cinnamate	74
Figure 3.3	Comparison of the ^{13}C spectra (100 MHz, $CDCl_3$) of *o*-methyl cinnamate and its carboxylic acid derivative	75
Figure 3.4	^{1}H NMR (400 MHz, $CDCl_3$) spectrum of *o*-formyl cinnamate	77
Figure 3.5	^{1}H NMR (400 MHz, $CDCl_3$) spectrum of indanone	78
Figure 3.6	^{13}C NMR (100 MHz, $CDCl_3$) spectrum of indanone	78
Figure 3.7	^{1}H NMR (400 MHz, $CDCl_3$) spectrum of *o*-formyl cinnamic acid	80
Figure 3.8	^{1}H NMR (400 MHz, $CDCl_3$) spectrum of crude reaction mixture of conversion of tolualdehyde to 1-(dichloromethyl)-2-methylbenzene	82
Figure 4.1	Optimization of the cytotoxicity assay on MDA-MB-231 cells	111
Figure 4.2	Validation of cytotoxicity assay on MDA-MB-231 cells using Paclitaxel	113
Figure 4.3	Determination of possible interaction between cell proliferation reagent and derivatives	113
Figure 4.4	Comparison of cytotoxic activity of cinnamate ester derivatives in MDA-MB-231 cells	117
Figure 4.5	Comparison of cytotoxic activity of cinnamic acid derivatives in MDA-MB-231 cells	119

LIST OF TABLES

Table 1.1	Plant-derived anti-cancer agents	4
Table 1.2	Microbe-derived anti-cancer agents	4
Table 1.3	Marine-organism derived anti-cancer agents	5
Table 2.1	Halogenated monoterpenes previously isolated from *P. cornutum*	26
Table 2.2	Halogenated monoterpenes previously isolated from *P. suhrii*	26
Table 2.3	Halogenated monoterpenes previously isolated from *P. corallorhiza*	27
Table 2.4	^{1}H NMR (400 MHz, $CDCl_3$) chemical shifts of halogenated monoterpenes isolated from *P. cornutum*	43
Table 2.5	^{1}H NMR (400 MHz, $CDCl_3$) chemical shifts of halogenated monoterpenes isolated from *P. corallorhiza*	54
Table 2.6	Anti-cancer activity (IC_{50} values) of halogenated monoterpenes isolated from *P. cornutum*, *P. suhrii* and *P. corallorhiza* against WHCO1 and against breast cancer cell lines (MCF7, MCF12A and MDA-MB-231)	56
Table 2.7	Masses and percentage yields of compounds isolated from *P. cornutum*	60
Table 2.8	Masses and percentage yields of compounds isolated from *P. corallorhiza*	61
Table 3.1	Cinnamate esters and carboxylic acid derivatives	71
Table 3.2	^{1}H NMR data (400 MHz) for ester derivatives in $CDCl_3$	87
Table 3.3	^{13}C NMR data (100 MHz) for ester derivatives in $CDCl_3$	88
Table 3.4	^{1}H NMR data (400 MHz) for carboxylic acid derivatives in $CDCl_3$	89
Table 3.5	^{13}C NMR (100 MHz) for carboxylic acid derivatives	90
Table 4.1	Derivatives tested on MDA-MB-231 cells for cytotoxicity	109
Table 4.2	Estimated IC_{50} values in μM concentrations	117

LIST OF SCHEMES

Scheme 1.1 Hepatic metabolism of halomon 10

Scheme 1.2 Bioisosteric exchange of uracil to 5-FU and its metabolism 15

Scheme 2.1 Proposed biosynthesis of cyclic and acyclic halogenated monoterpenes 23

Scheme 2.2 Extraction and isolation of secondary metabolites from *P. cornutum* 38

Scheme 2.3 Extraction and isolation of secondary metabolites from *P. corallorhiza* collected from Kalk Bay, Cape Town (South Africa) 45

Scheme 2.4 Extraction and isolation of secondary metabolites from *P. corallorhiza* collected from three sisters (South Africa) 46

Scheme 2.5 Extraction and isolation of secondary metabolites from *P. corallorhiza* collected from Noordhoek, Port Elizabeth 47

Scheme 2.6 Extraction and isolation of secondary metabolites from *P. corallorhiza* collected from Port Alfred 48

Scheme 3.1 Conversion of 10-deacetylbaccatin to paclitaxel and its structural analogue docetaxel 66

Scheme 3.2 Possible structural analogues of Plocornulide A 70

Scheme 3.3 General strategies used in the synthesis of cinnamic acid derivatives 72

Scheme 3.4 Preparation of *o*-methyl cinnamate and its free acid 73

Scheme 3.5 Preparation of *o*-bromo cinnamate and its free acid 76

Scheme 3.6 Preparation of *o*-formyl cinnamate 76

Scheme 3.7 Attempted synthesis of *o*-formyl cinnamic acid using Doebner modification reaction 78

Scheme 3.8 Proposed mechanism for the formation of indanone from phthaldialdehyde 79

Scheme 3.9 Aldehyde protection of *o*-formyl cinnamate and its hydrolysis 80

Scheme 3.10 Preparation of *o*-cyano cinnamate and its carboxylic acid derivative 81

Scheme 3.11 Conversion of tolualdehyde to *gem*-dichloromethyltoluene using BCl_3 82

Scheme 3.12 Proposed mechanism for the conversion of an aldehyde to gem-dichlorines using BCl_3 82

Scheme 3.13 Attempted synthesis of *o*-dichloromethyl cinnamate 83

Scheme 3.14 Conversion of tolualdehyde to *gem*-dichloromethyltoluene using $SOCl_2$ 83

Scheme 3.15 Conversion of *o*-formyl cinnamate to *o*-dichloromethyl cinnamate 84

Scheme 3.16 Attempted synthesis of *o*-dichloromethyl cinnamic acid by hydrolysis of the parent ester 85

Scheme 3.17 Conversion of *o*-formyl cinnamic acid to *o*-dichloromethyl cinnamic acid 85

Scheme 3.18 Esterification of o-trifluoromethyl cinnamic acid to o-trifluoromethyl cinnamate 86

Scheme 4.1 Reduction of MTT to a formazan salt by viable cells 107

Scheme 4.2 Reduction of WST-1 to a formazan salt by viable cells 107

LIST OF ABBREVIATIONS

ºC	Degrees Celsius
COSY	^{1}H-^{1}H Homonuclear Correlation Spectroscopy
d	Doublet
dd	Doublet of doublets
eV	Electron Volt
DCM	Dichloromethane
DEPT	Distortionless Enhancement by Polarization Transfer
DMSO	Dimethyl Sulphoxide
ESI-MS	Electronspray Ionization-Mass spectrometry
EtOAc	Ethyl Acetate
GC-MS	Gas chromatography-Mass spectrometry
HMBC	Heteronuclear Multiple Bond Correlation
HMT	Halogenated Monoterpenes
HSQC	Heteronuclear Single Quantum Coherence
HPLC	High Performance Liquid Chromatography
HREI-MS	High Resolution Electron Impact Mass Spectrometry
Hz	Hertz
IC_{50}	Inhibitory Concentration 50 %
IR	Infrared
J	Spin-Spin Coupling constant (Hz)
MeOH	Methanol
m	Multiplet
m/z	Mass to charge ratio
NCI	National Cancer Institute
NMR	Nuclear Magnetic Resonance Spectroscopy
ppm	Parts per million

q	Quartet
s	Singlet
t	Triplet
TLC	Thin Layer Chromatography
UV	Ultra violet

CHAPTER ONE:

Literature review

1.1 Introduction:

1.1.1 Breast Cancer

Breast cancer is characterized by the presence of benign/malignant cells in either glandular or ductal units of the breast tissue. Abnormal growths occur due to uncontrolled cell divisions of immortalized cells that do not respond to apoptotic mechanisms and may become invasive and spread to regional lymph nodes (metastasis) (Eleri Lloyd, 2011). Systemic organs that are likely to be involved in breast cancer metastasis include lungs, bones, liver, skin and soft tissues (Chambers et al., 2002).

1.1.2 Causes and symptoms

Cancer cells are thought to arise due to mutations occurring at DNA level, thereby resulting in the damage of genes involved in cell division. Causes of such mutations could be tobacco smoke, asbestos, arsenic, radiation (ionizing and non-ionizing), infections, environmental pollutants, etc. (Anand et al., 2008). Symptoms of the disease vary from lumps in the breast to swellings and skin changes. No obvious signs can be observed unless properly examined and diagnosed by a medical practitioner. Once the cancer has metastasized, symptoms are related to the organ(s) affected.

1.1.3 Epidemiology and risk factors

It is estimated that about 1.3 million women are diagnosed with breast cancer each year worldwide, and 465 000 die from the disease, with mortality rates being high in developing countries (Eleri Lloyd, 2011). In Africa, the disease has been on the rise with reported cases increasing as much as 5% every year. The cost of treating metastatic breast cancer in Africa, North America and Asia was estimated to be $68 million, $3.8 billion and $143 million respectively in 2006, costs which are mostly likely to be higher at the present times (Groot et al., 2006). It is quite clear that breast cancer can pose a significant economic burden on governments and the world as a whole (Remak and Brazil, 2004) if intervention protocols are not put in place.

Incidences of breast cancer increase with age, mostly above 50 years. Risk factors include late menopause, breast feeding, parity, prolonged use of exogenous hormones, alcohol consumption, obesity, genetic predisposition (born with a certain genetic mutation that statistically increases one's chances of developing cancer later in life), etc. (Popat and Smith, 2006). Identification of such factors is essential in initiating chemoprevention strategies in patients that are most likely to develop the disease in the future.

1.1.4 Classification of breast cancer

Due to different morphological appearances, molecular features and location of carcinoma in the breast tissue, several classifications of cancer types have been made, with ductal carcinomas being considered non-life threatening (Rakha and Chan, 2011; Veronesi et al., 2005).

Currently, classification according to molecular features and biomarkers such as hormone receptors (HR) i.e., oestrogen receptors (ER) and progesterone receptors (PR), and human epidermal growth factor 2 receptors (HER 2), is important in breast cancer and gives an indication of treatment response by patients (Gluz et al., 2009; Rakha et al., 2007). HR+ and HER 2- tumours constitute the largest proportion of breast cancer cases reported and normally respond to hormonal therapy. Tumours with neither HR nor HER 2 expressions are termed triple negative breast cancers (TNBC) and are difficult to treat with poor prognosis (Dent et al., 2007). TNBC constitute 10-20% of all breast cancer cases (Carey et al., 2006) and is most prevalent in African populations (Hammond et al., 2010). Targeted therapies are unavailable for this class of cancer and more work is underway to best treat patients suffering from TNBC.

1.1.5 Current treatment (chemotherapy) and short-falls

Several treatment options/regimens have been in use to improve overall survival of patients. The use of high doses of non-specific toxic agents has been the main strategy for treating cancer. Since approximately 70% of patients have tumours expressing ER and/or PR receptors, hormonal therapy (HT) is considered pivotal in the management of the disease (Awada et al., 2003). The first drug which had major impact on chemotherapy in the 1970s was tamoxifen (**1.1**), an oestrogen receptor antagonist, and was considered a gold standard (Jordan, 1988) though other drugs/regimen are slowly taking over. Second and third generation aromatase inhibitors e.g. anastrozole (**1.2**) that inhibit synthesis of oestrogen by

blocking activity of aromatase enzyme have challenged the use of tamoxifen (**1.1**) as first line treatment in advanced cancers (Nabholtz et al., 2000).

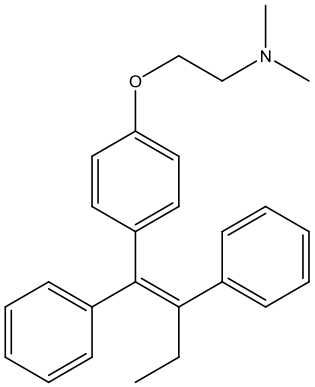

tamoxifen (1.1)

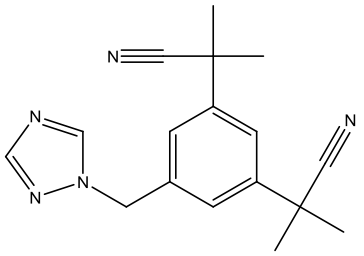

anastrozole (1.2)

Nowadays targeted therapies containing hormonal therapy (e.g Herceptin) can be used in combination with other classes of drugs, depending on the characteristics of the cancer. Chemotherapy normally will contain medicines from the anthracyclines (e.g. doxorubicin, epirubicin) and taxanes (e.g. paclitaxel, docetaxel) classes with sometimes the addition of antimetabolites (e.g. methotrexate, fluorouracil) as adjuvant therapy after lumpectomy. Vinca alkaloids, gemcitabine, capecitabine, and ixabepilone are being used as third line treatment or in later treatment of metastatic breast cancer (Rivera, 2010). Tamoxifen (**1.1**) has since been introduced as a preventive measure in reducing oestrogen-receptor positive breast cancer (Cuzick et al., 2003; Veronesi et al., 2005) in people at high risk of developing the disease.

Undesirable adverse side effects of current anti-cancer drugs lead to poor patient compliance and adherence. Chemotherapy has been demonstrated to affect normal rapidly dividing cells of the body, especially cells of the blood, mouth, intestinal tract, nose, nails and hair. Current microtubule targeted therapies e.g. paclitaxel and vinca alkaloids result in sensory and motor neuropathy (Carlson and Ocean, 2011). Hormonal therapy e.g. Herceptin has been shown to possess severe cardiovascular, gastrointestinal and cutaneous side effects (Metzger Filho et al., 2010). Attempts have been underway in trying to reduce the toxic side effect profiles of chemotherapy. New agents are required that specifically target tumour related molecules i.e., that possess selective cytotoxicity. Several molecular pathways have been of interest to scientists that can be explored further; oestrogen receptor pathway, tyrosine kinase signal transduction pathway, cell cycle regulation pathway, apoptosis pathway and angiogenesis pathway (Awada et al., 2003). New drug candidates and new drug targets have to be

discovered. Natural products offer a wide variety of novel cytotoxic compounds that are worthwhile investigating and pursuing as anti-cancer drug leads.

1.2 Natural products: Possible new drug leads

For the past decade, the use of natural products as means for drug discovery has increased drastically. Natural products offer a rich and unexplored source of therapeutic leads to pharmaceutical industries (Corson and Crews, 2007). More and more attention is being given to compounds of natural origin due to the limitations associated with combinatorial chemistry and high-through put screening methods (Molinari, 2009). Before the introduction of these computational models, natural products were key elements in drug discovery processes for over a century. Several drugs have already been developed from natural compounds (McRae et al., 2007; William, 2000) and Tables 1.1 - 1.3 show anti-cancer agents derived from plants, microbes and marine organisms as compiled by (Da Roche et al., 2001) in the article natural products in anti-cancer therapy.

Table 1.1: Plant-derived anti-cancer agents

Compound	Cancer use
Vincristine	Leukaemia, lymphoma, breast, lung, paediatric solid tumours
Vinblastine	Breast, lymphoma, renal cancer
Paclitaxel	Ovary, breast, lung, bladder cancer
Docetaxel	Breast, lung cancer

Table 1.2: Microbe-derived anti-cancer agents

Compound	Cancer use
Actinomycin	Sarcoma and germ-cell cancers
Bleomycin	Germ-cell, cervix, head and neck cancers
Daunomycin	Leukaemia
Doxorubicin	Lymphoma, breast, ovary, lung and sarcomas
Epirubicin	Breast cancer

Table 1.3: Marine-organism derived anti-cancer agents

Compound	Cancer use	Mechanism of action
Citarabine	Leukaemia, lymphoma	Inhibition of DNA synthesis
Bryostatin	Experimental	Activation of protein kinase c
Dolastatin	Experimental	Inhibition of microtubules
Ecteinascidin 743	Experimental	Alkylation of DNA
Aplidine	Experimental	Inhibition of cell cycle progression
Halichondrin B	Experimental	Interaction with tubulin

Improvements in deep sea sample collection and technologies in structure elucidation and synthesis have allowed a shift of focus to marine organisms as sources of drug leads (Da Roche et al., 2001). A large number of novel compounds have been isolated from marine algae with exciting cytotoxic activity. Red algae (Rhodophyta) commonly known as red seaweeds, are the most important and are believed to produce many biologically active compounds compared to other species (El Gamal, 2011). In nature they occupy parts of the sea, lake or river that are close to the shore i.e., littoral zones. Their basic appearance consists of a thallus that make up the algal body, a leaf-like structure known as the lamina, a stipe which acts as the stem although it might be absent and a holdfast that attaches to the surface of a rock or base of the ocean. In terms of size, it varies from a few centimetres to several metres in length. Cytotoxic activity of extracts from these algae and from all species in nature is attributed to molecules referred to as secondary metabolites (El Gamal, 2011).

Secondary metabolites (natural products) are organic compounds that are not required for the immediate survival of species. They do not play any role in the growth, development or reproduction of the organism. Their presence in organisms is not clearly understood but it is believed they promote the spread and dominance of species in an ecological setting (McRae et al., 2007). They are responsible for warding off bacteria, insects, fungi and in some cases animals that threaten the survival of species. They therefore provide a protective role to organisms and it is this phenomenon that makes natural products important drug leads (Stamp, 2003). Their complex structures, potent biological activity and novelty offer opportunities for the discovery of new drug leads and identification of new drug targets in a biological system.

In the following section some of the important issues in the discovery and development of anti-cancer agents from the marine environment are discussed using two examples.

1.3 Examples of promising natural products as marine anti-cancer agents

1.3.1 Halichondrin B

Halichondrin B (**1.3**) is a macrocyclic polyether first isolated from the sponge *Halichondria okadai* (Uemura et al., 1985), that exhibited cytotoxic activity by inhibiting cell division of cancerous cells. It was included in pre-clinical studies by the National Cancer Institute (NCI) in 1992 in which it demonstrated high toxicity against blood cancer cells i.e., leukaemia. However further developments were hindered by difficulties in collecting sufficient material and the lengthy processes in the synthesis of the natural compound. Discovery of the C1-C38 moiety as the pharmacophoric element in the macrocyclic lactone led to the development and synthesis of ER-086526 (**1.4**) (Towle et al., 2001) which is also known as E7389, NSC 707389 (Perez, 2009) and ER-076349 (**1.5**). Assessment of more than 180 macrocylic ketones resulted in the development of the above mentioned analogues and their structural difference being the substituent at C35, either an alcohol or amine functionality. The analogues differed in structure to Halichondrin B by replacing a lactone ester at C1, a methyl functionality at C31 and a tricyclic system C29-C38 on halichondrin B with a ketone, methoxy group and a five-membered ring respectively.

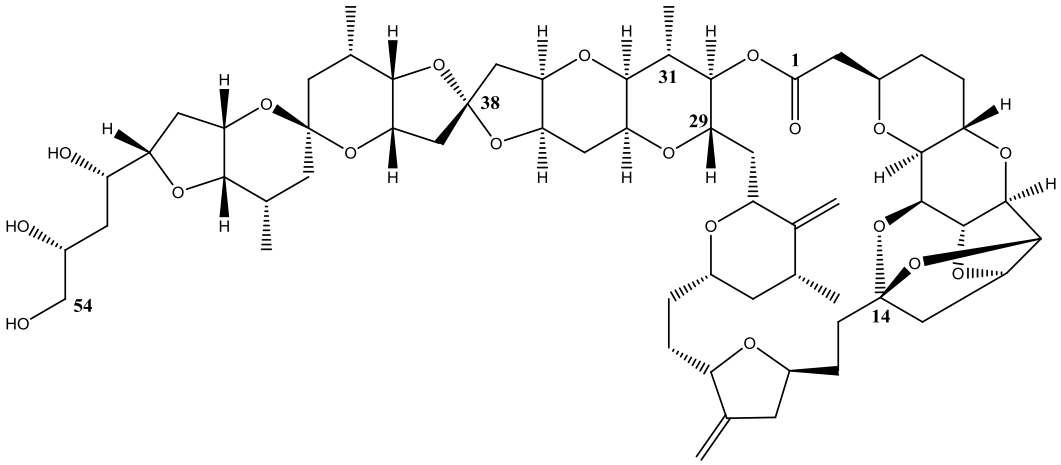

halichondrin B (1.3)

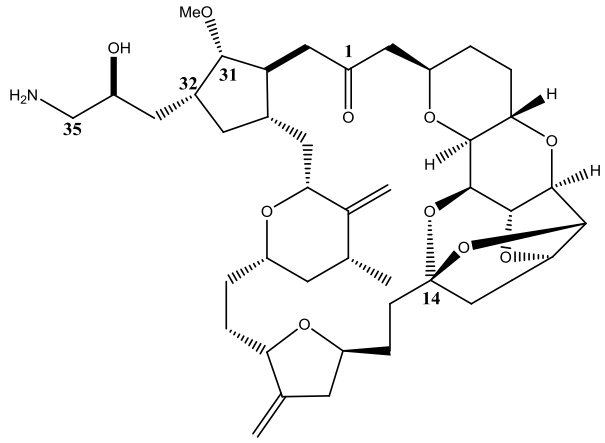

ER-086526 (1.4)

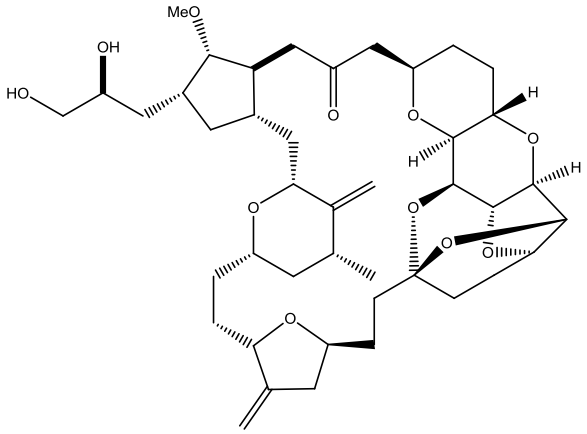

ER-076349 (1.5)

When tested against human cell lines, the alcohol (ER-076349) showed twice the activity compared to the amine (ER-086526), and both being 5-10 times more active than vinblastine (**1.6**) and paclitaxel (**1.7**) used in the experiments as reference standards (Bai et al., 1991; Towle et al., 2001).

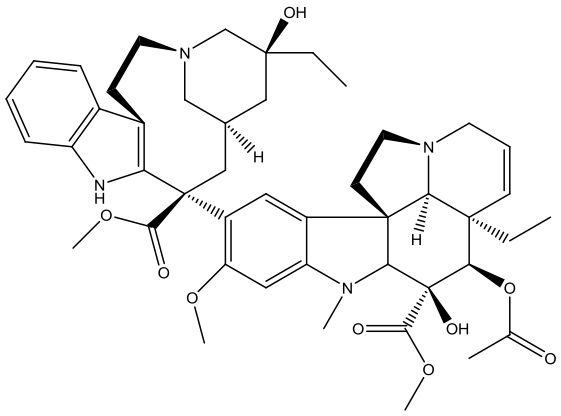

vinblastine (1.6)

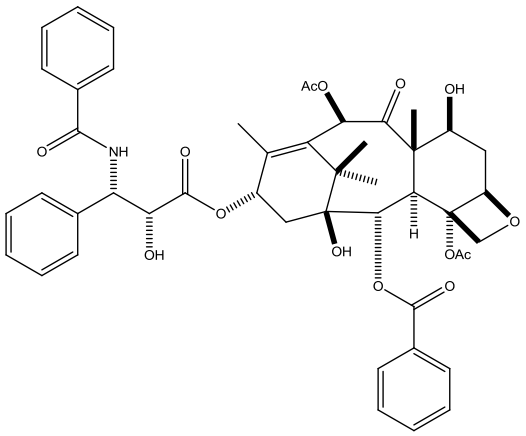

paclitaxel (1.7)

Activity of the analogues was comparable to the natural product but with greater activity in lung and breast cancer cells (Fang, 2004).

The mechanism of action of these compounds was identified as tubulin-based antimitotic. They disrupt microtubule formation during mitosis of rapidly dividing cells i.e., cancer cells. However, their interaction with tubulin is somehow different and specific in comparison to other tubulin depolymerizers e.g., Vinca alkaloids, dolastatins etc. A different interaction to the known mechanism may aid in unique tumour specificities and other desirable clinical outcomes (Bai et al., 1991), hence the interest in this natural product.

Despite ER-076346 (**1.5**) showing greater cytotoxicity in *in-vitro* studies, ER-086526 (**1.4**) showed better efficacy when *in-vivo* studies were conducted, particularly in MDA-MB-435 breast and COLO 205 colon cancer models. Possible explanations for the observed trends could be that ER-076346 (**1.5**) is more readily metabolized *in-vivo* than ER-086526 (**1.4**), compromising on bioavailability and efficacy. The mitotic block as a result of ER-086526 (**1.4**) was also shown to be less reversible than that induced by ER-076346 (**1.5**), rendering ER-086526 (**1.4**) more cytotoxic and a better lead for drug development. Further investigations are however required to fully ascertain these explanations (Towle et al., 2001).

ER-086526 (**1.4**) has been pursued further and has since entered phase I, II and III of clinical trials against advanced and metastatic breast cancer. It is now known as Eribulin and has a half-life of 40 hours with minimal renal excretion (Tan et al., 2009). The drug is metabolized by cytochrome P450 but has been shown not to influence metabolism of other drugs (Zhang et al., 2008). Eribulin has promising drug outcomes when used as a single agent in patients with locally advanced disease or in those with metastatic breast cancer that have become resistant to taxanes and anthracyclines (Cortes et al., 2011).

1.3.2 Halomon

Halomon (**1.8**) is a secondary metabolite isolated from the red seaweed *Portieria hornemannii* that belongs to the Rhodophyta class (red algae). It is a well-known halogenated monoterpene that has received worldwide attention since it possesses selective cytotoxicity properties ideal in cancer therapy (Fuller et al., 1994; Stallard and Faulkner, 1974).

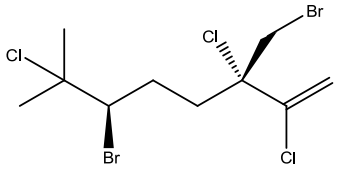

1.8

Halomon (**1.8**) was considered a novel anti-tumour agent by the NCI, as it displayed interesting activities in human tumour, disease-oriented *in-vitro* screens (Fuller et al., 1992). Cytotoxic selectivity was observed to be towards renal, brain, colon and lung cancer cells with less sensitivity in leukaemia and melanomas. Its mechanism of action is unclear, but it has been shown to be different from that of electrophilic alkylating agents by computerized pattern-recognition studies (Egorin et al., 1997). Halomon was therefore selected as a pre-clinical drug for development due to its potentially unique mechanism of action and selective

cytotoxicity to cell lines. Several other related metabolites to halomon, both acyclic and cyclic were also screened for cytotoxic activity which allowed Structural Activity Relationships (SARs) to be deduced.

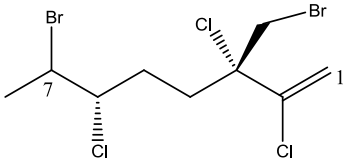

1.9

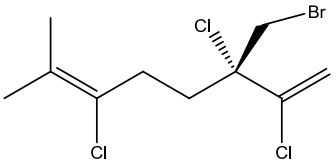

1.10

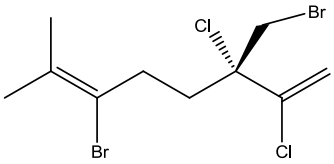

1.11

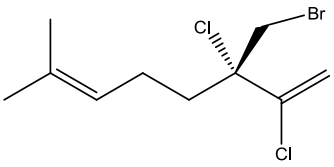

1.12

Compounds **1.9-1.11** had comparable activity to halomon (**1.8**), with compound **1.12** being weakly active. The halogen at C-7 was shown to be unessential for activity considering compounds **1.10** and **1.11** displayed cytotoxic properties. Halogen removal at C-6 in compound **1.12** resulted in a weak/inactive metabolite, showing the necessity of a halogen at that position. Compounds with a halogen at C-2 also exhibited cytotoxic behaviour rendering its presence necessary for activity.

From the list of carbocyclic compounds isolated from *Portieria hornemannii*, compound **1.13** and **1.14** were weakly cytotoxic in comparison to compounds **1.9-1.11.** Compound **1.15** possessed noticeable activity which could be compared to halomon (**1.8**).

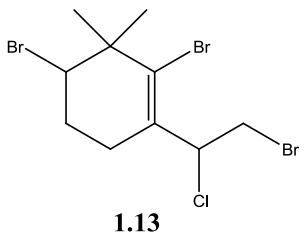

1.13

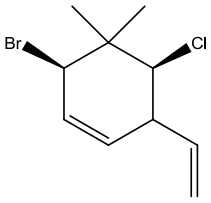

1.14

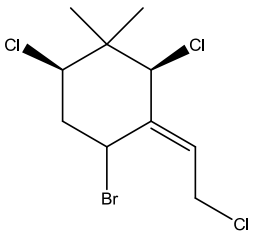

1.15

However, cytotoxic profiles obtained for the cyclic and acyclic compounds showed little correlation to halomon (**1.8**) in terms of selectivity. Minimal differential response to cell lines was noted, prompting research on halomon (**1.8**) which had exceptional properties to the rest of the class of halogenated monoterpenes from *Portieria hornemannii*.

In pre-clinical trials, experiments were conducted to determine the enzymes responsible for the metabolism of halomon (**1.8**), and the metabolites formed by carrying out *in-vitro* metabolism studies using mice and human liver preparations (Egorin et al., 1997). Cytochrome P450 isoforms are majorly linked to metabolism of halogenated compounds (Koop, 1992) and hepatic metabolism of halomon has been established with minimal urinary excretion (Egorin et al., 1996). NADPH is required as a co-factor and halomon (**1.8**) is metabolized to the following metabolites; **1.16** and **1.17.** The structures of metabolites formed were determined by mass spectroscopy.

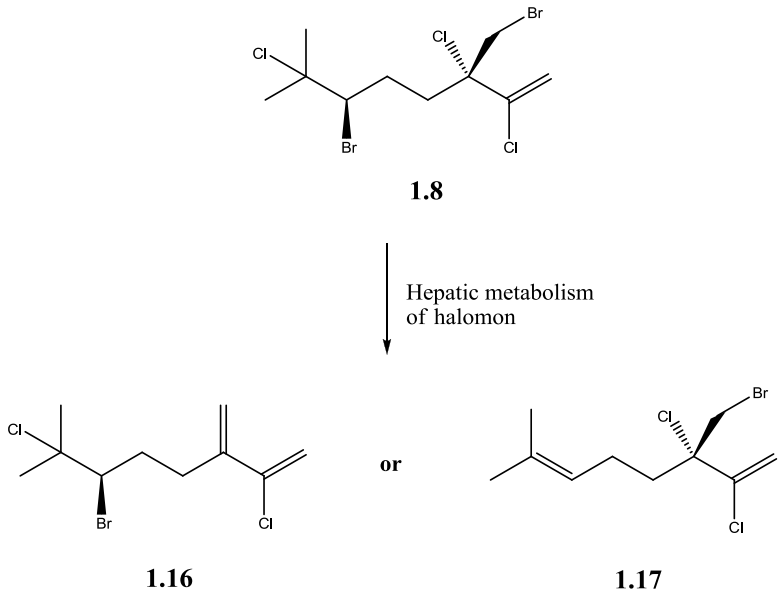

Scheme 1.1 Hepatic metabolism of halomon (**1.8**)

Halomon is rapidly metabolized *in-vivo* and the enzyme responsible for its metabolism is still yet to be identified (Egorin et al., 1997). The connection between the metabolism of halomon/metabolites and the mechanism of action/biological activity remains to be explored though the NCI has dropped halomon as a potential anti-cancer drug due to likely toxic effects presented with the high degree of halogens on its structure.

1.4 Halogenated compounds from marine environment

In light of selective cytotoxicity displayed by halomon (**1.8**) (Fuller et al., 1994), interest has risen to explore biological activity of halogenated compounds. It is quite evident that halomon (**1.8**) targets a certain pathway/protein that is specific to cancer cells. An understanding of such a phenomenon will enable the development of targeted therapies that target tumour-related molecules and thereby reduce the side effect profiles of chemotherapy.

1.4.1 Cytotoxic activity of halogenated compounds

Cytotoxicity studies conducted with several metabolites isolated from *Plocamium* species have demonstrated the same phenomenon of selective toxicity (De Ines et al., 2004). Studies on *Laurencia* have also displayed the presence of cytotoxic metabolites in its extracts. Both species belong to the Rhodophyta class that is common for producing a variety of halogenated compounds.

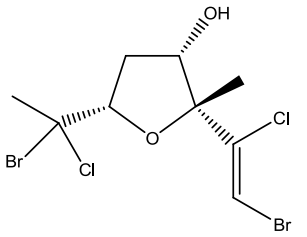

1.18

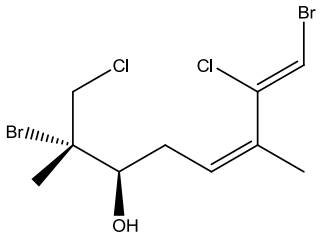

1.19

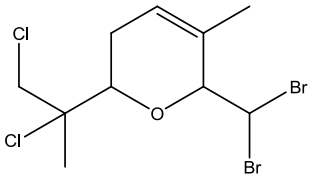

1.20

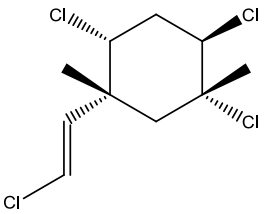

1.21

Compounds **1.18 – 1.21** were isolated from *Plocamium cartilagineum* and displayed selective cytoxicity when exposed to CT26 (murine colon adenocarcinoma), SW480 (human colon carcinoma), HeLa (human cervical adenocarcinoma) and a mammalian non-tumor cell line CHO (Chinese hamster ovary cells). Compound **1.20** was more specific to human colon adenocarcinoma SW480 and caused irreversible damage to cells (De Ines et al., 2004).

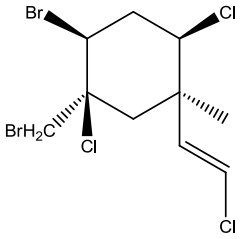

1.22

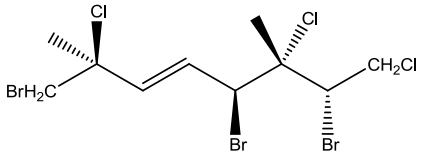

1.23

Plocamium hamatum presented with two metabolites, compound **1.22** and **1.23** that showed moderate cytotoxicity (Konig et al., 1999). Secondary metabolites from *Plocamium cornutum* (Antunes et al., 2011)(Lawson, 2010) and *Plocamium corallorhiza* (Knott et al., 2005) displayed cytotoxic activities against breast and oesophageal cancer cell lines and these will be discussed in detail in chapter 2.

From *Laurencia* species, several metabolites with interesting cytotoxic properties have been isolated. To mention a few, compound **1.24** known as Laurinterol (LOEL), has been isolated from *Laurencia okamurai* and it inhibits growth of melanoma cell lines by inducing apoptosis without the occurrence of serious adverse effects. Its effect is dose dependent as 10 μg/ml of product inhibits 50% of melanoma cells, with 1 μg/ml inhibiting 30%. LOEL (**1.24**) has since been considered an invention for preventing and inhibiting melanoma (El Gamal, 2011). Compounds **1.25-1.27** from *Laurencia obtuse* have shown remarkable cytotoxic activity with compound **1.27** having an ED_{50} value of 0.3 μg/ml against a P388 cell line. Compounds **1.28-1.30**, also from the same species (*L. obtuse*) were tested against a Chinese hamster ovary (CHO) cell line and compound **1.29** showed greater cytotoxic activity than **1.28** and **1.30.** A lot more metabolites from various *Laurencia* species have been tested which have moderate to great cytotoxic activity and further research is required to ascertain their full potential as candidates for cancer therapy.

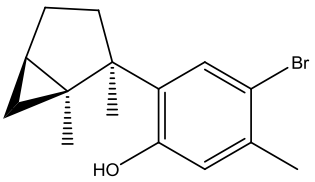

1.24

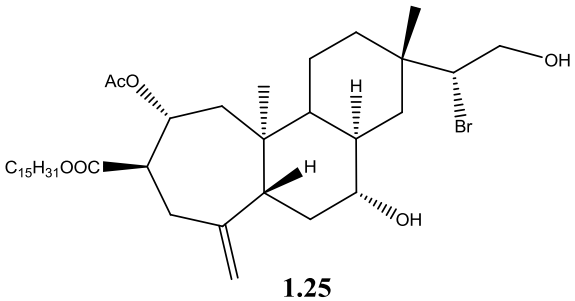

1.25

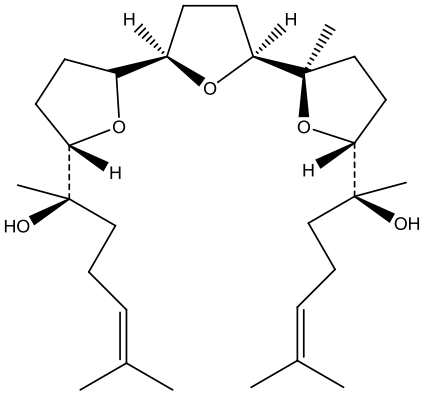

1.26

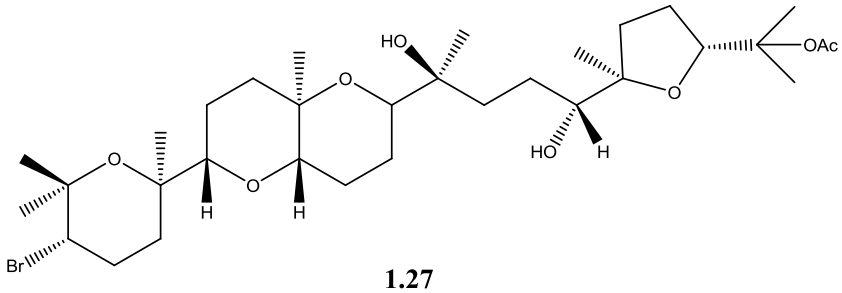

1.27

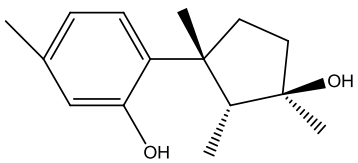

1.28

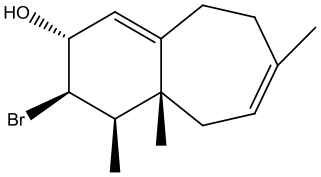

1.29

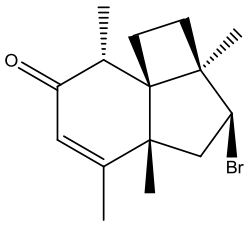

1.30

1.4.2 Medicinal chemistry of halogens

Structural activity relationships conducted on halomon (**1.8**) and related compounds demonstrate the importance of having halogens on the molecule. Chlorine and bromine appear to be the most common halogens used by nature to increase biological activity of secondary metabolites (Neumann et al., 2008) and this is assumed to occur in several ways.

a) Bulky flanking groups e.g., halogens can result in volumetric and conformational changes. Their presence on the molecule enables occupation of the entire active site of a molecular target in a biological system, including the deeper pockets, thereby enhancing binding affinity of the compound to the target site (Greenbaum et al., 2004; Monforte et al., 2009).

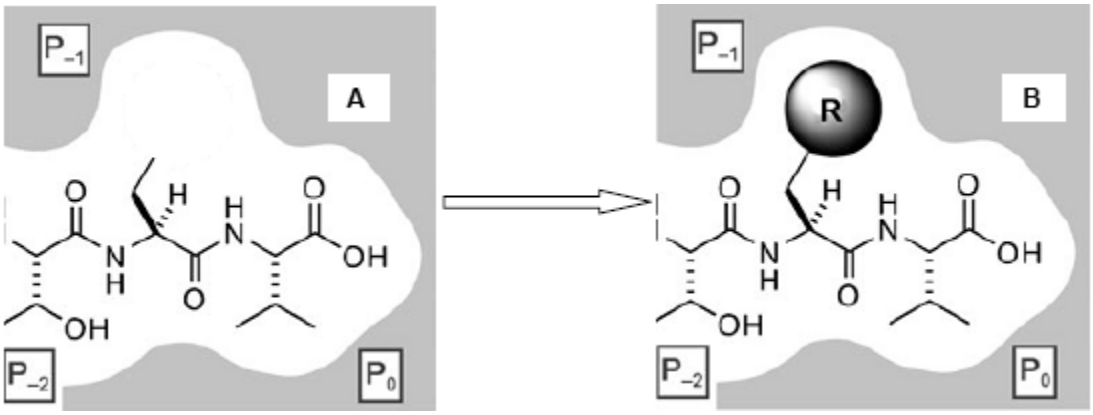

Figure 1.1: General view of how a bulk group enhances binding affinities: A) without and B) with one designated R group (Hernandes et al., 2010).

b) Incorporation of halogens enhances lipophilic nature of molecules, resulting in an increase in membrane permeability. Development of CNS drugs has been demonstrated to use halogenation to improve blood brain barrier (BBB) permeability (Gentry et al., 1999). Biological activity is observed when the active compound reaches the active site, of which membrane permeability is key.

c) Though effect is less pronounced, halogens have shown tendencies to form intermolecular bonds equivalent to hydrogen bonds but of lower energy. Such interactions contribute to the stability of the complexes formed when a compound interacts with its biological site, improving on biological activity (Metrangolo and Resnati, 2008; Metrangolo and Resnati, 2001).

Incorporation of halogens in the synthesis of final compounds has been documented in almost 25% of the total number of papers/patents published related to medicinal chemistry. Estimates were based on searches recorded in five bibliographic databases: ISI Web of Science, Scifinder, Science Direct, ACS and Wiley Co in October 2009 (Hernandes et al., 2010). A common example demonstrating the influence of halogens on biological activity is the exchange of hydrogen by fluorine in uracil (**1.31**) to yield 5-fluorouracil (**1.32**) (5-FU), an anti-cancer drug (Scheme 1.2).

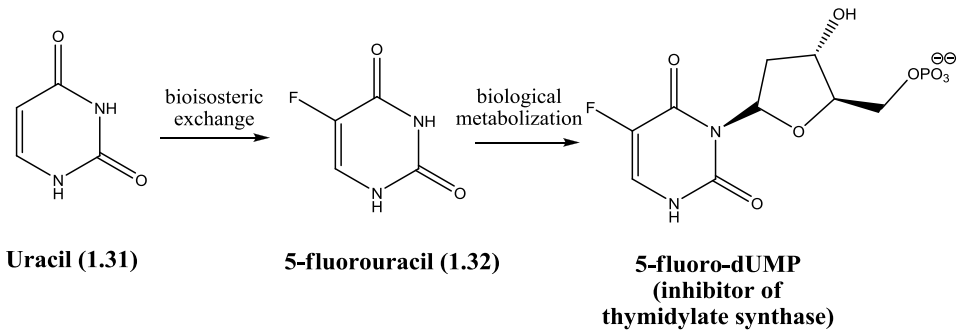

Scheme 1.2 Bioisosteric exchange of uracil to 5-FU and its metabolism

Fluorine enhances binding affinity of 5-FU on thymidylate synthase, hence inhibits pyrimidine biosynthesis. Therefore fluorine chemistry can be explored further to determine its influence on binding affinities of drug candidates. It's no question that halogens play a role in ensuring activity profiles of compounds. However little knowledge is known regarding the extent of their influence which was one of the objectives of this project.

1.5 Aims and objectives

Selective cytotoxicity is key in reducing the side effect profiles of chemotherapy. New drug targets are required for better clinical outcomes to be observed. Halogenated monoterpenes show great potential to be developed into newer drug hits/leads that can be used in developing new targeted therapies since they demonstrate selective cytotoxicity. Halogenation of these molecules seems important for activity and is worthwhile pursuing the effect of halogens on the activity of metabolites.

Therefore the main aim of this project was to explore the medicinal chemistry of halogenated monoterpenes isolated from *Plocamium cornutum* and *Plocamium corallorhiza* as potential anti-cancer agents against breast cancer cell lines with the following objectives:

1) Isolating a selection of halogenated monoterpenes for preliminary structure-activity studies in a breast cancer cell line
2) Synthesizing selected derivatives of halogenated monoterpene inspired inhibitors of cancer cell growth using a fragment based-type approach
3) Conducting cell-based *in-vitro* studies with synthesized derivatives against a breast cancer cell line.
4) Determination of pharmacophoric elements and the effect of halogens on cytotoxic activity from *in-vitro* studies conducted

References

Anand, P., Kunnumakara, A.B., Sundaram, C., Harikumar, K.B., Tharakan, S.T., Lai, O.S., Sung, B., Aggarwal, B.B., 2008. Cancer is a Preventable Disease that Requires Major Lifestyle Changes. Pharmaceutical Research, 25, 2097-2116.

Antunes, E.M., Afolayan, A.F., Chiwakata, M.T., Fakee, J., Knott, M.G., Whibley, C.E., Hendricks, D.T., Bolton, J.J., Beukes, D.R., 2011. Identification and in vitro anti-oesophageal cancer activity of a series of halogenated monoterpenes isolated from the South African seaweeds *Plocamium suhrii* and *Plocamium cornutum*. Phytochemistry (Elsevier), 72, 769-772.

Awada, A., Cardoso, F., Atalay, G., Giuliani, R., Mano, M., Piccart, M.J., 2003. The pipeline of new anti-cancer agents for breast cancer treatment in 2003. Critical Reviews in Oncology/Hematology, 48, 45-63.

Bai, R., Paull, K.D., Herald, C.L., Malspeis, L., Pettit, G.R., Hamel, E., 1991. Halichondrin B and homohalichondrin B, marine natural products binding in the vinca domain of tubulin. Discovery of tubulin-based mechanism of action by analysis of differential cytotoxicity data. Journal of Biological Chemistry, 266, 15882-15889.

Carey, L.A., Perou, C.M., Livasy, C.A., Dressler, L.G., Cowan, D., Conway, K., Karaca, G., Troester, M.A., Tse, C.K., Edmiston, S., Deming, S.L., Geradts, J., Cheang, M.C.U., Nielsen, T.O., Moorman, P.G., Earp, H.S., Millikan, R.C., 2006. Race, Breast Cancer Subtypes, and Survival in the Carolina Breast Cancer Study. JAMA: The Journal of the American Medical Association, 295, 2492-2502.

Carlson, K., Ocean, A.J., 2011. Peripheral Neuropathy with Microtubule-Targeting Agents: Occurrence and Management Approach. Clinical Breast Cancer, 11, 73-81.

Chambers, A.F., Groom, A.C., MacDonald, I.C., 2002. Metastasis: Dissemination and growth of cancer cells in metastatic sites. Nature Reviews Cancer, 2, 563-572.

Corson, T.W., Crews, C.M., 2007. Molecular Understanding and Modern Application of Traditional Medicines: Triumphs and Trials. Cell, 130, 769-774.

Cortes, J., Montero, A.J., Gluck, S., 2011. Eribulin mesylate, a novel microtubule inhibitor in the treatment of breast cancer. Cancer Treatment Reviews, 2012 April., 38(2):143-51

Cuzick, J., Powles, T., Veronesi, U., Forbes, J., Edwards, R., Ashley, S., Boyle, P., 2003. Overview of the main outcomes in breast-cancer prevention trials. The Lancet, 361, 296-300.

da Rocha, A., Lopes, R.M., Schwartsmann, G., 2001. Natural products in anti-cancer therapy. Current Opinion in Pharmacology, 1, 364-369.

de Ines, C., Argandona, V.H., Rovirosa, J., San-Martin, A., Diaz-Marrero, A.R., Cueto, M., Gonzalez-Coloma, A., 2004. Cytotoxic activity of halogenated monoterpenes from Plocamium cartilagineum. Z. Naturforsch. , C: Journal of Biological sciences, 59, 339-344.

Dent, R., Trudeau, M., Pritchard, K.I., Hanna, W.M., Kahn, H.K., Sawka, C.A., Lickley, L.A., Rawlinson, E., Sun, P., Narod, S.A., 2007. Triple-Negative Breast Cancer: Clinical Features and Patterns of Recurrence. Clinical Cancer Research, 13, 4429-4434.

Egorin, M.J., Rosen, D.M., Benjamin, S.E., Callery, P.S., Sentz, D.L., Eiseman, J.L., 1997. In vitro metabolism by mouse and human liver preparations of halomon, an antitumor halogenated monoterpene. Cancer Chemotherapy and Pharmacology, 41, 9-14.

Egorin, M.J., Sentz, D.L., Rosen, D.M., Ballesteros, M.F., Kearns, C.M., Callery, P.S., Eiseman, J.L., 1996. Plasma pharmacokinetics, bioavailability, and tissue distribution in CD2F1 mice of halomon, an antitumor halogenated monoterpene isolated from the red algae Portieria hornemannii. Cancer Chemotherapy and Pharmacology, 39, 51-60.

El Gamal, A.A., 2011. Biological Importance of Marine Algae. John Wiley & Sons, Ltd, 1-35.

Eleri Lloyd, D., 2011. Breast cancer. Medicine, 40, 5-9.

Fang, Francis G. Synthetic Studies on the Halichondrin B Analog, E7389. Abstracts, 56th Southeast Regional Meeting of the American Chemical Society, Research Triangle Park, NC, United States, November 10-13 , GEN-083. 2004. American Chemical Society.
Ref Type: Conference Proceeding

Fuller, R.W., Cardellina, J.H., II, Kato, Y., Brinen, L.S., Clardy, J., Snader, K.M., Boyd, M.R., 1992. A pentahalogenated monoterpene from the red alga Portieria hornemannii produces a novel cytotoxicity profile against a diverse panel of human tumor cell lines. Journal of Medicinal Chemistry, 35, 3007-3011.

Fuller, R.W., Cardellina, J.H., II, Jurek, J., Scheuer, P.J., Alvarado-Lindner, B., McGuire, M., Gray, G.N., Steiner, J.R., Clardy, J., 1994. Isolation and Structure/Activity Features of Halomon-Related Antitumor Monoterpenes from the Red Alga Portieria hornemannii. Journal of Medicinal Chemistry, 37, 4407-4411.

Gentry, C.L., Egleton, R.D., Gillespie, T., Abbruscato, T.J., Bechowski, H.B., Hruby, V.J., Davis, T.P., 1999. The effect of halogenation on blood-brain barrier permeability of a novel peptide drug. Peptides, 20, 1229-1238.

Gluz, O., Liedtke, C., Gottschalk, N., Pusztai, L., Nitz, U., Harbeck, N., 2009. Triple-negative breast cancer: current status and future directions. Annals of Oncology, 20, 1913-1927.

Greenbaum, D.C., Mackey, Z., Hansell, E., Doyle, P., Gut, J., Caffrey, C.R., Lehrman, J., Rosenthal, P.J., McKerrow, J.H., Chibale, K., 2004. Synthesis and Structure-Activity Relationships of Parasiticidal Thiosemicarbazone Cysteine Protease Inhibitors against Plasmodium falciparum, Trypanosoma brucei, and Trypanosoma cruzi. Journal of Medicinal Chemistry, 47, 3212-3219.

Groot, M.T., Baltussen, R., Uyl-de Groot, C.A., Anderson, B.O., Hortobagyi, G.N., 2006. Costs and Health Effects of Breast Cancer Interventions in Epidemiologically Different Regions of Africa, North America, and Asia. The Breast Journal, 12, S81-S90.

Hammond, M.E., Hayes, D.F., Dowsett, M., Allred, D.C., Hagerty, K.L., Badve, S., Fitzgibbons, P.L., Francis, G., Goldstein, N.S., Hayes, M., Hicks, D.G., Lester, S., Love, R., Mangu, P.B., McShane, L., Miller, K., Osborne, C.K., Paik, S., Perlmutter, J., Rhodes, A., Sasano, H., Schwartz,J .N., Sweep, F.C.G., Taube, S., Torlakovic, E.E., Valenstein, P., Viale, G., Visscher, D., Wheeler, T., Williams, R.B., Wittliff, J.L., Wolff, A.C., 2010. American Society of Clinical Oncology/College of American Pathologists Guideline Recommendations for Immunohistochemical Testing of Estrogen and Progesterone Receptors in Breast Cancer. Journal of Clinical Oncology, 28, 2784-2795.

Hernandes, M., Cavalcanti, S., Moreira, D., de Azevedo Junior, W., Leite, A., 2010. Halogen Atoms in the Modern Medicinal Chemistry: Hints for Drug Design. Current Drug Targets, 11, 303-314.

Jordan,V.C., 1988. The development of tamoxifen for breast cancer therapy: A tribute to the late Arthur L. Walpole. Breast Cancer Research and Treatment, 11, 197-209.

Knott, M.G., Mkwananzi, H., Arendse, C.E., Hendricks, D.T., Bolton, J.J., Beukes, D.R., 2005. Plocoralides A-C, polyhalogenated monoterpenes from the marine alga Plocamium corallorhiza. Phytochemistry (Elsevier), 66, 1108-1112.

Konig, G.M., Wright, A.D., Linden, A., 1999. Plocamium hamatum and its monoterpenes: chemical and biological investigations of the tropical marine red alga. Phytochemistry, 52, 1047-1053.

Koop, D.R., 1992. Oxidative and reductive metabolism by cytochrome P450 2E1. FASEB Journal, 6, 724-730.

Lawson, J; M.Sc thesis; Analysis of the anti-cancer activity of novel indigenous algal compounds in breast cancer: Towards the development of a model for screening anti-cancer stem cell activity (2009).

McRae, J., Yang, Q., Crawford, R., Palombo, E., 2007. Review of the methods used for isolating pharmaceutical lead compounds from traditional medicinal plants. The Environmentalist, 27, 165-174.

Metrangolo, P., Resnati, G., 2008. Halogen Versus Hydrogen. Science, 321, 918-919.

Metrangolo, P., Resnati, G., 2001. Halogen Bonding: A Paradigm in Supramolecular Chemistry. Chemistry. A European Journal, 7, 2511-2519.

Metzger Filho, O., Saini, K.S., Azim Jr, H.A., Awada, A., 2010. Prevention and management of major side effects of targeted agents in breast cancer. Critical Reviews in Oncology/Hematology.

Molinari, G., 2009. Natural Products in Drug Discovery: Present Status and Perspectives Pharmaceutical Biotechnology. In: Guzmaín, C.A., Feuerstein, G.Z. (Eds.), Springer New York, 13-27.

Monforte, A.M., Logoteta, P., Ferro, S., Luca, L.D., Iraci, N., Maga, G., Clercq, E.D., Pannecouque, C., Chimirri, A., 2009. Design, synthesis, and structure-activity relationships of 1,3-dihydrobenzimidazol-2-one analogues as anti-HIV agents. Bioorganic and Medicinal Chemistry, 17, 5962-5967.

Nabholtz, J.M., Buzdar, A., Pollak, M., Harwin, W., Burton, G., Mangalik, A., Steinberg, M., Webster, A., von Euler, M., for the Arimidex Study Group, 2000. Anastrozole Is Superior to Tamoxifen as First-Line Therapy for Advanced Breast Cancer in Postmenopausal Women: Results of a North American Multicenter Randomized Trial. Journal of Clinical Oncology, 18, 3758-3767.

Neumann, C.S., Fujimori, D.G., Walsh, C.T., 2008. Halogenation Strategies In Natural Product Biosynthesis. Chemical Biology. (Cambridge, MA, U. S.), 15, 99-109.

Perez, E.A., 2009. Microtubule inhibitors: Differentiating tubulin-inhibiting agents based on mechanisms of action, clinical activity, and resistance. Molecular Cancer Therapeutics, 8, 2086-2095.

Popat, S., Smith, I.E., 2006. Breast cancer. Update on Cancer Therapeutics, 1, 187-210.

Rakha, E.A., Chan, S., 2011. Metastatic Triple-negative Breast Cancer. Clinical Oncology, 23, 587-600.

Rakha, E.A., El-Sayed, M.E., Green, A.R., Lee, A.H.S., Robertson, J.F., Ellis, I.O., 2007. Prognostic markers in triple-negative breast cancer. Cancer, 109, 25-32.

Remak, E., Brazil, L., 2004. Cost of managing women presenting with stage IV breast cancer in the United Kingdom. British Journal of Cancer, 91, 77-83.

Rivera, E., 2010. Management of Metastatic Breast Cancer: Monotherapy Options for Patients Resistant to Anthracyclines and Taxanes. American Journal of Clinical Oncology, 33.

Stallard, M.O., Faulkner, D.J., 1974. Chemical constituents of the digestive gland of the sea hare Aplysia californica. I. Importance of diet. Comparative Biochemistry and Physiology. B, 49, 25-35.

Stamp, N., 2003. Out of the Quagmire of Plant Defense Hypotheses. The Quarterly Review of Biology, 78, 23-55.

Tan, A.R., Rubin, E.H., Walton, D.C., Shuster, D.E., Wong, Y.N., Fang, F., Ashworth, S., Rosen, L.S., 2009. Phase I Study of Eribulin Mesylate Administered Once Every 21 Days in Patients with Advanced Solid Tumors. Clinical Cancer Research, 15, 4213-4219.

Towle, M.J., Salvato, K.A., Budrow, J., Wels, B.F., Kuznetsov, G., Aalfs, K.K., Welsh, S., Zheng, W., Seletsky, B.M., Palme, M.H., Habgood, G.J., Singer, L.A., DiPietro, L.V., Wang, Y., Chen, J.J., Quincy, D.A., Davis, A., Yoshimatsu, K., Kishi, Y., Yu, M.J., Littlefield, B.A., 2001. In vitro and in vivo anti-cancer activities of synthetic macrocyclic ketone analogues of halichondrin B. Cancer Research, 61, 1013-1021.

Uemura, D., Takahashi, K., Yamamoto, T., Katayama, C., Tanaka, J., Okumura, Y., Hirata, Y., 1985. Norhalichondrin A: an antitumor polyether macrolide from a marine sponge. Journal of the American Chemistry Society, 107, 4796-4798.

Veronesi, U., Boyle, P., Goldhirsch, A., Orecchia, R., Viale, G., 2005. Breast cancer. The Lancet, 365, 1727-1741.

William, R., 2000. The role of natural products in a modern drug discovery program. Drug Discovery Today, 5, 39-41.

Zhang, Z.Y., King, B., Pelletier, R., Wong, Y., 2008. Delineation of the interactions between the chemotherapeutic agent eribulin mesylate (E7389) and human CYP3A4. Cancer Chemotherapy and Pharmacology, 62, 707-716.

CHAPTER TWO:

Isolation of halogenated monoterpenes from *Plocamium cornutum and Plocamium corallorhiza*

2.1 Introduction

The family Plocamiaceae (order Plocamiales, phylum Rhodophyata) is well known for producing a wide variety of halogenated terpenes with diverse biological activities (König et al., 1999). Interest in these natural products has increased since the discovery of halomon (**1.8**) (Scheme 2.1), an acyclic monoterpene, that demonstrated selective anti-tumour activity (Fuller et al., 1994). The more than 100 halogenated monoterpenes from the genus *Plocamium* appear to originate *via* halogenation reactions of either myrcene (**2.1**) or ocimene (**2.2**) monoterpene units (Kladi et al., 2005; Wise et al., 2002) whose precursor is geranyl diphosphate (Scheme 2.1).

Halogenation reactions in the marine environment are thought to be facilitated mainly by vanadium–dependent haloperoxidases that catalyse oxidation of halides (Br^- and Cl^-) and their incorporation into organic molecules in the presence of hydrogen peroxide (Carter-Franklin and Butler, 2004; Neumann et al., 2008; Ohsawa et al., 2001; Winter and Moore, 2009). Other proposed mechanisms include use of Heme-Fe haloperoxidases and Flavin-Dependent halogenases to aid in halogenation of terpene molecules. In rare instances, direct halide incorporation can occur at electrophilic sites on the molecule. Such chemical modifications have enabled species to adapt to a given environment and give rise to a series of compounds that are worthwhile exploring for biological activity.

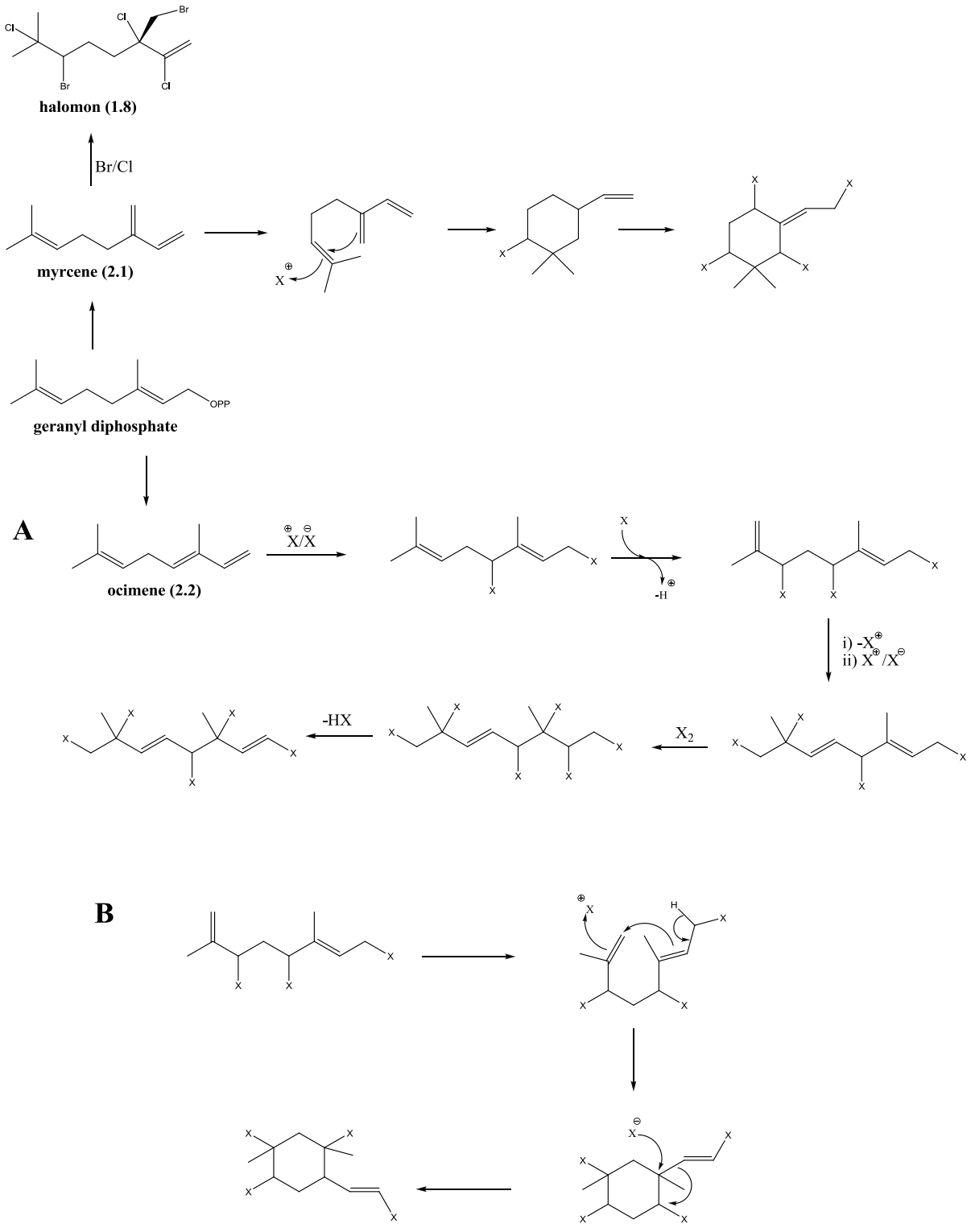

Scheme 2.1: Proposed biosynthesis of cyclic (A) and acyclic (B) halogenated monoterpenes (Wise et al., 2002)

2.1.1 Biological activity of acyclic and cyclic halogenated monoterpenes

Interestingly, chlorinated and brominated natural products are more common than iodinated ones. The importance of the halogen substituent has been confirmed in well-known biologically active natural products e.g., vancomycin, salinosporamide A, neomangicol A and B (Neumann et al., 2008).

Numerous studies have been conducted to determine the biological activities of halogenated monoterpenes. The functions of these metabolites in nature, are related to their ecological roles e.g., herbivore deterrence, anti-algal and anti-fouling activities (König et al., 1999). *In-vitro* studies have demonstrated other biological activities that include anti-microbial, antifungal, ichthyotoxic, antiplasmodial and cytotoxic activities (Kladi et al., 2005). As briefly discussed in chapter 1, many of the halogenated monoterpenes from the genus *Plocamium* have shown potential as sources of hit or lead compounds that can be used in research and pharmaceutical industries. To mention a few, several cyclic and acyclic polyhalogenated monoterpenes have been isolated from *P. violaceum*, in particular violacene (**2.3**) and plocamene B (**2.4**) that have been reported to show insecticidal activity and growth inhibitory activity against mosquito larvae (Crews and Kho, 1975). Plocamene D (**2.5**) and Plocamene E (**2.6**) from *P. cartilagineum* have exhibited the same inhibitory effect towards mosquito larvae at comparable levels to commercial products (Kladi et al., 2005). Two polyhalogenated acyclic metabolites (**2.7**) and (**2.8),** once found in the digestive gland of sea hare *Aplysia californica* (Ireland et al., 1976), have been isolated from *P. pacificum*. The two metabolites (**2.7** and **2.8**) have displayed moderate anti-fungal activities against *Cladosporium cucumerium.* Plocoralides B (**2.9**) and C (**2.10**) also once found in the digestive gland of sea hare *Aplysia californica,* have been isolated from *P. corallorhiza* and possess moderate activity against an oesophageal cancer cell line WHCO1 (Knott et al., 2005). Compound **2.8** has also been isolated from *P. costatum* and showed potential anti-fouling properties (El Gamal, 2011). Halogenated monoterpenes therefore possess a wide range of activities that are promising in the development of new drug treatments.

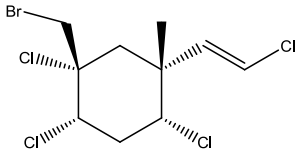

2.3

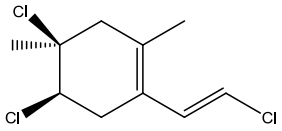

2.4

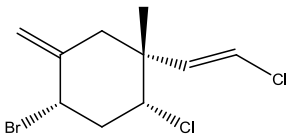

2.5

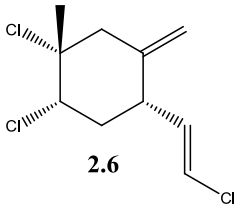

2.6

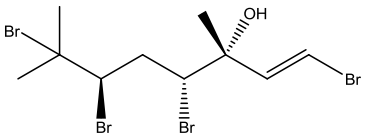

2.7

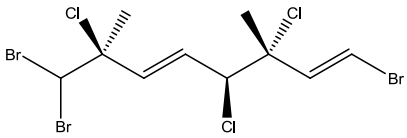

2.8

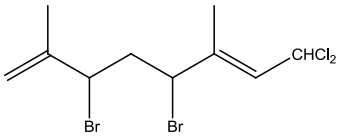

2.9

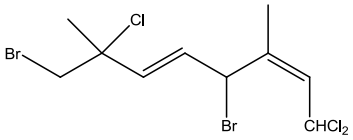

2.10

2.1.2 Halogenated monoterpenes from South African *Plocamium* spp.

Bioactivity guided isolation has been key in accessing metabolites that possess biological activity from natural products. Halogenated monoterpenes from South African marine algae; *P. cornutum*, *P. corallorhiza* and *P. suhrii* have shown promising antiplasmodial activities against a chloroquine sensitive strain of *Plasmodium falciparum* (Afolayan et al., 2009) and cytotoxic activities towards an oesophageal cancer cell line (WHCO1). The cytotoxicity has been demonstrated to be comparable to that of *cis*-platin, a known chemotherapeutic drug (Antunes et al., 2011). However minute quantities of these metabolites in nature always prompt for continuous extraction and isolation for further research to be conducted. Tables 2.1, 2.2 and 2.3 list the secondary metabolites that have been isolated by our research group from *P. cornutum*, *P. corallorhiza* and *P. suhrii* collected along the South African south-east coast line.

Table 2.1: Halogenated monoterpenes previously isolated from *P. cornutum* [a, b]

No.	Structure	No.	Structure
2.11	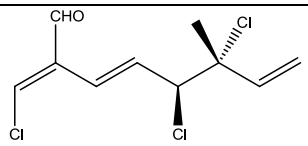	**2.14**	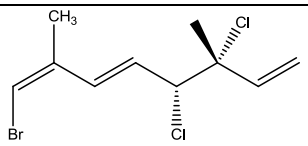
2.12	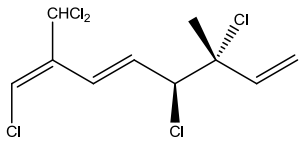	**2.15**	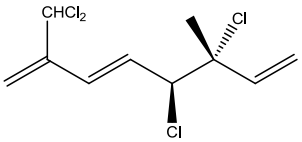
2.13	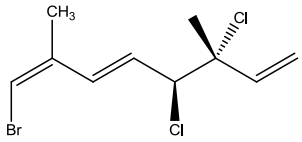		

[a] Afolayan, 2008
[b] Afolayan et al., 2009

Table 2.2: Halogenated monoterpenes previously isolated from *P. suhrii* [a]

No.	Structure	No.	Structure
2.16	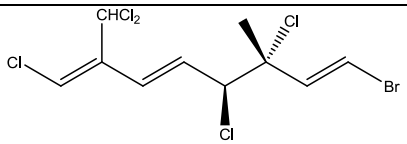	**2.19**	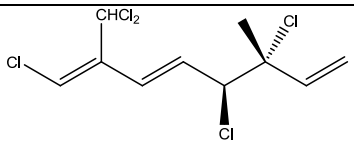
2.17	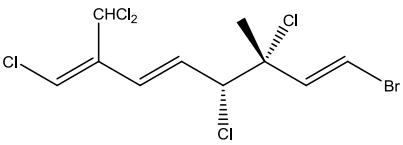	**2.20**	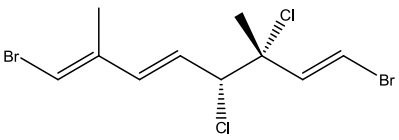
2.18	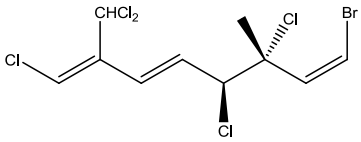	**2.21**	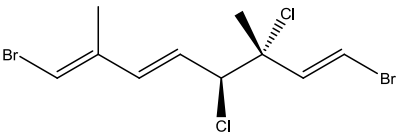

[a] Antunes et al., 2011

Secondary metabolites from *P. cornutum* and *P. suhrii* are closely related, with the only difference being the presence of a terminal bromine at position 1 in metabolites from *P. suhrii*. *P. corallorhiza* show distinct differences when compared to the previous species. In particular, the presence of *gem*-dichloro- or aldehyde moieties at position 1 is characteristic of the main *P. corallorhiza* metabolites.

Table 2.3: Halogenated monoterpenes previously isolated from *P. corallorhiza* [a-e]

No.	Structure	No.	Structure
2.9	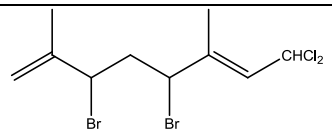	**2.29**	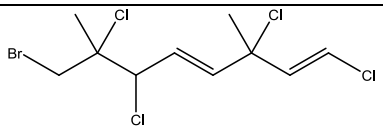
2.10	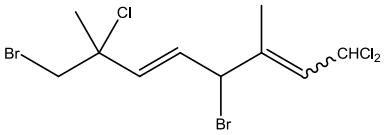	**2.30**	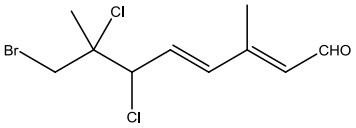
2.22	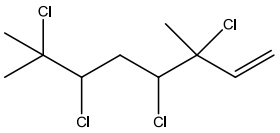	**2.31**	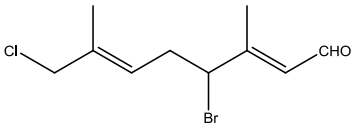
2.23	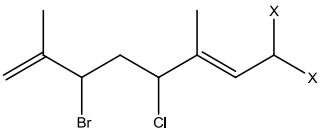 x = Cl or Br	**2.32**	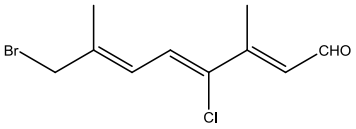
2.24	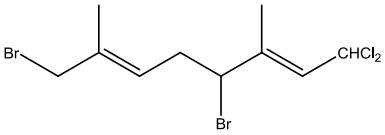	**2.33**	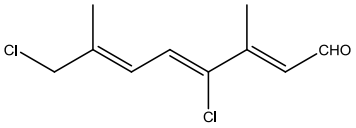
2.25	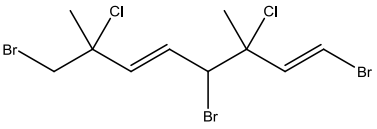	**2.34**	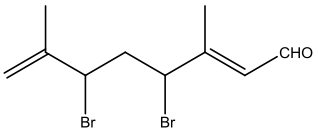
2.26	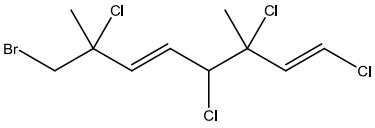	**2.35**	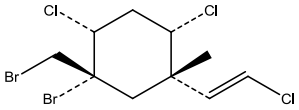
2.27	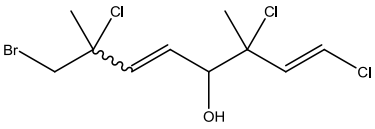	**2.36**	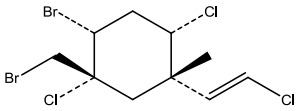
2.28	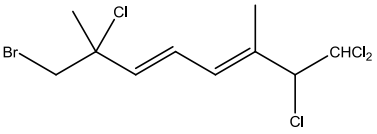	**2.37**	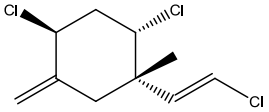

[a] Knott, 2003
[b] Mkwananzi, 2005
[c] Mann, 2008
[d] Knott et al., 2005
[e] Mann et al., 2007

2.1.3 Chapter Aims

This work forms part of a larger multidisciplinary project whose aim is to identify potential drug leads or drug targets for the treatment of breast cancer. Screening of a small library of natural products identified a number of halogenated monoterpenes as potential leads (de la Mare et al., 2012). With the need to further explore the chemical and anti-cancer activities of these active halogenated monoterpenes, the main objectives of this part of the project were to:

a) Identify reliable sources of halogenated monoterpenes by investigating geographical variations of metabolites from selected collection sites.
b) Extract and isolate target compounds from *P. corallorhiza* and *P. cornutum* for further studies.

A B

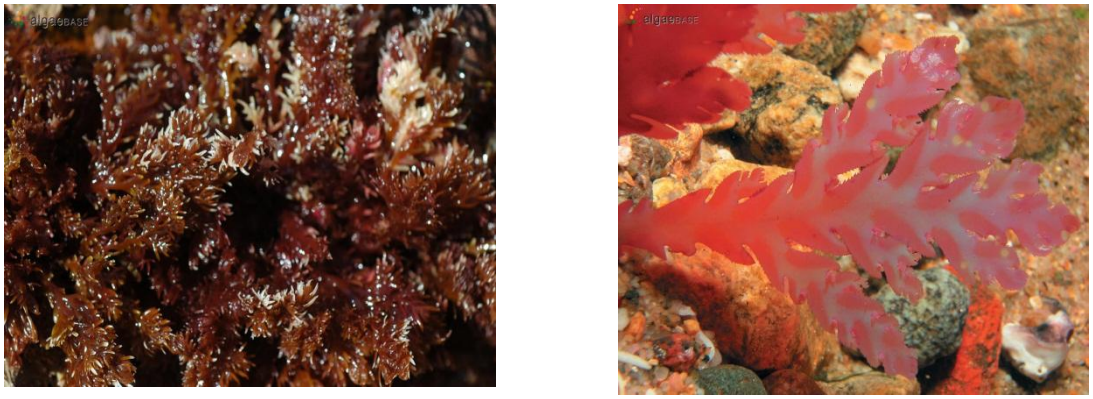

Figure 2.1: Photographs of A) *P. cornutum* B) *P. corallorhiza*
(Photographs adopted from http://www.algaebase.org/search/species/detail/?species_id=2831, http://www.algaebase.org/search/species/detail/?species_id=2830. Web accessed: 19 Dec 2011)

2.2 Results and discussion

Initial attempts to isolate larger quantities of halogenated monoterpenes from South African seaweeds have been frustrated by the apparent geographical variation and instability of these compounds. We therefore developed a simple, rapid, small-scale (*ca.* 1 g of wet alga), ultra-sound assisted extraction method for the rapid screening of crude extracts of algae. This method provides sufficient organic extract for analysis by ^{1}H NMR spectroscopy and or GC-MS analysis. Although the GC methods are more sensitive, we favoured the use of ^{1}H NMR spectroscopy because i) the halogenated monoterpene aldehydes in particular, degrade under conditions employed for GC-FID or GC-MS and ii) we were mainly interested in compounds that were present in large enough amounts (several milligram quantities) to allow their isolation and chemical and biological characterization.

In the following sections, we consider the effect of transit times (from collection site to laboratory) and solvents on metabolic profiles, and intra- and inter-site variation of halogenated monoterpenes.

2.2.1 Effect of transit times and solvents on the metabolite profiles of *P. corallorhiza*[1]

Before addressing issues of geographical and or seasonal variation of metabolites, we had to consider the possibility of some metabolites being artefacts of the extraction process. Although the chemical reactivity of halogenated monoterpenes have not been studied in detail, it is likely that these compounds may undergo dehydrohalogenation, halogen substitutions and rearrangement of halogen atoms.

Usually, algal specimens are collected from sites 70-150 km away from the laboratory. One site (Port Alfred) was selected for this study. Samples were collected, flash frozen on-site in liquid nitrogen and crushed immediately. Portions of the crushed alga (~ 1 mL) were transferred to 10 ml centrifuge tubes and immediately extracted with four different solvents: CH_2Cl_2-MeOH (A), no solvent (B), ethanol (C) and acetone (D).[2] Sample B was treated in the same way as A except that it was first stored on ice (during transportation to the lab) before being extracted. All samples were analysed by ^{1}H NMR spectroscopy in duplicate. The ^{1}H NMR profiles (δ 5 – 11 ppm)[3] of the crude extracts (A, C and D) (Figure 2.2) were

[1] This could not be done for the other *Plocamium* spp because their collection sites were too far from the lab.
[2] Solvents were added to the samples at the site of collection and stored on ice during transport to the laboratory (1-2 h).
[3] This region shows the most important differences in the spectra.

almost identical, indicating that no one solvent is more selective than the other. Interestingly, extract B displayed the presence of aldehyde signals at ~ δ 9.85 and δ 10.20 that are absent in the other extracts, signalling more metabolites extracted with this solvent system. We have not made any attempts to identify compounds in these extracts. However, a preliminary analysis indicates that they are different to those previously reported from this algae. Although outside the scope of this study, the chemical reactivity (stability) of these compounds may be worth investigating.

As for the effect of transit times on metabolite profiles, the ^{1}H NMR spectra obtained for A and B showed differences though similar solvent systems had been used. Sample B was extracted at the laboratory and qualitatively, more metabolites were extracted from this fraction. The differences can be attributed to levels of moisture in the samples that masked the amount of material that can be extracted in sample A though further investigation is required. It was therefore concluded that transit times have a significant effect on metabolite profiles. This may be overcome by "pickling" the algae in a suitable solvent during transportation to the lab.

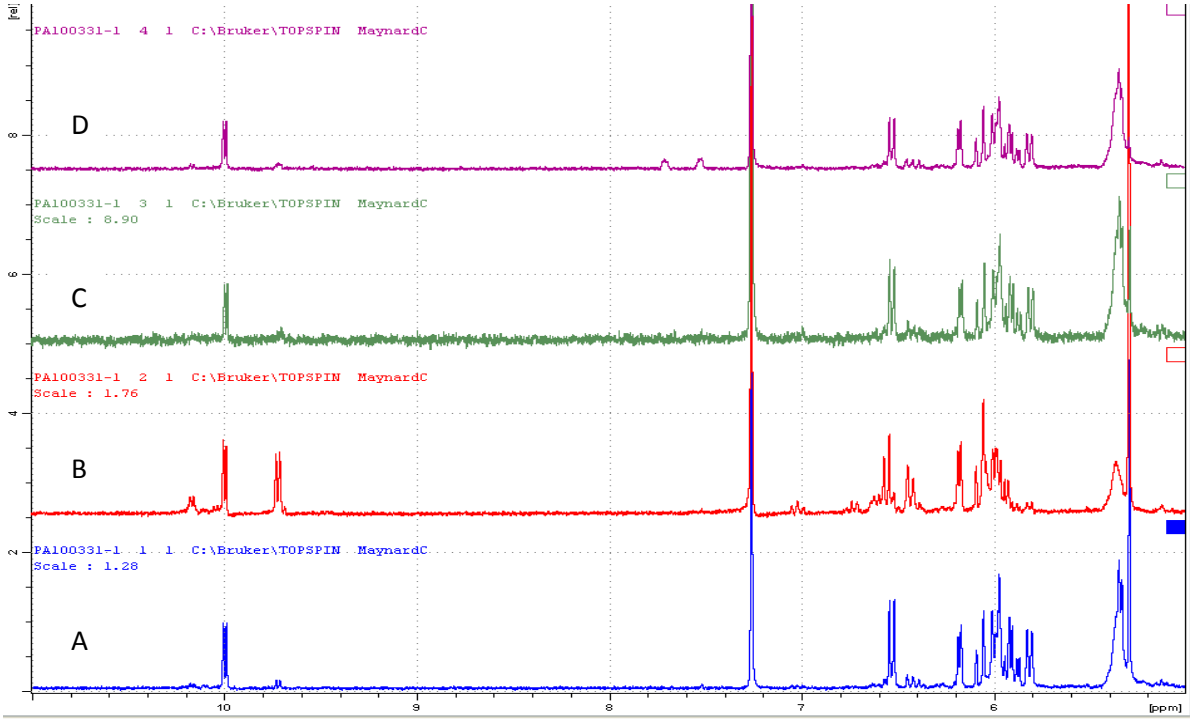

Figure 2.2: ^{1}H NMR profiles (400 MHz, $CDCl_3$) of *P. corallorhiza* crude extracts using different solvents

(A)- DCM/MeOH 2:1 (B)- DCM/MeOH 2:1 after storing on ice (C)-ethanol (D)-acetone

2.2.2 Intra- and inter-site variation of secondary metabolites from *Plocamium* spp

As previously highlighted (chapter 1), secondary metabolites are produced in response to environmental stimuli and metabolic profiles may differ from site to site. With our continual search for halogenated monoterpenes, assessment of metabolic profiles of *Plocamium* spp distributed along the South African south-east coast became essential in determining actual locations that can be visited for recollection and isolation of specific secondary metabolites for further research. Geographical variations of metabolites were conducted at three sites: Kenton-on-Sea, Noordhoek (Port Elizabeth) and Port Alfred, taking into account intra-site and inter-site variations.

Small scale ultra-sound assisted extractions were carried out on specimens of *P. corallorhiza* collected from the three sites mentioned above. Algal samples were collected during the same period, stored on ice during transport to the lab and frozen, only to be partially thawed just before extraction. ^{1}H NMR spectra of CH_2Cl_2-MeOH (2:1) extracts of individual algae were acquired on a 600 MHz Bruker NMR spectrometer and compared with spectra of known compounds previously isolated from *P. corallorhiza.*

Before comparing geographical variations of metabolites one needs to ensure that there are no intra-site variations. Individual plants were collected at each site and extracted and analysed separately. When considering the ^{1}H NMR profiles of the individual plants collected from Noordhoek, at least three "chemotypes" can be observed, A & B, C & D and E (Figure 2.3)**.** The most pronounced differences could be observed in the downfield regions of the spectra from δ 9.6 – δ 10.2. Spectra A, B and E displayed ^{1}H NMR signals at δ 9.7-10.05 which are characteristic of metabolites containing an aldehyde functionality. Spectra C and D contained only two main aldehyde signals at δ 10.05.

Compared to the Noordhoek collection, *P. corallorhiza* from Port Alfred and Kenton-on-Sea[4] demonstrated minimal intra-site variations. Figure 2.4 shows spectra of different samples collected at Port Alfred containing three major metabolites. Several other metabolites with aldehyde moieties were also present but in minute quantities due to the weak signal intensities observed in the region δ 10.00 and δ 10.20 (Figure 2.4).

[4] Spectra for Kenton-on-Sea for intra-site variations are available in the supplementary data

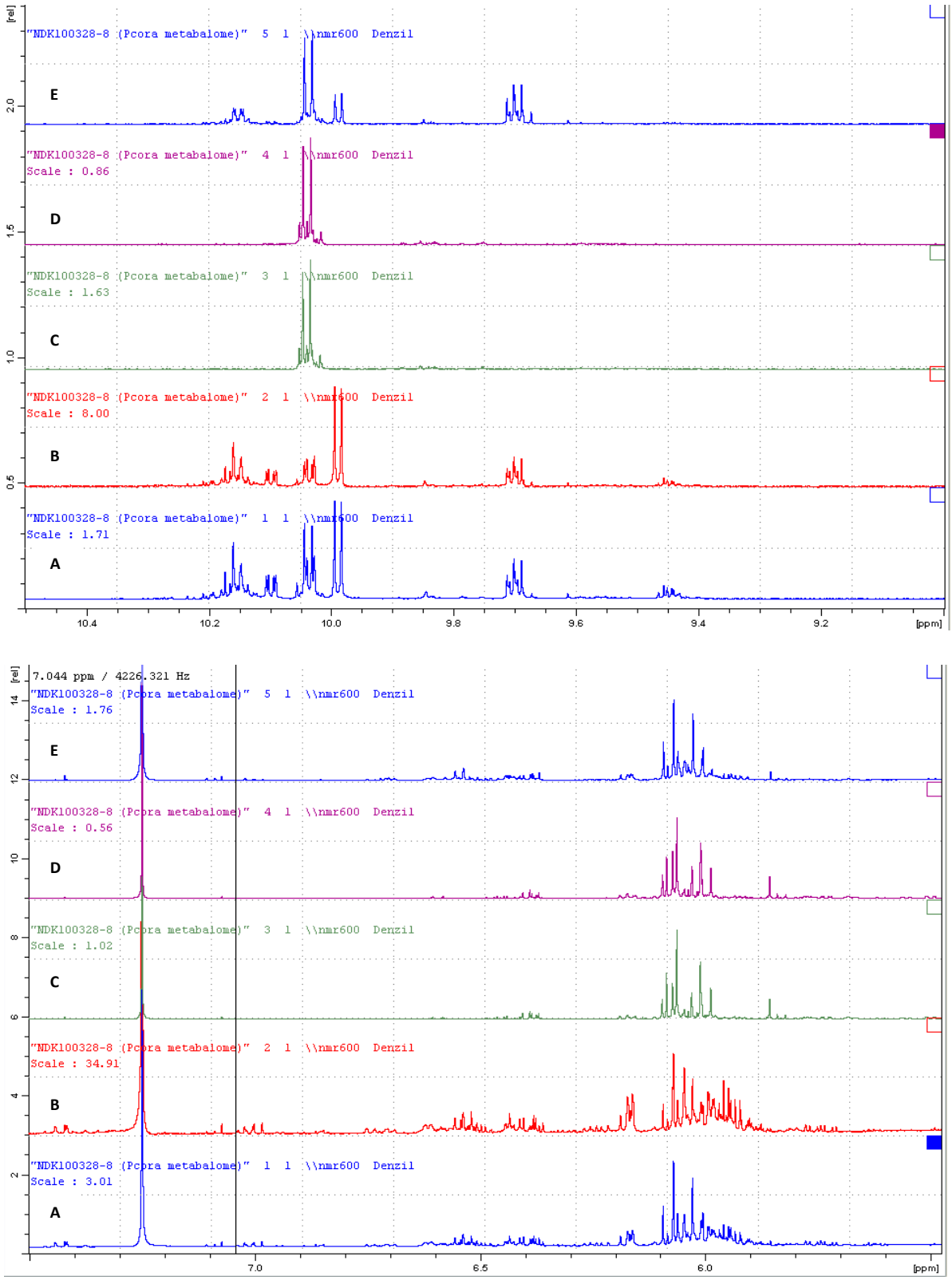

Figure 2.3: Expansions of ^{1}H NMR profiles (600 MHz, $CDCl_3$) of crude extracts (A-E) obtained from individual *P. corallorhiza* plants from Noordhoek (Port Elizabeth, South Africa). Top: 9 - 10.6 ppm, bottom: 5.5 – 7.5 ppm

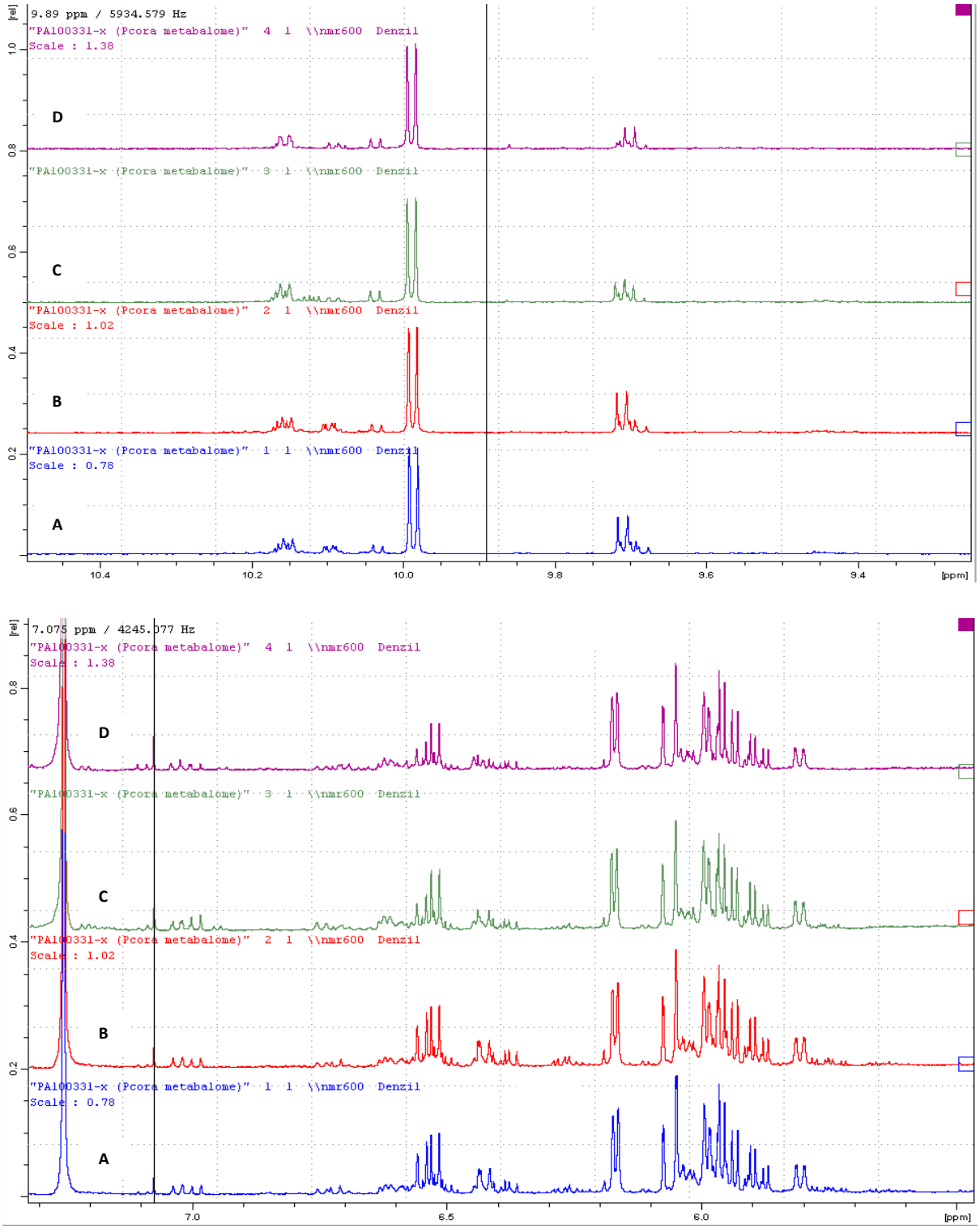

Figure 2.4: Expansions of ^{1}H NMR profiles (600 MHz, $CDCl_3$) of crude extracts (A-D) obtained from individual *P. corallorhiza* plants collected from Port Alfred, South Africa. Top: 9.25 – 10.5 ppm, bottom: 5.5 – 7.3 ppm

Such intra-site variations in metabolite profiles especially from *P. corallorhiza* from Noordhoek (Port Elizabeth) nullified the purpose of doing an inter-site variation study. Reasons for chemical composition differences are not clear, and a more in depth study might be required taking into consideration environmental factors of respective pools where the algae were collected e.g., water tonicity, bacterial content, stage of development of the specimen etc. Determination of specific sites that can be visited to collect samples that yield previously isolated molecules became relatively impossible as metabolite profiles differed in samples collected from the same site. The search for metabolites would therefore rely on trial and error in collecting samples, presenting with challenges in accessing these compounds for further work.

The same study was conducted on *P. cornutum*, analysing specimens from Kalk Bay (Cape Town), Kenton-on-Sea, and Noordhoek (Port Elizabeth). Fresh algal samples of *P. cornutum* could not be located at Port Alfred. Small scale ultra-sound assisted extractions yielded crude extracts that were analysed by ^{1}H NMR spectroscopy, and attempts were made to identify the compounds present in *P. cornutum* extracts (Figure 2.5).

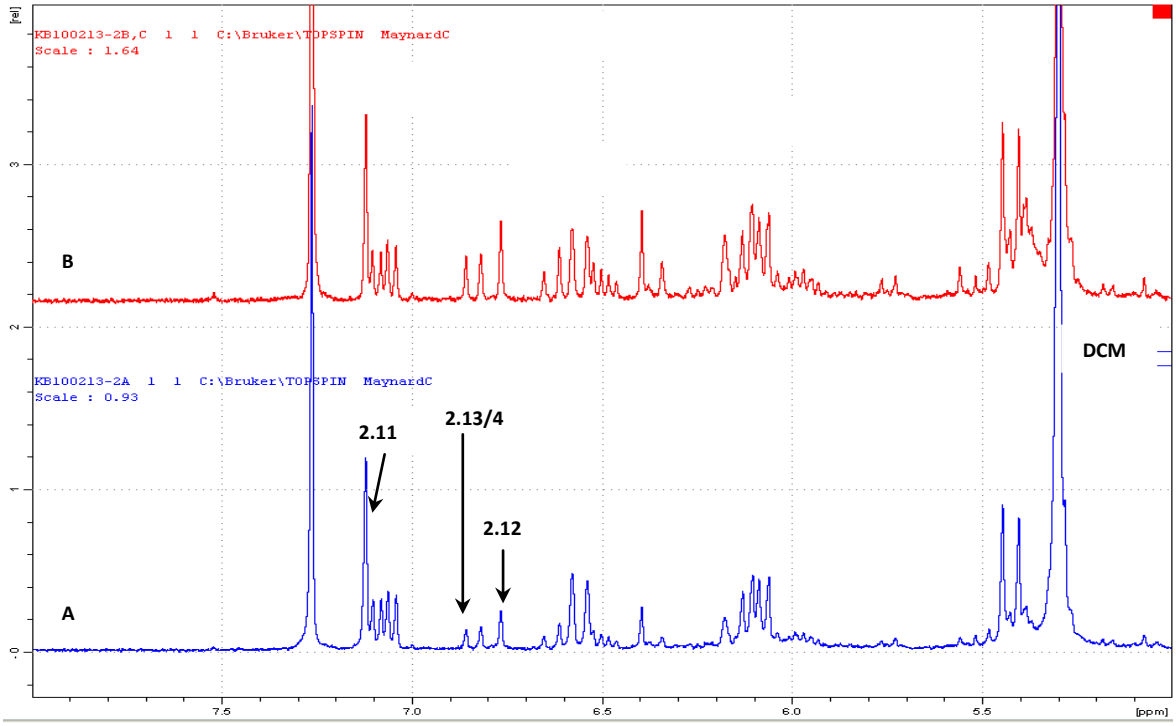

Figure 2.5: Expansion of ^{1}H NMR profiles (400 MHz, $CDCl_3$) of crude extracts (A & B) obtained from individual *P. cornutum* plants at Kalk Bay, Cape Town (South Africa)[5]

[5] Full ^{1}H NMR spectra for *P. cornutum* extracts collected from Kalk bay are present in the supplementary data.

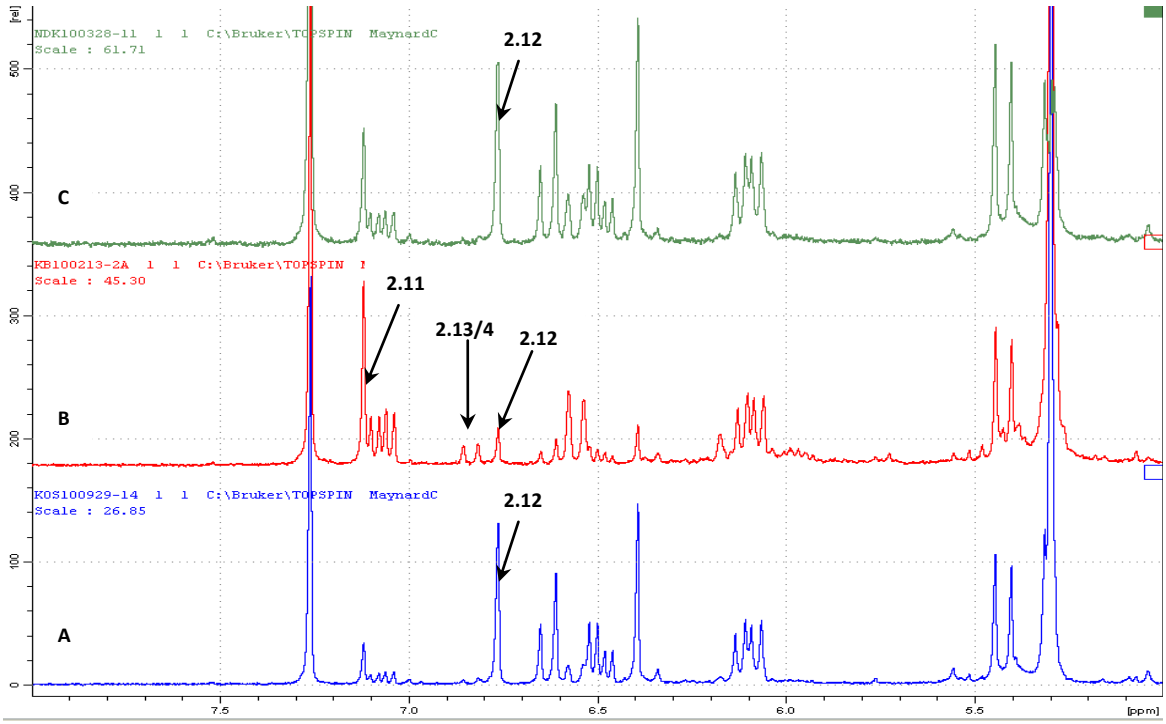

Figure 2.6: Expansion of ^{1}H NMR profiles (400 MHz, $CDCl_3$) of crude extracts (A-C) obtained from *P. cornutum* plants collected at Kenton-on-Sea (A), Kalk Bay (Cape Town) (B) and Noordhoek (Port Elizabeth) (C)[6]

Intra-site variation studies conducted on specimen collected from Kalk Bay (Cape Town) showed insignificant ^{1}H NMR differences (Figure 2.6). No variation was observed in the metabolite profiles. The crude extracts however showed compound **2.11** as the major metabolite due to the intense signals at ~ δ 9.0 and ~ δ 7.1 in comparison with the other peaks. Compounds **2.12 – 2.14** however existed in minute quantities.

An inter-site variation study was carried out with samples collected from Kalk Bay (Cape Town), Kenton-on-Sea and Noordhoek (Port Elizabeth). The ^{1}H NMR spectra of the crude extracts displayed differences in the region δ 5.5 – 7.5 (Figure 2.7). *P. cornutum* from Kenton-on-Sea and Noordhoek (Port Elizabeth) showed the presence of two main metabolites, compound **2.11** and **2.12** (Figure 2.7), with **2.12** being predominately abundant especially in specimen from Kenton-on-Sea. This was noted by the difference in signal intensities at ~ δ 6.8 and ~ δ 9.0 for compound **2.12** and **2.11** respectively. Samples from Noordhoek (Port Elizabeth) showed that compound **2.11** was also present in fairly large amounts but **2.12** still being abundant.

[6] Full ^{1}H NMR spectra for *P. cornutum* extracts collected from Kalk bay are present in the supplementary data.

Four metabolites (**2.11-2.14**) were identified in crude extracts from Kalk Bay, as previously discussed and **2.11** was the major metabolite with the others in diminished amounts. Two additional peaks were observed on the ^{1}H NMR spectrum at ~ δ 7.0 corresponding to compounds **2.13** and **2.14**. These signals were absent in extracts from Kenton-on-Sea and Noordhoek (Port Elizabeth). Compound **2.11**, was however the most abundant metabolite in Kalk Bay samples, judging by the intensity of the signal at ~ δ 9.0, in comparison to the others. Inter-site variations in metabolite profiles were noted favouring Kalk Bay (Cape Town) as a good source for a wider range of metabolites from *P. cornutum.* Isolation of either compound **2.11** or **2.12** could be carried out on algal samples from Kenton-on-Sea or Noordhoek (Port Elizabeth).

The main purpose of this study was to identify specific sites that will allow for more focused collection strategies in order to access those metabolites of interest for further chemical and biological studies. It is obvious that the situation is much more complex than what was initially anticipated. Our current knowledge can be summarised as follows:

- Metabolite profiles for *P. corallorhiza* change over a period of a few hours after collection
- Although there is some consistency in metabolite profiles from different collection sites, *P. corallorhiza* from Noordhoek shows significant intra-site variation
- *P. cornutum* also shows significant inter-site variation in metabolite profiles but this is mainly due to different concentrations of metabolites

2.2.3 Isolation and characterization of halogenated monoterpenes from *P. cornutum*

P. cornutum (KB100213-1) was collected from Kalk Bay (Cape Town) and extracted in CH_2Cl_2: MeOH (2:1) after soaking in MeOH for 1 h. The crude extract (Figure 2.8) was fractionated by column chromatography to give 9 fractions of increasing polarity (Scheme 2.2). Fraction B was further purified by column chromatography (hexane-EtOAc 95:5) to give 5 fractions (A-E) with B being compound **2.11**. Fraction A was further purified by normal phase HPLC (hexane 100%) to yield 4 metabolites (F-I) (compounds **2.12 - 2.15**) (Scheme 2.2). The different metabolites were identified by comparing their ^{1}H NMR spectra to those reported in literature.

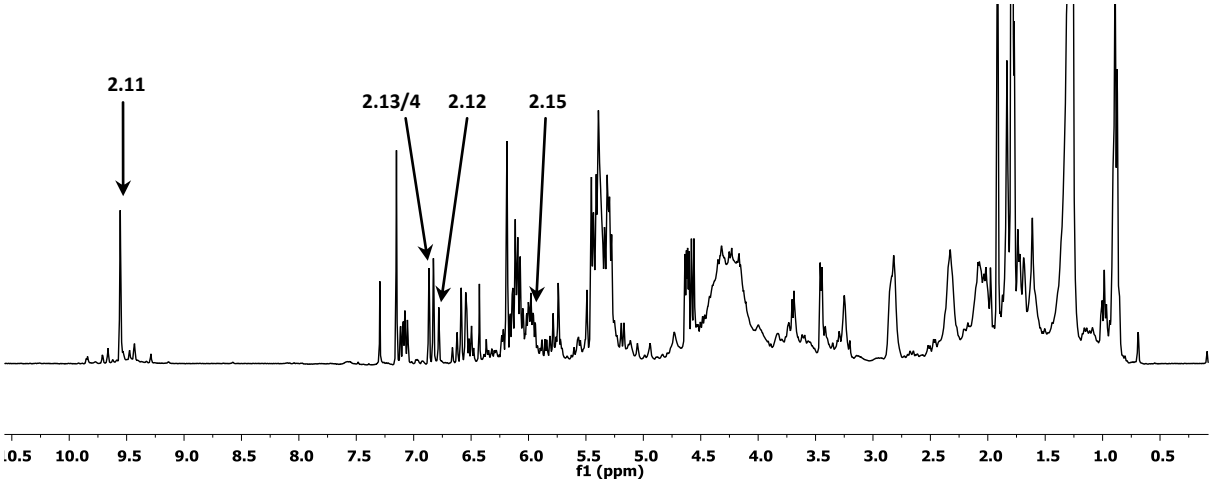

Figure 2.7: Crude ^{1}H NMR ($CDCl_3$, 400 MHz) spectrum of *P. cornutum* collected from Kalk Bay, Cape Town (South Africa)

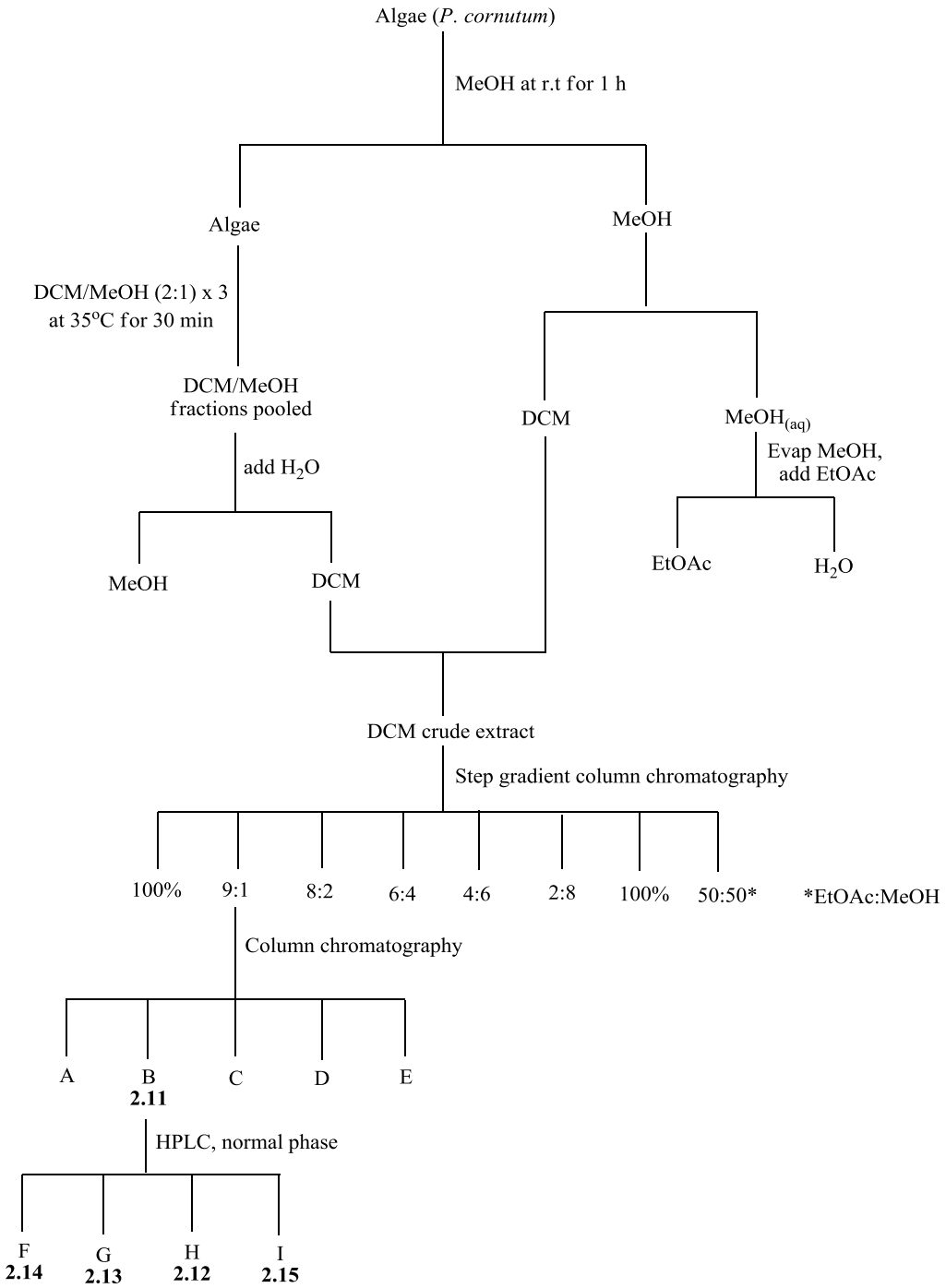

Scheme 2.2 Extraction and isolation of secondary metabolites from *P. cornutum.*[7,8]

[7] $MeOH_{(aq)}$ fractions were also pooled and extracted using EtOAc as shown above.

[8] Step gradient solvents systems are in the ratio of Hexane: EtOAc

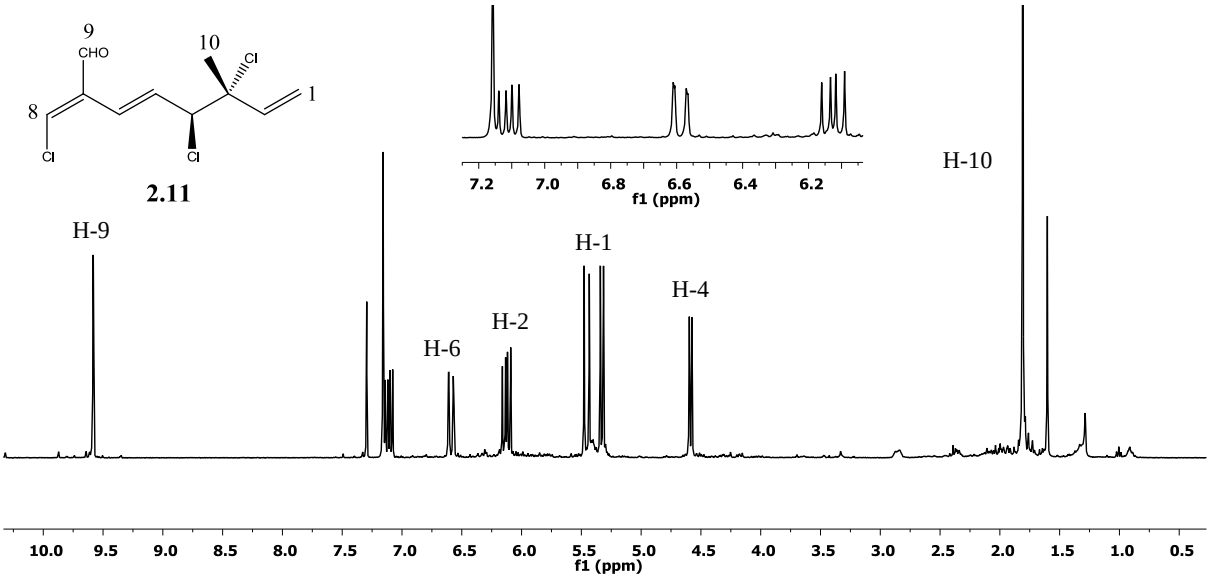

Figure 2.8: ^{1}H NMR (400 MHz, $CDCl_3$) spectrum of **2.11**

The ^{1}H NMR spectrum of **2.11** displayed two terminal methylene protons indicated by doublets at δ 5.33 (d, *J* = 10.6 Hz, H-1a) and δ 5.47 (d, *J* = 17.1, H-1b). These two protons were coupled to a methine proton at δ 6.13 (dd, *J* = 17.1, 10.6 Hz, H-2) giving a -CH=CH_2 structural motif. A doublet peak at δ 4.59 (d, *J* = 8.8 Hz, H-4) represented a halomethine functionality coupled to olefinic methine protons at δ 7.11 (dd, *J* = 15.9, 8.8 Hz, H-5). The latter was also coupled to an olefinic methine at δ 6.57 (d, *J* = 15.9 Hz, H-6) resulting in a –CH=CH-CHX substructure. A coupling constant of 15.9 Hz signified the presence of an alkene moiety with *E* geometry. A more deshielded singlet olefinic proton signal was observed at δ 7.16 (H-8), a doublet at δ 9.58 (d, *J* = 2.0 Hz, H-9) that represented a -CHO functionality and a singlet at δ 1.81 (s, H-10) corresponding to a methyl group. The above data are consistent with cartilagineal that was first isolated from *P. cartilagineum* (Crews and Kho, 1975).

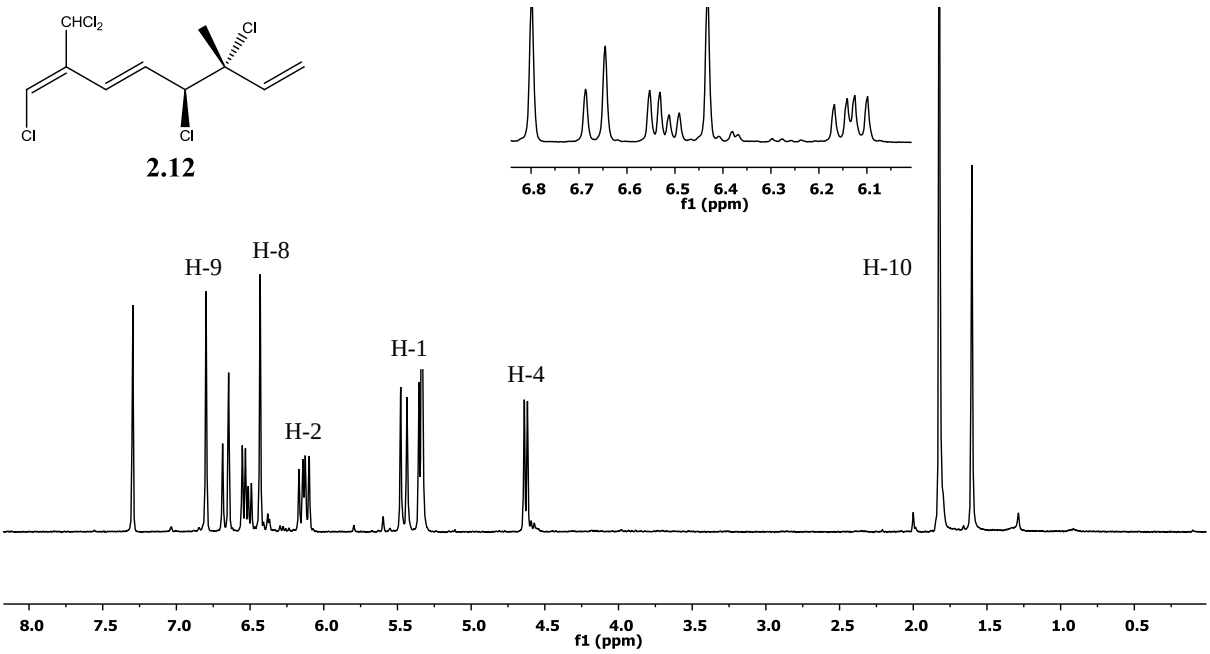

Figure 2.9: ^{1}H NMR (400 MHz, $CDCl_3$) spectrum of **2.12**

The ^{1}H NMR data for **2.12** had similar features to those of **2.11**. It showed two terminal methylene protons at δ 5.34 (d, *J* = 10.7 Hz, H-1a) and δ 5.46 (d, *J* = 17.1 Hz, H-1b) coupled to a methine proton at δ 6.13 (dd, *J* = 17.0, 10.7 Hz, H-2), a halomethine functionality at δ 4.63 (d, *J* = 8.5 Hz, H-4) coupled to olefinic methine protons at δ 6.52 (dd, *J* = 16.2, 8.5 Hz, H-5) and δ 6.67 (d, *J* = 16.3 Hz, H-6) and two more deshielded methines at δ 6.43 (s, H-8) and δ 6.80 (s, H-9). A methyl peak was also present at δ 1.82 (s, H-10). The main difference between the ^{1}H NMR spectra of **2.11** and **2.12** was the appearance of a singlet signal at δ 6.80 (s, H-9) corresponding to -$CHCl_2$ and the disappearance of the aldehyde signal at δ 9.58 (d, *J* = 2.0 Hz, H-9). The ^{1}H NMR data are consistent with compound **2.12** previously reported by Abreu and Galindro (1996).

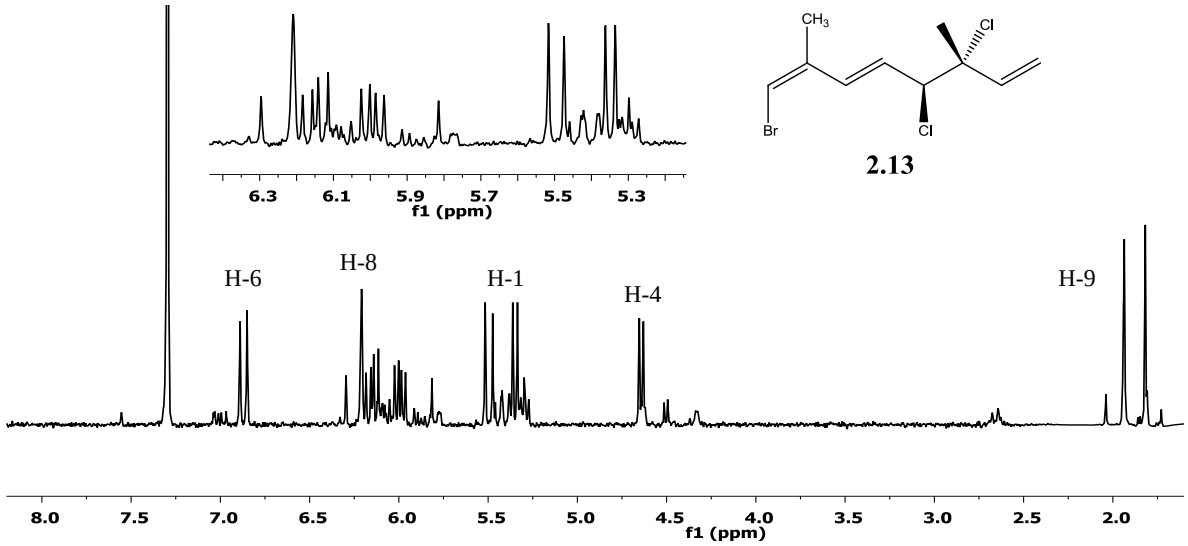

Figure 2.10: ^{1}H NMR (400 MHz, $CDCl_3$) spectrum of **2.13**

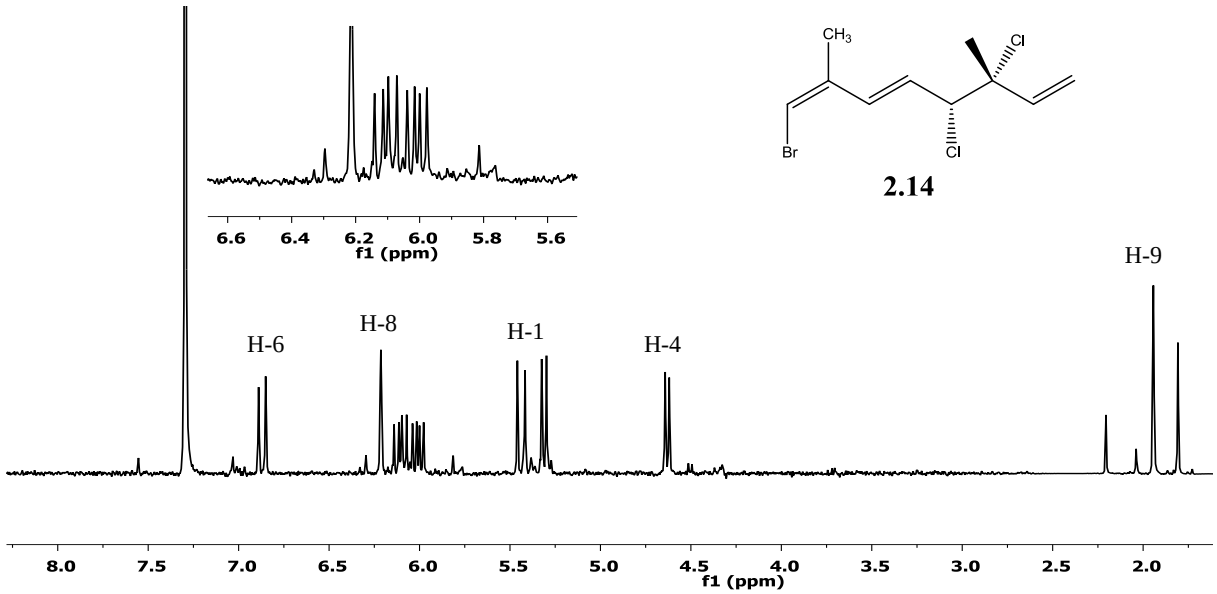

Figure 2.11: ^{1}H NMR (400 MHz, $CDCl_3$) spectrum of **2.14**

The ^{1}H NMR spectral features of **2.13** and **2.14** were also similar to those of compounds **2.11** and **2.12** with the presence of an additional methyl peak at δ 1.94 (s, H-9) in both spectra. However they lacked signals at δ 9.58 (s) and δ 6.80 (s) corresponding to -CHO and -$CHCl_2$ functionalities observed in **2.11** and **2.12** respectively. Previous studies had demonstrated the presence of diastereoisomers in extracts from *P. cornutum* and comparison of these spectra with literature confirmed the relative configuration at C-3 and C-4 (Afolayan et al., 2009).

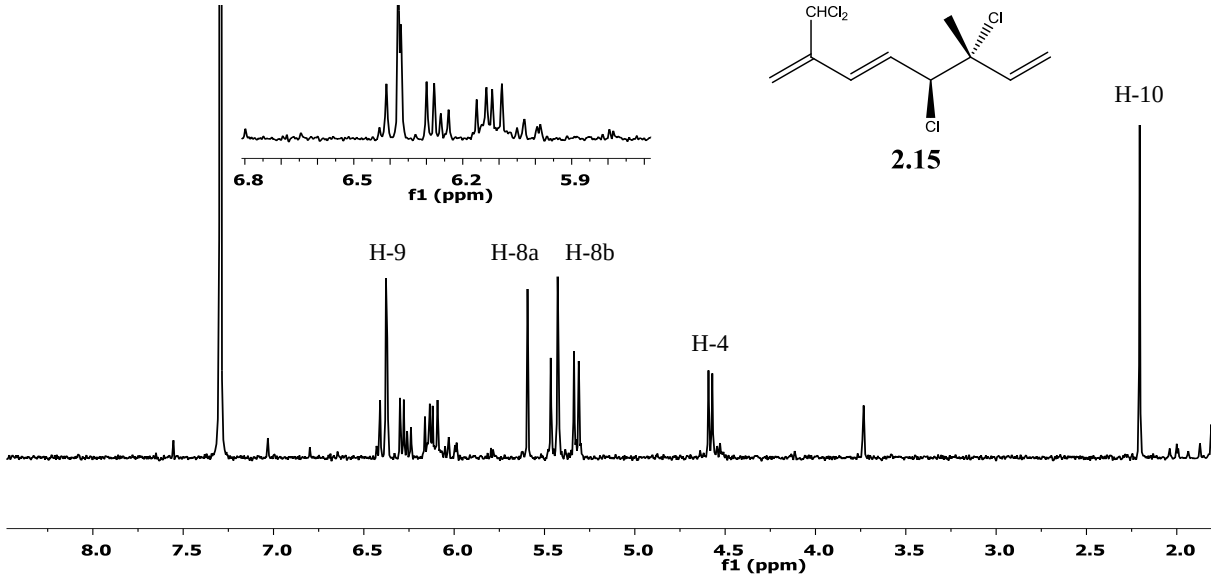

Figure 2.12: ^{1}H NMR (400 MHz, $CDCl_3$) spectrum of **2.15**

The ^{1}H NMR spectrum of **2.15** showed similar features to the ones described above. It displayed a -CH=CH_2 motif related to signals at δ 5.32 (d, *J* = 10.6 Hz, H-1a), δ 5.45 (d, *J* = 17.0 Hz, H-1b), δ 6.13 (dd, *J* = 17.1, 10.6 Hz, H-2). A -CH=CH-CHX- functionality was noted corresponding to olefinic methines at δ 6.27 (dd, *J* = 16.0, 8.5 Hz, H-5) and δ 6.37 (d, *J* = 16.0 Hz, H-6), coupled to a halomethine proton at δ 4.35 (d, *J* = 8.5 Hz, H-4). A methyl singlet peak was also present at δ 1.81 (s, H-10) and three deshielded olefinic protons at δ 6.41 (s, H-9) and δ 5.43 (s, H-8a) and δ 5.59 (s, H-8b) showing a terminal alkene. The ^{1}H NMR data are consisted with values reported in literature (Afolayan, 2008).

Table 2.4: ^{1}H NMR (400 MHz, $CDCl_3$) chemical shifts of halogenated monoterpenes isolated from *P. cornutum*

	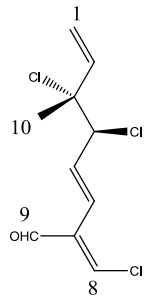	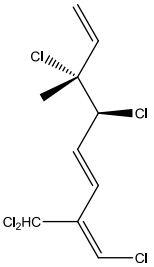	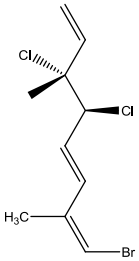	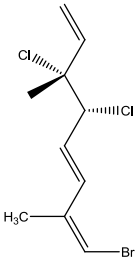	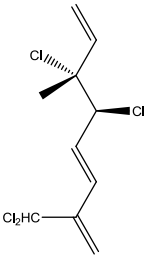
	2.11	**2.12**	**2.13**	**2.14**	**2.15**
Carbon No.	δ_H, multi, J(Hz)	δ_H, multi, J(Hz)	δ_H, multi, J(Hz)	δ_H, multi, J(Hz)	δ_H, multi, J(Hz)
1	5.33, d, 10.6	5.34, d, 10.7	5.35, d, 10.7	5.31, d, 10.7	5.32, d, 10.6
	5.47, d, 17.1	5.46, d, 17.1	5.50, d, 16.9	5.44, d, 17.0	5.45, d, 17.0
2	6.13, dd, 17.1,	6.13, dd, 17.1,	6.15, dd, 16.9,	6.11, dd, 17.0,	6.13, dd, 17.1,
	10.6	10.7	10.7	10.7	10.6
3	-	-	-	-	-
4	4.59, d, 8.8	4.63, d, 8.5	4.64, d, 9.2	4.63, d, 9.0	4.58, d, 8.5
5	7.11, dd, 15.9, 8.8	6.52, dd, 16.2, 8.5	5.99, dd. 15.4, 9.2	6.01, dd, 15.6, 9.1	6.27, dd, 16.0, 8.5
6	6.57, d, 15.9	6.67, d, 16.3	6.87, d, 15.6	6.87, d, 15.5	6.37, d, 16.0
7	-	-	-	-	-
8	7.16, s	6.43, s	6.21, s	6.21, s	5.59, s
					5.43, s
9	9.58, d, 2.0	6.80, s	1.94, s	1.94, s	6.41, s
10	1.81, s	1.82, s	1.81, s	1.81, s	1.81, s

2.2.4 Isolation and characterization of halogenated monoterpenes from *P. corallorhiza*

The significant variation in metabolites from *P. corallorhiza* necessitated the extraction of specimens collected from different sites. These were Kalk Bay (Cape Town), Three Sisters, Noordhoek (Port Elizabeth) and Port Alfred

P. corallorhiza (Kalk Bay, Cape town; KB100213-1)
P. corallorhiza was collected from Kalk Bay, Cape Town and extracted in CH_2Cl_2: MeOH (2:1) after soaking in MeOH for 1 h (Scheme 2.3). The ^{1}H NMR spectrum of the crude extract displayed the presence of one major compound, **2.26** and did not prompt for further fractionation.

P. corallorhiza (Three Sisters; TSO90311-2)
P. corallorhiza collected from Three Sisters near Port Alfred was extracted in a similar way as above in CH_2Cl_2: MeOH (2:1) after soaking in MeOH for 1 h. The crude extract was fractionated by column chromatography to give 9 fractions of increasing polarity. Fraction 9:1 was further purified by column chromatography (hexane-EtOAc 95:5) to give 6 fractions (A-F) with fraction E, and F being pure compounds of **2.33** and **2.34** respectively (Scheme 2.4).

P. corallorhiza (Noordhoek, Port Elizabeth; NDK100328-10)
P. corallorhiza collected from Noordhoek (Port Elizabeth) was also extracted in CH_2Cl_2: MeOH (2:1) and the crude extract fractionated by column chromatography of increasing polarity to give 9 fractions. Fraction 9:1 was further purified by column chromatography (hexane-EtOAc 95:5) to give 6 fractions (A-F). Fraction E was determined to be compound **2.38**, with further purification of fraction B by thin layer chromatography (hexane-EtOAc 95:5) yielding compound **2.37** (Scheme 2.5). Purification of the 8:2 fraction also gave compound **2.37**.

P. corallorhiza (Port Alfred, PA100730-4a)
Algal samples collected from Port Alfred were also extracted as discussed above. The 9:1 and 8:2 fractions were further purified by column chromatography using hexane-EtOAc 95:5 and hexane-EtOAc 85:15 respectively. 6 fractions (A-F) from the 9:1 extract gave fractions D and E as compound **2.34**. Fraction H from the 8:2 extract also yielded compound **2.34** as the major metabolite (Scheme 2.6).

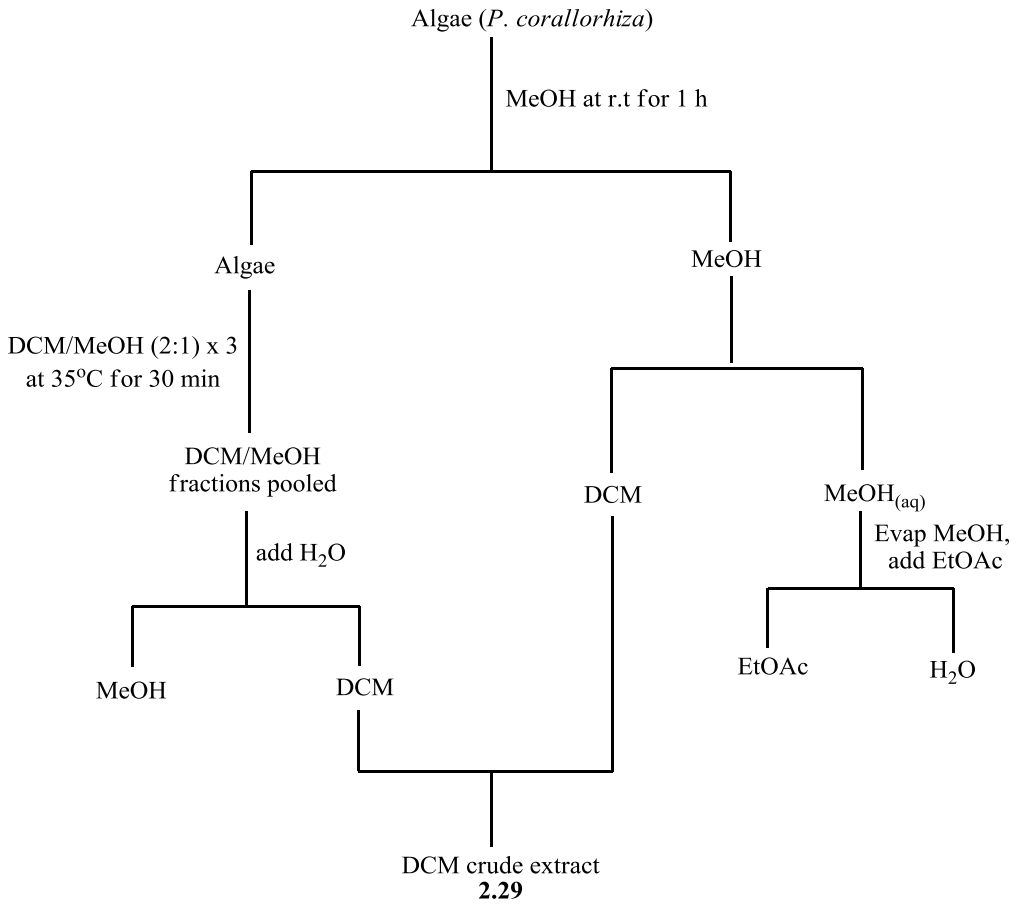

Scheme 2.3: Extraction and isolation of secondary metabolites from *P. corallorhiza* collected from Kalk Bay, Cape Town (South Africa)

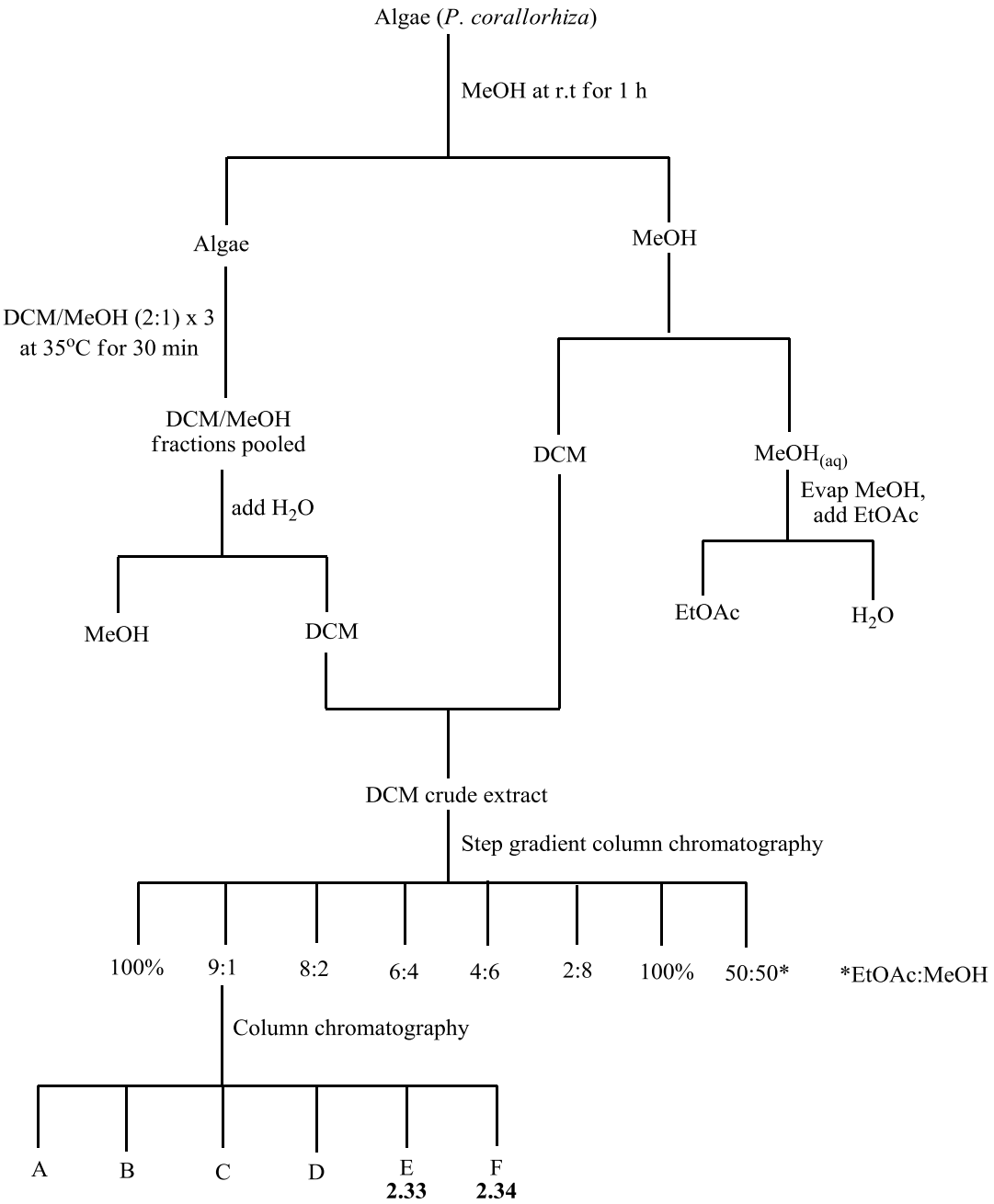

Scheme 2.4: Extraction and isolation of secondary metabolites from *P. corallorhiza* collected from Three Sisters (South Africa)

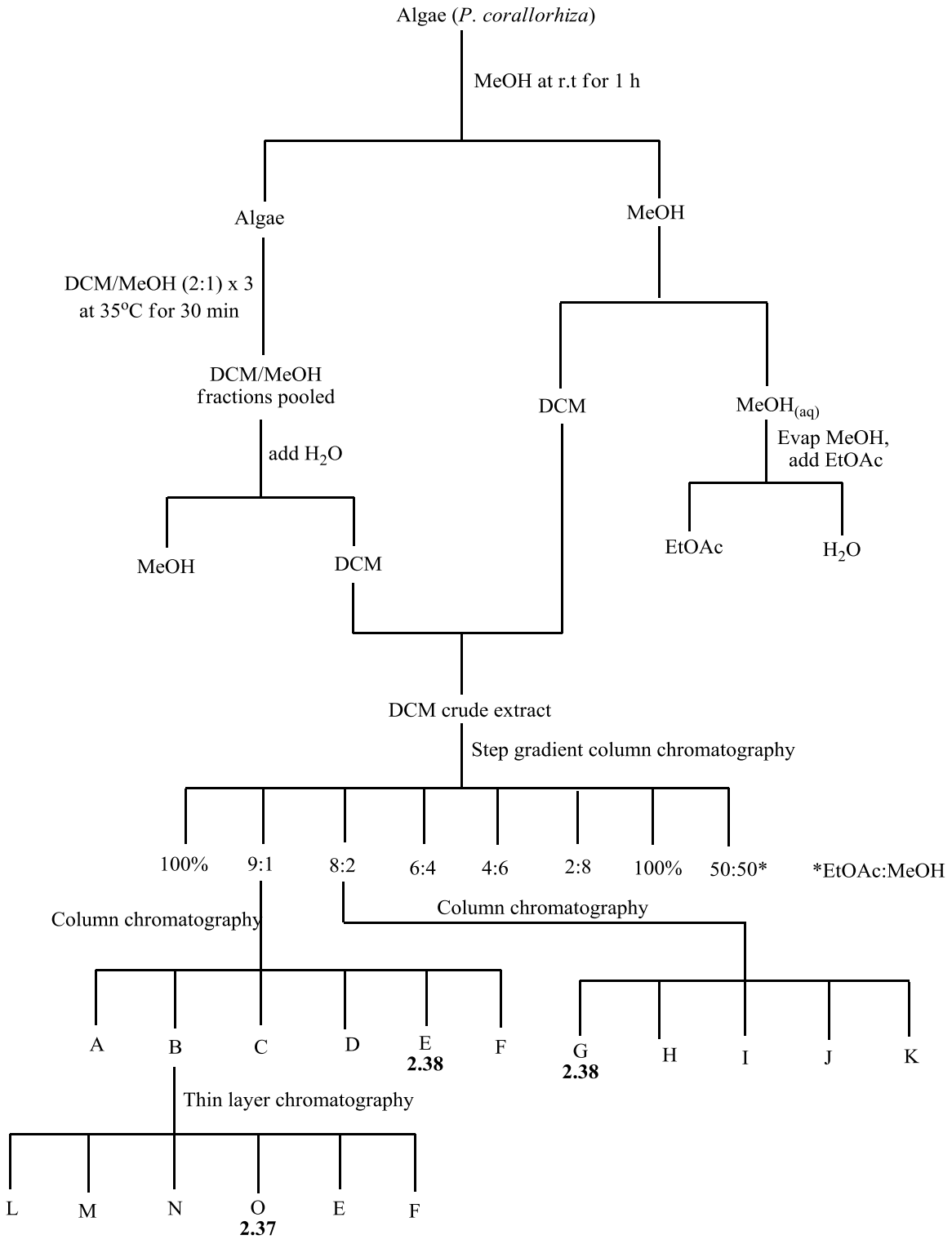

Scheme 2.5: Extraction and isolation of secondary metabolites from *P. corallorhiza* collected from Noordhoek (Port Elizabeth).

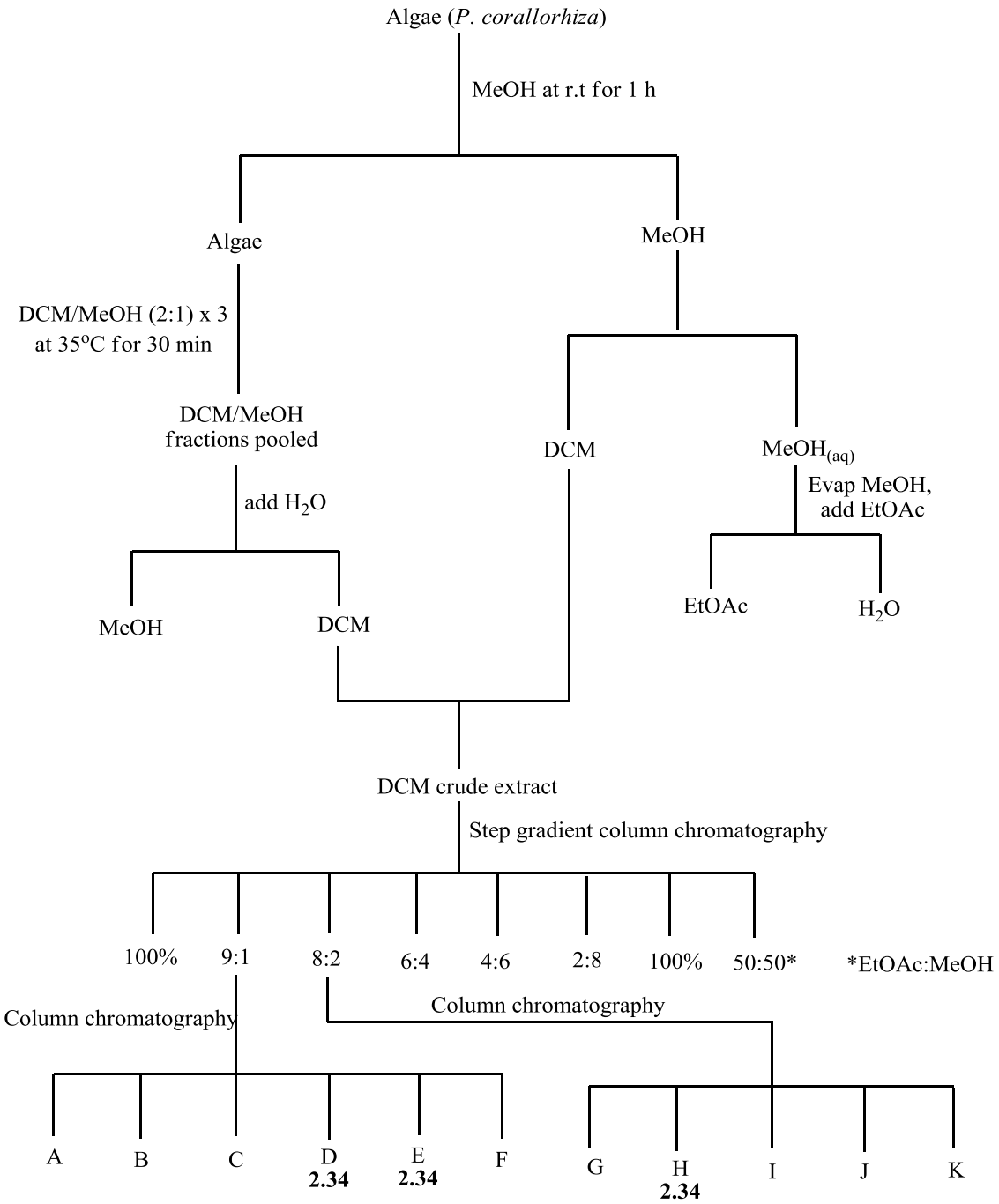

Scheme 2.6: Extraction and isolation of secondary metabolites from *P. corallorhiza* collected from Port Alfred[9][10].

[9] $MeOH_{(aq)}$ fractions were also pooled together and extracted using EtOAc as shown above
[10] Step gradient solvents systems are in the ratio of Hexane: EtOAc

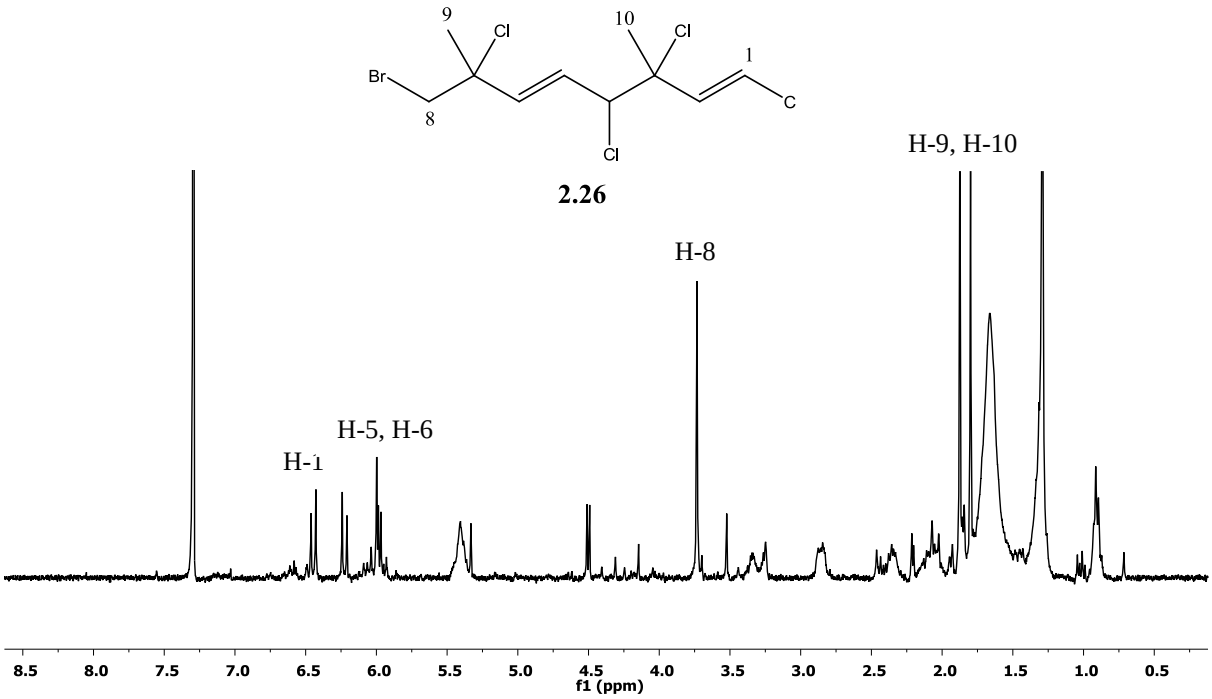

Figure 2.13: ^{1}H NMR (400 MHz, $CDCl_3$) spectrum of **2.26**

The ^{1}H NMR spectrum of **2.26** displayed the presence of two mutually coupled methines at δ 6.42 (d, *J* = 13.5 Hz, H-1) and δ 6.24 (d, *J* = 13.5 Hz, H-2). A halomethine proton was observed at δ 4.51 (d, 7.5 Hz, H-4), together with a two proton multiplet at δ 5.99 (H-5, H-6). A methylene pair singlet attached to a bromine was noted at δ 3.52 (s, H-8) and two methyl groups represented by signals at δ 1.79 (s H-10) and δ 1.87 (s H-9), consistent with compound **2.26** previously reported by Knott (2003) The ^{1}H NMR data are consistent with values reported in literature (Stierle et al., 1979).

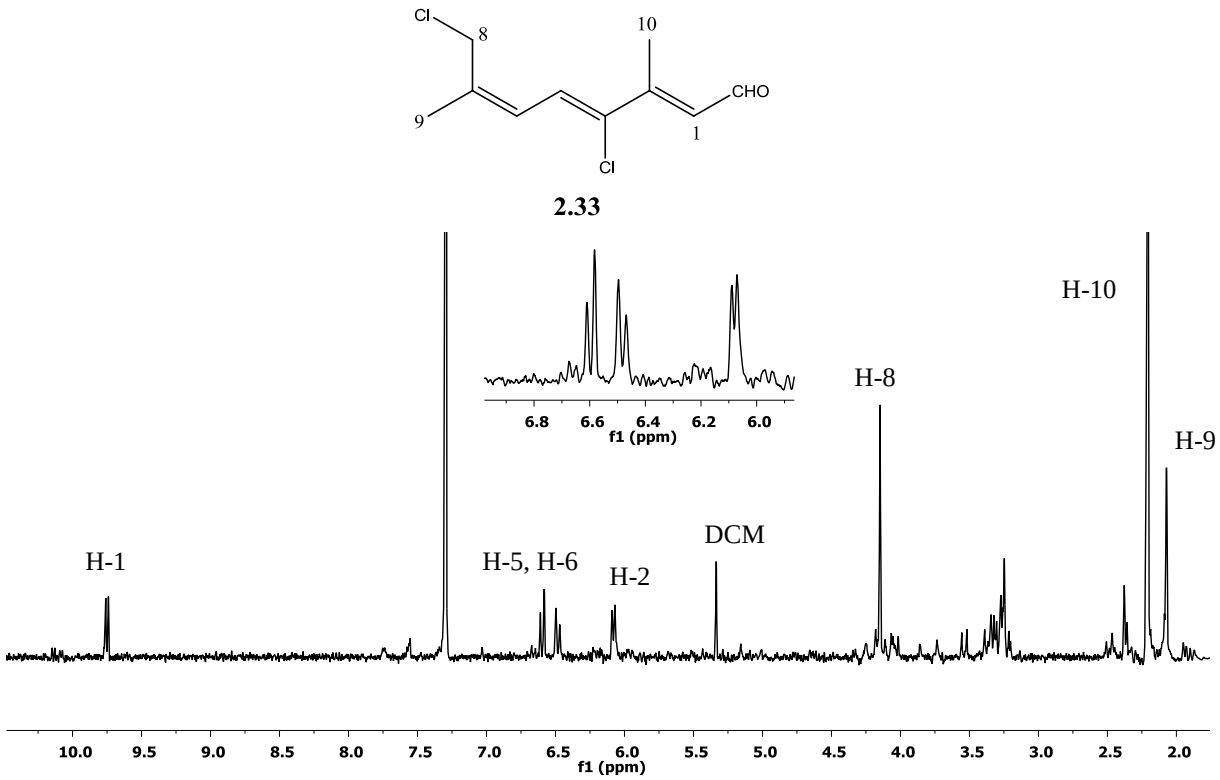

Figure 2.14: ^{1}H NMR (400 MHz, $CDCl_3$) spectrum of **2.33**

The ^{1}H NMR spectrum of **2.33** indicated the presence of an aldehydic doublet signal at δ 9.75 (d, *J* = 7.3 Hz, H-1) coupled to an olefinic proton at δ 6.07 (d, *J* = 7.3 Hz, H-2). Two mutually coupled vinylic protons were apparent and were represented by signals at δ 6.60 (d, *J* = 11.1 Hz, H-5) and δ 6.50 (d, *J* = 11.0 Hz, H-6). A halomethylene singlet was also noted at δ 4.15 (s, H-8), together with two methyl signals at δ 2.07 (s, H-9) and δ 2.21 (s, H-10) corresponding to compound **2.33**. The ^{1}H NMR data are consistent with values reported by Mann (2008).

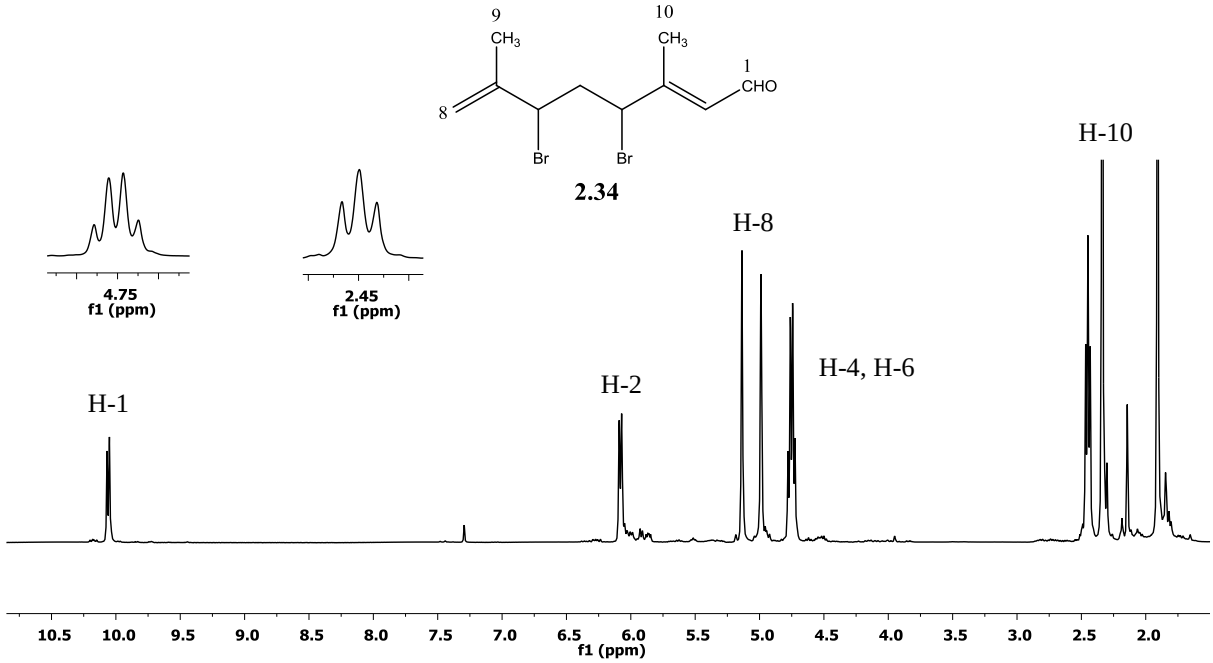

Figure 2.15: ^{1}H NMR (400 MHz, $CDCl_3$) spectrum of **2.34**

The ^{1}H NMR spectrum of **2.34** indicated the presence of an aldehydic proton at δ 10.05 (d, *J* = 7.5 Hz, H-1) coupled to a vinylic proton at δ 6.08 (d, *J* = 7.5 Hz, H-2). An overlap of signals was noted at δ 4.75 (dd, *J* = 7.5 Hz, H-4 and H-6) due to two halomethines at positions 4 and 6 existing in similar and chemical environments. These two protons are coupled to a methylene pair at signal δ 2.59 (t, *J* = 7.0 Hz H-5) resulting in a –CHX-CH_2-CHX structural motif. A terminal alkene was also apparent from signals at δ 5.00 (s, H-8a) and δ 5.18 (s, H-8b), and two methyl groups represented by signals at δ 1.90 (s, H-9) and δ 2.38 (s, H-10). The structure was therefore determined to be compound **2.34** previously reported by Mkwananzi (2005) and Mann et al. (2007).

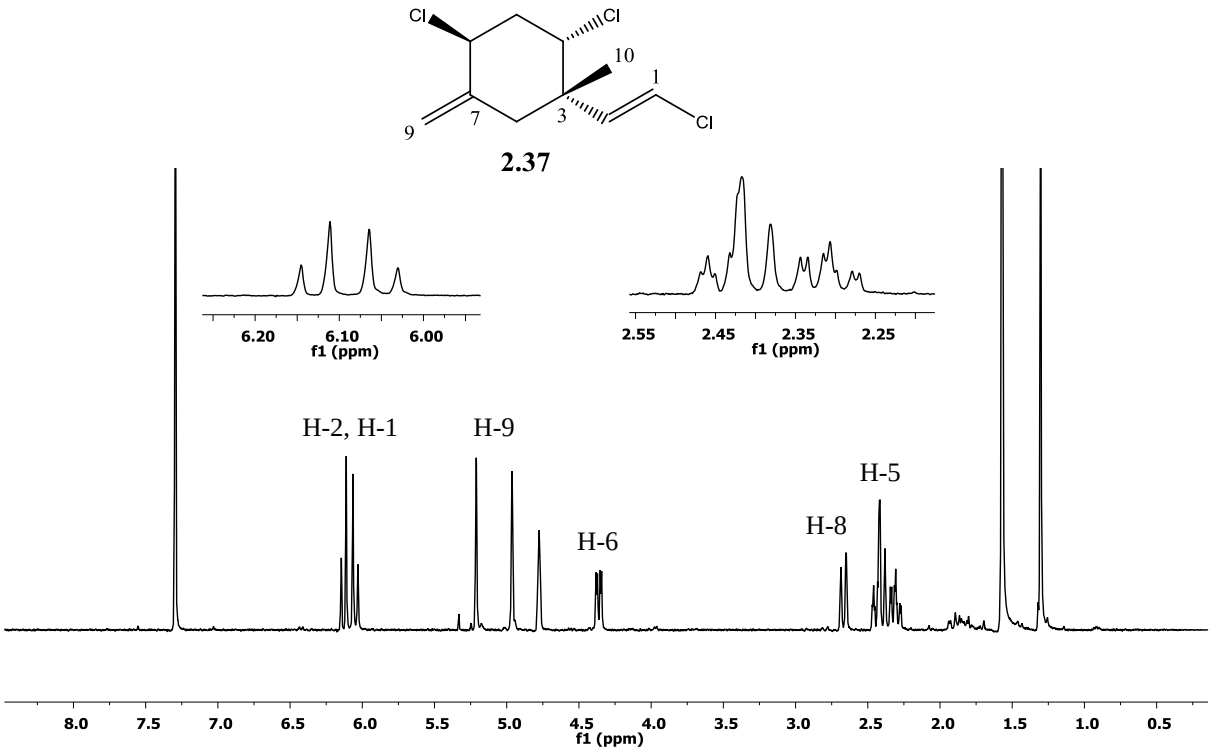

Figure 2.16: ^{1}H NMR (400 MHz, $CDCl_3$) spectrum of **2.37**

The ^{1}H NMR spectrum of **2.37** showed the presence of two mutually coupled olefinic protons at signals δ 6.05 (d, *J* = 13.7 Hz, H-1) and δ 6.13 d, *J* = 13.7 Hz, H-2) bonded to a halogen giving a -CH=CHX structural motif. Signals at δ 4.96 (H-9a) and δ 5.21 (H-9b) displayed a terminal alkene functionality (-C=CH_2). Two halomethine signals were present at δ 4.37 (d, *J* = 11.4 Hz, H-6) and δ 4.78 (br, s, H-4), while two methylenes were represented by signals at δ 2.33 – δ 2.42 (H-5a and H-5b), δ 2.67 (d, *J* = 14.4 Hz, H-8a) and δ 2.33 (d, *J* = 14.9, H-8b). This ^{1}H NMR data are consistent with the metabolite previously isolated by Mann (2008) (Stierle and Sims, 1979).

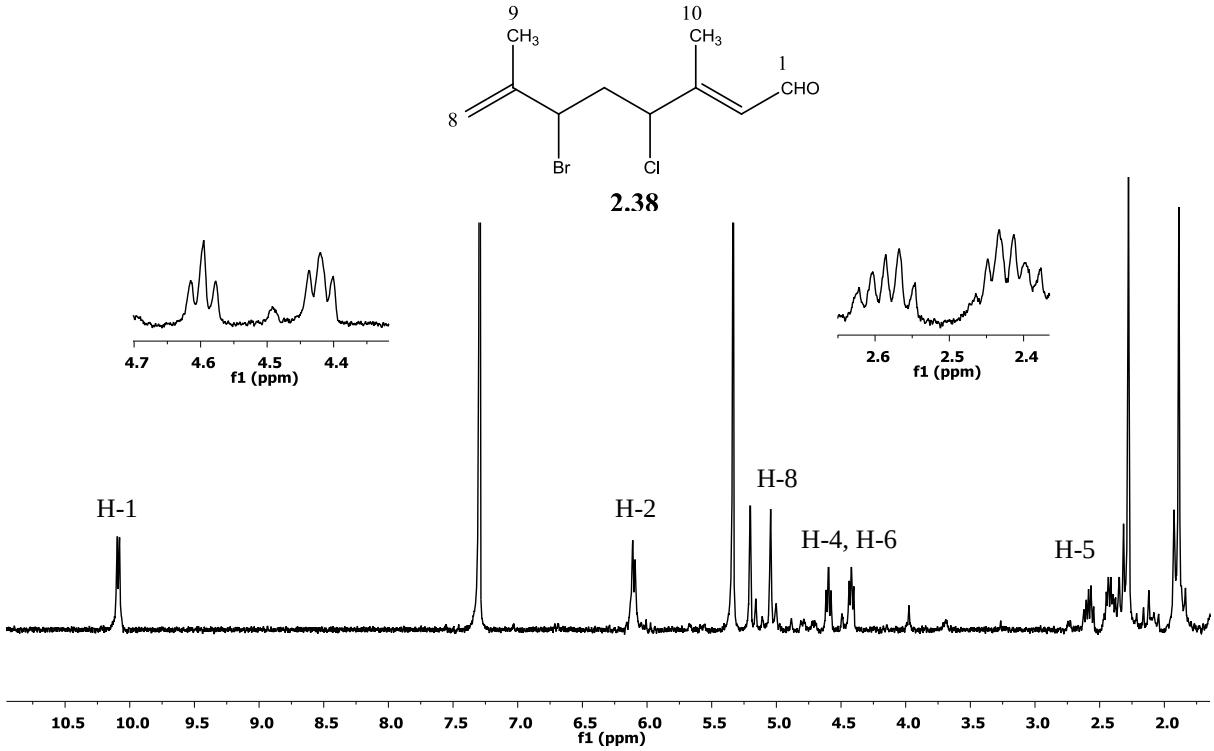

Figure 2.17: ^{1}H NMR (400 MHz, $CDCl_3$) spectrum of **2.38**

The ^{1}H NMR spectrum of **2.38** had similar spectral features to compound **2.34**. It also showed an aldehydic proton represented by the signal at δ 10.10 (d, *J* = 7.4 Hz, H-1) coupled to a vinylic proton at δ 6.08 (d, *J* = 7.4 Hz, H-2), a terminal double bond from signals at δ 5.04 (s, H-8a) and δ 5.21 (s, H-8b) while a –CHX-CH_2-CHX system was suggested by peaks at δ 4.42 (t, J = 7.4 Hz, H-6), δ 2.42-2.59 (H-5a and H-5b) and δ 4.60 (t, J = 7.4 Hz, H-4). The final part of the spectrum consists of two methyl signals at δ 1.89 (s, H-9) and δ 2.29 (s, H-10). The ^{1}H NMR data are consistent with values previously reported for **2.38** by Mann (2008).

Table 2.5: ^{1}H NMR (400 MHz, $CDCl_3$) chemical shifts of halogenated monoterpenes isolated from *P. corallorhiza*

	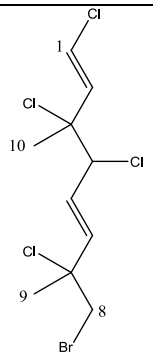	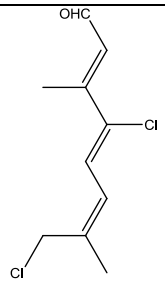	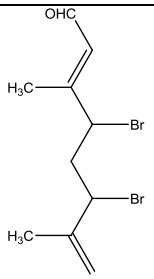	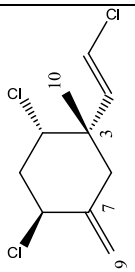	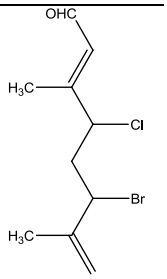
	2.26	**2.33**	**2.34**	**2.37**	**2.38**
Carbon No.	δ_H, multi, J(Hz)	δ_H, multi, J(Hz)	δ_H, multi, J(Hz)	δ_H, multi, J(Hz)	δ_H, multi, J(Hz)
1	6.42, d, 13.5	9.75, d, 7.3	10.05, d, 7.5	6.05, d ,13.7	10.10, d, 7.4
2	6.24, d, 13.5	6.07, d,7.3Hz	6.08, d, 7.5	6.13, d, 13.7	6.08, d, 7.4
3	-	-	-	-	-
4	4.51, d. 7.5	-	4.75, dd, 7.5	4.78,	4.60, t, 7.4
5	5.99, m	6.60, d, 11.1	2.59, t, 7.0	2.33 - 2.42	2.42-2.59,
6	5.99, m	6.50, d, 11.0	4.75,dd, 7.5	4.37, d, 11.4	4.42, t, 7.4
7	-	-	-	-	-
8a	3.52, s	4.15, s,	5.00, s	2.67, d, 14.4	5.04, s,
8b			5.18, s	2.33, d, 14.9	5.21, s,
9	1.87, s	2.07, s,	1.90, s	4.96, s 5.21, s	1.89, s
10	1.79, s	2.21, s,	2.38, s	1.30, s	2.29, s

2.2.5 Biological activity of halogenated monoterpenes

Cell based assays conducted on an oesophageal cancer cell line (WHCO1) and breast cancer cell lines (MCF7, MCF12A and MDA-MB-231) with the above discussed metabolites confirmed the cytotoxic nature of these molecules. Cytotoxic studies involving breast cancer occasionally include the MCF12A breast cancer cell line, which is an immortalized breast epithelial cell line (Paine et al., 1992) that is commonly referred to as a "normal" breast tissue. It is included in assays to determine selective cytotoxicity of test compounds. Current drug designing approaches are aiming to reduce chemotherapy toxicity by developing agents that target cancer cells with minimal effect on normal human cells. Previous studies had made efforts in determining IC_{50} values of metabolites from *Plocamium* and some of the results obtained are tabulated below (Table 2.6).

Some selective cytotoxicity was demonstrated by compounds **2.10**, **2.26**, **2.30** and **2.34** given the noticeable differences in the IC_{50} values between MCF7s and MCF12As. Metabolites from *P. suhrii* (compounds **2.16 – 2.21**) displayed remarkable activity in the oesophageal cancer cell line (WHCO1). However selective cytotoxicity studies on these metabolites are still yet to be conducted. Compound **2.12** displayed the greatest activity in both oesophageal (WHCO1) and breast cancer cell lines, MCF7 and MDA-MB-231 with IC_{50} values of 17.8 µM, 3.55 µM and 6.15 µM respectively. However it showed minimal selective cytotoxicity with an IC_{50} value of 3.52 µM in the MCF12A breast cancer cell line that represents normal tissue. Distinct trends in activity could be noticed in metabolites from *P. cornutum* as substituents on position 7 of the molecule changed from $-CHCl_2$, to $-CH_3$. With such observable changes in activity, SAR studies could be conducted on secondary metabolites from *P. cornutum* and clear cut deductions made in terms of which components of the molecule are essential for activity, which formed the basis for chapter 3.

Table 2.6 Anti-cancer activity (IC_{50} values) of halogenated monoterpenes isolated from *P. cornutum, P. suhrii* and *P. corallorhiza* against WHCO1 (Antunes et al., 2011; Knott et al., 2005) and against breast cancer cell lines (MCF7, MCF12A and MDA-MB-231) (Lawson, 2009; de la Mare et al., 2012)[11]

Compound no.	WHCO1 (μM)	MCF7 (μM)	MCF12A (μM)	MDA-MB-231 (μM)
2.9	9.3	-	-	-
2.10	33.8	65.05	non-toxic	63.52
2.11	47.3	-	-	non-toxic
2.12	17.8	3.55	3.52	6.15
2.13	87.6	non-toxic	non-toxic	-
2.14	87.6	non-toxic	non-toxic	-
2.15	40.2	-	-	non-toxic
2.16	6.6	-	-	-
2.17	9.9	-	-	-
2.18	9.3	-	-	-
2.19	8.5	-	-	-
2.20	8.4	-	-	-
2.21	15.1	-	-	-
2.25	18.1	69.7	34.8	-
2.26	17.2	89.98	non-toxic	77.77
2.30	-	28.85	62.29	88.11
2.33	-	-	-	non-toxic
2.34	-	32.98	127.59	66.85
2.36	34.8	-	-	-
2.37	-	-	-	non-toxic
2.38	-	-	-	non-toxic

[11] IC_{50} values greater than 200 μM were considered as non-toxic

2.3 CONCLUSION

The above results have prompted us to focus our research on SARs related to halogenated monoterpenes, and map out essential components that are responsible for biological activity. However exploring the chemistry and biological activity of halogenated monoterpenes is associated with the following challenges:

- Stability: natural product compounds are highly unstable. (Coimbra et al., 2011). They are prone to degradation once extracted and isolated from algae.
- Quantities: concentrations of halogenated monoterpenes in algae are very low (Jung and Parker, 1997) and require frequent extractions to obtain the required compounds, which is cumbersome.
- Source: marine algae that produce these compounds are not easy to locate, identify or collect (Fuller et al., 1994; Jung and Parker, 1997). As highlighted earlier, geographical changes affect metabolite profiles and this decreases the easy of finding the same compound isolated previously for further studies to be done.

A solution was therefore to devise synthetic routes that can be used to synthesize halogenated monoterpene analogues and conduct SAR studies. Synthesis of these analogues is discussed in chapter 3.

2.4 Experimental

2.4.1 General experiments

Solvents

All solvents used for extractions and chromatography were of HPLC grade (Chromasolv) acquired from Sigma Aldrich South Africa.

Chromatography

Purification procedures were conducted using silica gel 60 (0.040-0.063 mm), 230-400 mesh ASTM Merck product. Thin layer chromatography experiments were run on TLC silica gel $60F_{254}$ 20 x 20 aluminium sheets and visualized using a Syngene UV lamb 230 V, 50 Hz with dual wavelengths 365 nm and 254 nm.

High Performance Liquid Chromatography

A Waters HPLC machine was used with Waters 1525 binary HPLC pump connected to a Waters 2487 Dual wavelength absorbance detector. A Whatman Partisil 10 (1 x 50 cm) normal phase column was used for purification.

Nuclear magnetic resonance (NMR)

NMR data (1D and 2D experiments) were acquired on a Bruker Avance 400 MHz and 600 MHz spectrometers. Chemical shifts were recorded in ppm and referenced to residual deuterated solvent ($CDCl_3$ δ_H 7.26, δ_C 77.0). All coupling constants are reported in Hz.

Plant material

Samples were collected along the south eastern coast of South Africa at low tides. Identification of different algae collected was assisted by Prof John J. Bolton of the department of Botany, University of Cape Town, South Africa. Voucher specimens were made and kept in our repository at Rhodes University, South Africa. Crude and pure extracts isolated were stored in vials at -20 ºC, covered with a thin film of hexane and flushed with argon/nitrogen.

2.4.2 Extraction procedures

2.4.2.1 Small-scale ultra-sound assisted extractions

This method was adopted for all small-scale extractions conducted in this project including geographical variation studies. Extractions were done in duplicates for comparison. For intra-site geographical variation studies, samples were collected from pools within 10-200 metres of each other on the same site and were extracted and analysed separately. The extraction procedure was done as outlined below:

- A sample of algae was crushed using a mortar and pestle after soaking it in liquid nitrogen. The resultant powders were packed in labelled centrifuge tubes to the 3 ml mark and MeOH (3 ml) added to each tube. The mixtures were sonicated for 2 minutes, followed by addition of DCM (6 ml). Another sonication period of 5 minutes was carried out, after which the mixtures were then centrifuged for 5 minutes. The DCM layer was pipetted out into size 6 vials and the solvent evaporated off on a rotavap. The remaining crude extracts were analysed by ^{1}H NMR.

2.4.2.2 Isolation and purification of secondary metabolites from *P. cornutum*

Samples of *P. cornutum* (collection code KB100213-1) were collected in February 2010 from Kalk Bay, Cape Town (South Africa). The algae was placed on ice during transportation and frozen at the laboratory until extracted. Protocols adopted for extraction, isolation and purification of metabolites are represented by the flow chart in Scheme 2.2**.**

Sufficient methanol was used to completely submerge the algae in a 1 L conical flask for 1 h. The solvent was decanted and the algae re-extracted 3 times with a 2:1 DCM-MeOH mixture at 35 ºC for 30 min. The methanol extract was further extracted with DCM (with the addition of sufficient H_2O to allow phase separation). Water was also added to the DCM-MeOH extract to allow phase separation. The DCM layers were combined and concentrated under reduced pressure to give crude extract A. The aqueous methanol layers were concentrated (to remove the MeOH) and re-extracted with EtOAc to give crude extract B after removal of solvent under reduced pressure.

The DCM crude extract (~ 1 g) was chromatographed on a silica column (10 g) using a step gradient protocol of increasing polarity from 100% hexane to 100% EtOAc and the column was finally washed with EtOAc-MeOH. Further column chromatography (silica, 10 g,

hexane-EtOAc, 95:5) of the hexane-EtOAc (9:1) fraction (120 mg) yielded fraction MC10-31A-E. MC10-31A was further purified by normal phase HPLC using 100% hexane as the mobile phase to give compounds MC10-32A-D. Dry weight of the algae after extraction was 43.79 g.

^{1}H NMR spectroscopy was used to characterize extracts obtained at each stage of the procedure. Fractions to further purify were chosen according to the NMR data acquired.

Table 2.7: Masses and percentage yields of compounds isolated from *P. cornutum*

Isolation Code	Compound No.	Mass (mg)	% yield
MC10-31B	**2.11**	18.2	0.041
MC10-32C	**2.12**	7.1	0.016
MC10-32B	**2.13**	2.3	0.005
MC10-32A	**2.14**	2.1	0.004
MC10-31D	**2.15**	1.0	0.002

^{1}H NMR data for compounds **2.11 – 2.15**, see Table 2.4.

2.4.2.3 Isolation and purification of secondary metabolites from *P. corallorhiza*

Samples of *P. corallorhiza* were collected in March 2010 from four sites (Kalk Bay, Kenton-on-Sea, Port Alfred and Noordhoek). The algae was transported on ice after which it was stored frozen. The protocols adopted for extraction, isolation and purification of metabolites from *P. corallorhiza* are shown in schemes 2.3-2.6.

The same general method discussed in section 2.4.2.2 for *P. cornutum* was used for the extraction of metabolites from *P. corallorhiza* collected from the four sites discussed. The DCM crude extract (~ 1 g) obtained from *P. corallorhiza* was chromatographed on a silica column (10 g) using a step gradient protocol of increasing polarity from 100% hexane to 100% EtOAc and the column finally washed with EtOAc-MeOH (1:1).

P. corallorhiza (Three Sisters; TSO90311-2)

Further column chromatography (silica, 10 g, hexane-EtOAc, 95:5) of the hexane-EtOAc (9:1) fraction (120 mg) yielded 6 fractions (A-F), with E (**2.33**) and F (**2.34**) being pure compounds. Dry weight of the algae after extraction was 61.37 g.

P. corallorhiza (Noordhoek, Port Elizabeth; NDK100328-10)

Further column chromatography (silica, 10 g, hexane-EtOAc, 95:5) of the hexane-EtOAc (9:1, 120 mg) fraction and hexane-EtOAc (8:2, 110 mg) (silica 10 g, hexane-EtOAc, 85:15) fraction yielded 6 (A-F) and 5 (G-K) fractions respectively. Fraction E was identified as compound **2.38** whilst further purification of fraction B by thin layer chromatography (mobile phase: hexane-EtOAc 95:5) yielded 6 more fractions (L-Q), with fraction O corresponding to compound **2.37.** Fraction G from the 8:2 (hexane-EtOAc) extract was similar to fraction E (**2.38**). Dry weight of the algae after extraction was 41.05 g.

P. corallorhiza (Port Alfred, PA100730-4a)

Further column chromatography (silica, 10 g, hexane-EtOAc, 95:5) of the hexane-EtOAc (9:1, 110 mg) fraction and of the hexane-EtOAc (8:2, 100 mg) (silica 10 g, hexane-EtOAc, 85:15) fraction yielded also 6 (A-F) and 5 (G-K) fractions respectively. Fractions D, E and H were similar and were identified as compound **2.34.** Dry weight of the algae after extraction was 31.02 g.

Table 2.8: Masses and percentage yields of compounds isolated from *P. corallorhiza*

Isolation Code	Compound No.	Mass (mg)	Dry weight of algae after extraction (g)	% yield
KB100213-1	**2.26**	1.5 g (crude)	112.12	1.338
TS090311-2	**2.33**	4.4	61.37	0.007
PA100730-4a	**2.34**	13.6	31.02	0.044
NDK100328-10	**2.37**	4.3	41.05	0.010
NDK100328-10	**2.38**	4.3	41.05	0.010

^{1}H NMR data for compounds **2.26, 2.33, 2.34, 2.37** and **2.38,** see Table 2.5.

It is important to note that secondary metabolites that were present in algae overlapped from one site to the next and these values refer to quantities obtained for specific metabolites isolated from a particular collection site.

References

Abreu, P.M., Galindro, J.M., 1996. Polyhalogenated Monoterpenes from Plocamium cartilagineum from the Portuguese Coast. Journal of Natural Products, 59, 1159-1162.

Afolayan, A.F., M.Sc thesis; Isolation and characterization of Anti-plasmodial metabolites from South African Marine Algae (2008).

Afolayan, A.F., Mann, M.G.A., Lategan, C.A., Smith, P.J., Bolton, J.J., Beukes, D.R., 2009. Antiplasmodial halogenated monoterpenes from the marine red alga Plocamium cornutum. Phytochemistry, 70, 597-600.

Antunes, E.M., Afolayan, A.F., Chiwakata, M.T., Fakee, J., Knott, M.G., Whibley, C.E., Hendricks, D.T., Bolton, J.J., Beukes, D.R., 2011. Identification and in vitro anti-esophageal cancer activity of a series of halogenated monoterpenes isolated from the South African seaweeds Plocamium suhrii and Plocamium cornutum. Phytochemistry (Elsevier), 72, 769-772.

Carter-Franklin, J.N., Butler, A., 2004. Vanadium Bromoperoxidase-Catalyzed Biosynthesis of Halogenated Marine Natural Products. Journal of the American Chemistry Society, 126, 15060-15066.

Coimbra, M., Isacchi, B., van Bloos, L., Torano, J.S., Ket, A., Wu, X., Broere, F., Metselaar, J.M., Rijcken, C.J.F., Storm, G., Bilia, R., Schiffelers, R.M., 2011. Improving solubility and chemical stability of natural compounds for medicinal use by incorporation into liposomes. International Journal of Pharmaceutics, 416, 433-442.

Crews, P., Kho, E., 1975. Plocamene B. New cyclic monoterpene skeleton from a red marine alga. Journal of Organic Chemistry, 40, 2568-2570.

de la Mare, J., Lawson, J.C., Chiwakata, M.T., Beukes, D.R., Edkins, A.L., Blatch, G.L.,2012 – Quinones and halogenated monoterpenes of algal origin show anti-proliferative effects against breast cancer cells in vitro. Accepted in Investigational New Drugs. Doi:10.1007/s10637-011-9788-0

El Gamal, A.A., 2011. Biological Importance of Marine Algae. John Wiley & Sons, Ltd, 1-35.

Fuller, R.W., Cardellina, J.H., II, Jurek, J., Scheuer, P.J., Alvarado-Lindner, B., McGuire, M., Gray, G.N., Steiner, J.R., Clardy, J., et,a., 1994. Isolation and Structure/Activity Features of Halomon-Related Antitumor Monoterpenes from the Red Alga Portieria hornemannii. Journal of Medicinal Chemistry, 37, 4407-4411.

Ireland, C., Stallard, M.O., Faulkner, D.J., Finer, J., Clardy, J., 1976. Some chemical constituents of the digestive gland of the sea hare Aplysia californica. The Journal of Organic Chemistry, 41, 2461-2465.

Jung, M.E., Parker, M.H., 1997. Synthesis of Several Naturally Occurring Polyhalogenated Monoterpenes of the Halomon Class. Journal of Organic Chemistry, 62, 7094-7095.

Kladi, M., Vagias, C., Roussis, V., 2005. Volatile halogenated metabolites from marine red algae. Phytochemistry Reviews, 3, 337-366.

Knott, M.G., 2003. The natural product chemistry of South African Plocamium species (MSc thesis). Rhodes University, Grahamstown, South Africa.

Knott, M.G., Mkwananzi, H., Arendse, C.E., Hendricks, D.T., Bolton, J.J., Beukes, D.R., 2005. Plocoralides A-C, polyhalogenated monoterpenes from the marine alga Plocamium corallorhiza. Phytochemistry (Elsevier), 66, 1108-1112.

König, G.M., Wright, A.D., De,N., 1999. Halogenated Monoterpenes from Plocamium costatum and Their Biological Activity. Journal of Natural Products, 62, 383-385.

König, G.M., Wright, A.D., Linden, A., 1999. Plocamium hamatum and its monoterpenes: chemical and biological investigations of the tropical marine red alga. Phytochemistry, 52, 1047-1053.

Lawson, J., 2009. Analysis of the anti-cancer activity of novel indigenous algal compounds in breast cancer: Towards the development of a model for screening anti-cancer stem cell activity (MSc thesis). Rhodes University, Grahamstown, South Africa.

Mkwananzi, H.B., (2005). The study of Plocamium corallorhiza secondary metabolites and their biological activity (MSc thesis). Rhodes University, Grahamstown, South Africa.

Mann, M.G.A., (2008). An investigation of the antimicrobial and antifouling properties of marine algal metabolites (MSc thesis). Rhodes University, Grahamstown, South Africa.

Mann, M.G.A., Mkwananzi, H.B., Antunes, E.M., Whibley, C.E., Hendricks, D.T., Bolton, J.J., Beukes, D.R., 2007. Halogenated Monoterpene Aldehydes from the South African Marine Alga Plocamium corallorhiza. Journal of Natural Products, 70, 596-599.

Neumann, C.S., Fujimori, D.G., Walsh, C.T., 2008. Halogenation Strategies In Natural Product Biosynthesis. Chemical Biology. (Cambridge, MA, U. S.), 15, 99-109.

Ohsawa, N., Ogata, Y., Okada, N., Itoh, N., 2001. Physiological function of bromoperoxidase in the red marine algae, Corallina pilulifera: production of bromoform as an allelochemical and the simultaneous elimination of hydrogen peroxide. Phytochemistry, 58, 683-692.

Paine, T.M., Soule, H.D., Pauley, R.J., Dawson, P.J., 1992. Characterization of epithelial phenotypes in mortal and immortal human breast cells. International Journal of Cancer, 50, 463-473.

Stierle, D.B., Sims, J.J., 1979. Marine natural products: Polyhalogenated cyclic monoterpenes from the red alga plocamium cartilagineum of antarctica. Tetrahedron, 35, 1261-1265.

Stierle, D.B., Wing, R.M., Sims, J.J., 1979. Marine natural products-XVI: Polyhalogenated acyclic monoterpenes from the red alga plocamium of antarctica. Tetrahedron, 35, 2855-2859.

Winter, J.M., Moore, B.S., 2009. Exploring the Chemistry and Biology of Vanadium-dependent Haloperoxidases. Journal of Biological Chemistry, 284, 18577-18581.

Wise, M.L., Rorrer, G.L., Polzin, J.J., Croteau, R., 2002. Biosynthesis of marine natural products: Isolation and characterization of a myrcene synthase from cultured tissues of the marine red alga Ochtodes secundiramea. Archieves of Biochemistry and Biophysics, 400, 125-132.

CHAPTER THREE:

Synthesis of halogenated monoterpene inspired inhibitors of cancer cell growth

3.1 Introduction

In chapter 2, we identified a number of halogenated monoterpenes which displayed good biological activities against various cancer cell lines. Unreliable supply of the natural products due to seasonal and geographical variations and relative instability of the active compounds made a more in-depth study of their anti-cancer properties problematic. In order to address this problem we embarked on developing simplified synthetic analogues/"fragments" of the natural products so as to study their activity in more detail.

Identification of agents active against human cancers has been largely dependent upon the screening of natural products and their analogues (Shu, 1998). Analogue development aims to enhance potency and improve pharmacokinetic and physical properties of a lead molecule. This subsequently furnishes compounds that are suitable for use as drug candidates. However the development of newer agents from natural products presents with challenges that are not commonly encountered with synthetic compounds. (Da Roche et al., 2001).

3.1.1 Lead optimization of natural products

Natural products normally display biological activities that can be optimized by structural manipulation. Compounds extracted and isolated from nature can act either as precursors for semi-synthetic compounds or as templates for totally different synthetic compounds (Nicolaou et al., 1996). In certain instances, attempts are made to fully synthesize natural products in the laboratory due to inadequate quantities being available from natural sources. For example it has been estimated that for a single dose of paclitaxel (Taxol, **1.7**)[1], one yew tree has to be cut down (Azzoli et al., 2009). Although synthesis is the preferred method for the production of drugs, the often complex structures of natural products such as paclitaxel (**1.7**) present significant challenges to the synthetic chemists (Gloer, 2000).

[1] The generic name paclitaxel is used here as opposed to Taxol® which is a registered Britol-Myers-Squib product

Rather than isolating the target compound itself, harvesting of biosynthetic intermediates can serve as a solution. Conversion of the intermediate to the actual lead can then be effected by synthetic methods. Furthermore, this gives opportunities for synthesizing analogues of the final compound which can be more potent / effective than the natural product. Paclitaxel (**1.7**) is one such example that is manufactured from its biosynthetic intermediate, 10-deacetylbaccatin III (**3.1**) through a four stage process. Its analogue docetaxel (**3.2**) is considered more potent than paclitaxel itself (Baker et al., 2006).

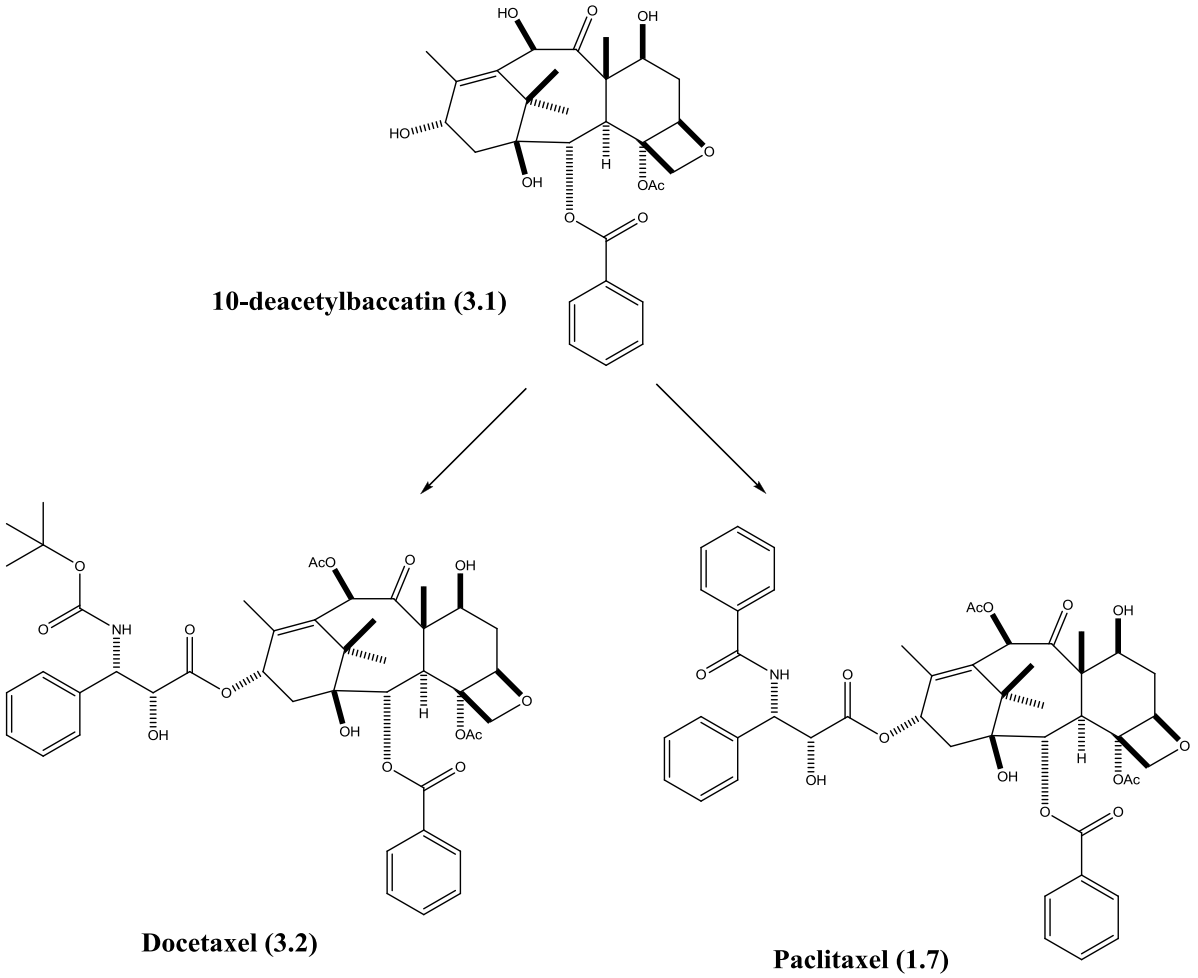

Scheme 3.1: Conversion of 10-deacetylbaccatin (**3.1**) to paclitaxel (**1.7**) and its structural analogue docetaxel (**3.2**)

3.1.2 Fragment-Based Drug Design[2]

Intense commercial pressure to increase drug discovery productivity has led to new technologies being developed to improve quality and efficiency of this process (Lanter et al., 2011). Success is mainly governed by two key issues in target-based drug design. The biological target (receptor or enzyme) linked to the onset or progression of the disease has to be identified, and therapeutic agents that can moderate activity of that protein receptor or enzyme with minimal side effects/adverse reactions have to be developed (Hajduk and Greer, 2007). Therefore newer technologies like the chemical fragment approach have gained momentum in drug discovery processes.

Fragment-based drug design was pioneered by Jencks and Ariens who postulated that drug-like molecules are a combination of two or more binding epitopes or fragments (Rees et al., 2004). They highlighted the importance of using small fragments in the discovery of new hits/leads for drug design. Therefore, a drug lead can be fragmented into small pieces or discrete entities e.g., aryl group, carboxylate etc. (Hajduk and Greer, 2007). The main advantage of this approach is that it simplifies computational analysis of ligand binding and allows mapping of elements required for enzyme binding (Foloppe, 2011). The same principles can be used identify functional groups or fragments that are essential for biological activity. Recent literature has addressed the properties of small molecules that are required to produce good lead compounds and this is in relation to Lipsinki's rule of five which determines a drug's suitability to be taken as an oral dosage form (Oprea, 2002). With the chemical fragment approach, several attractive features have been noted:

- Compounds screened are less since there is limited chemical diversity when dealing with small fragments.
- A higher proportion of atoms in a fragment are directly involved in the binding to a biological target and that allows the role of each functional group in that active site or receptor to be visualized.
- Chemical optimization is favourable, with the transition of a hit to a lead or a lead to a drug yielding a final molecule that has a molecular weight still within the required range of lead-likeness or drug-likeness (Zartler and Shapiro, 2005).

[2] Here we have adopted a very literal definition of fragment-based drug design to mean an approach whereby the structure of a complex molecule may be simplified by "fragmenting" it into potentially active parts which can be tested for activity. No specific target is implied.

The fragments identified for biological activity maybe optimized to leads and eventually into drugs, or combined with other fragments to provide synergistic effects (Carr et al., 2005). However every determination of a pharmacophoric fragment may not lead to the development of a drug but might be incorporated in another drug molecule to make it potent/enhance activity/lessen side effect profiles. This was the case with the development of artemisinin derivatives for the treatment of chloroquine-resistant strains of malaria. The drawback with artemisinin (**3.3**) was poor bioavailability (Titulaer et al., 1990). Several studies highlighted the importance of the peroxide bridge in the molecule and that it was responsible for the mechanism of action of artemisinin (Brown, 2006). Such a realization led to the synthesis of first and second generations of artemisinin derivatives in the hope of improving bioavailability and potency. The second generation artemisinin derivatives have a different structural skeleton to artemisinin but contain the peroxide bridge.

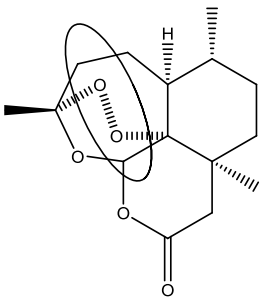

Artemisinin (3.3)

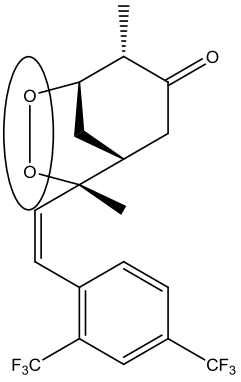

Arteflene (3.4)

Arteflene (**3.4**) is a second generation drug containing the endoperoxide bridge and is also active against chloroquine-resistant *Plasmodium falciparum* (Hofheinz et al., 1994). The presence of a small fragment from artemisinin rendered first and second generation derivatives active, and it can be concluded that once an important pharmacophore [3] is identified on a natural product molecule, that same fragment can be built into other molecules to impact activity.

[3] A pharmacophore is a group of atoms or functional groups responsible for a compound's biological activity.

3.1.3 Rationale

Figure 3.1 summaries some of the main structure-activity relationships for the halogenated monoterpenes tested in chapter two. Caution should be exercised when interpreting the cytotoxicity data for these compounds due to observed instabilities. It's also more informative to consider the activities of compounds within a source organism/structural class. In the *P. cornutum* group it is clear that the 7-dichloromethyl group, followed by a 7-aldehyde group seems to be more important for activity while a 7-methyl group at the same position shows a decrease in activity. Conversely, in the *P. suhrii* group all compounds with and without the 7-dichloromethyl moiety show similar activity. The only consistent theme in this group of compounds is the 3, 4-dichloro substitution pattern. The halogenation patterns in *P. corallorhiza* metabolites are even more complex which makes it difficult to draw any specific conclusions in terms of structure-activity relationships. However, it seems that the dichloromethyl or aldehyde moieties at position 1 give the most active compounds.

It is tempting to suggest that all the halogenated monoterpenes are likely to interact with biological targets via covalent bonding. However this does not explain the reported selectivity of these compounds. Furthermore, the cytotoxicity profiles of halomon-related compounds do not correspond to that of known DNA alkylating agents (Fuller et al., 1992; Fuller et al., 1994).

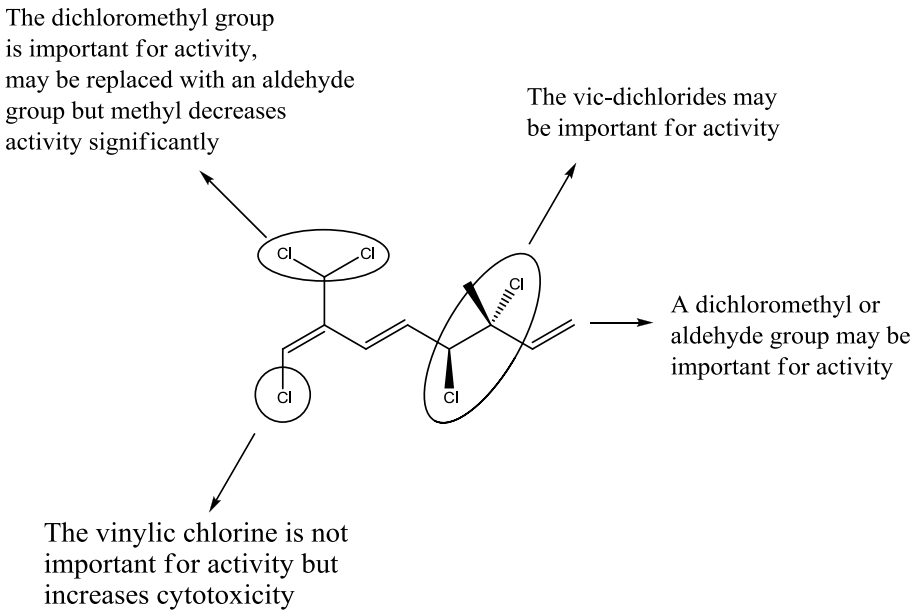

Figure 3.1: Summary of structure-activity information for halogenated monoterpenes from South African *Plocamium* spp

In this study we wished to systematically study the effect of different functional groups on the cytotoxicity of halogenated monoterpenes. As previously mentioned, stability issues related to natural products present with challenges that hinder progress in exploring their medicinal chemistry. However in this project, it was hypothesized that the C_5-C_8 diene system could be replaced with an aromatic ring. This would facilitate the introduction of selected functional groups into the ring. The presence of three sets of chlorines on these molecules should be noted; geminal chlorines, vicinal chlorines and a vinyl chlorine, and it is assumed that cytotoxic activity might be related to their orientation. Therefore an investigation into the positioning of the chlorines formed the basis for synthesis of HMT analogues. The dissection of compound **2.12** is presented in scheme 3.2**,** with various fragments to be explored on. The main focus of this part of the research was to explore the importance of the dichloromethyl moiety and selected isosteres on cytotoxic activity against a breast cancer cell line. This approach seemed reasonable since the anti-cancer drug, mitotane (**3.6**) also incorporates this aromatic and dichloromethyl moieties. It is quite possible that by making such drastic changes to the lead natural product that one may change its target in a cell based assay. Confirmation of the target can only be done once an optimized structure has been developed.

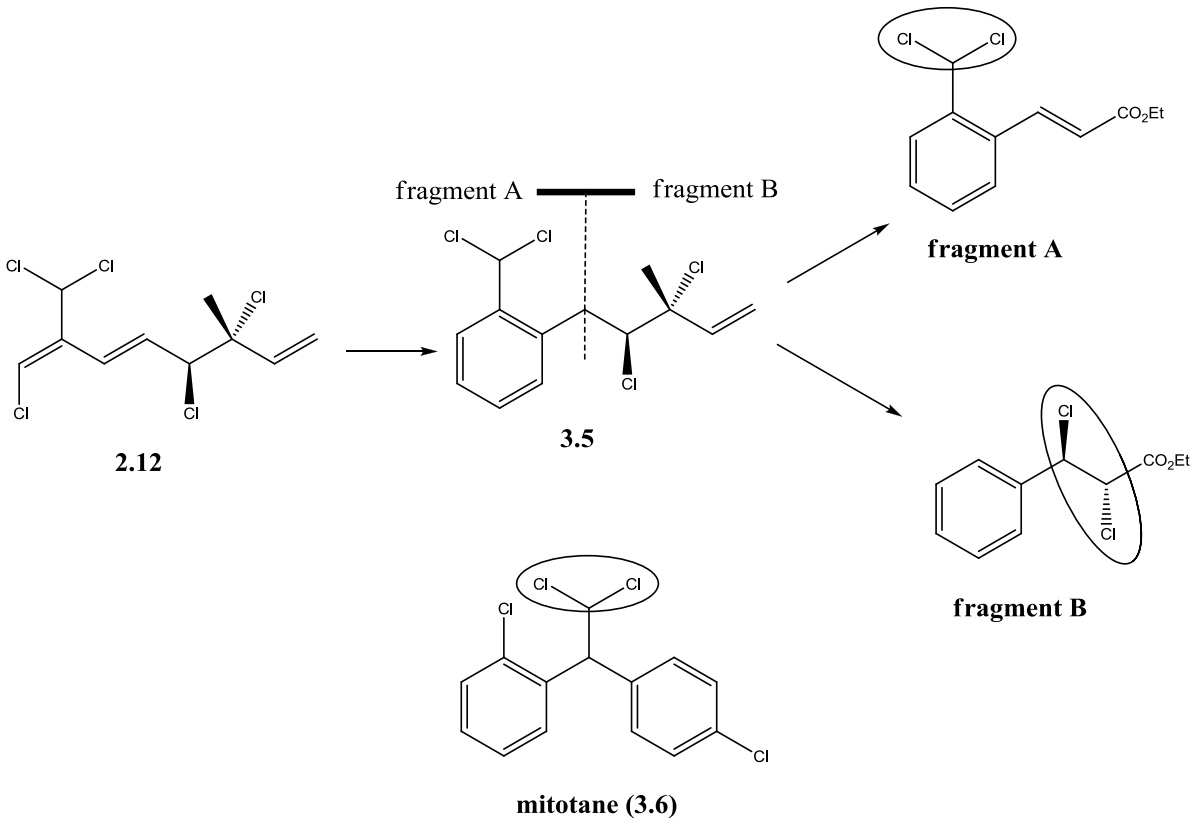

Scheme 3.2: Possible structural analogues of Plocornulide A (**2.12**)

Biological activity related to each set of chlorines was to be assessed in turn, thereby yielding several sets of fragments, as indicated above. Combinations will then be attempted i.e., geminal and vicinal chlorines or vinyl and geminal chlorines, resulting in subsequent series of other fragments, in the process determining any changes in cytotoxic properties. The relevance of geminal chlorines was assessed by varying substituents on position 7, thereby synthesizing a series of cinnamate esters and their carboxylic acid derivatives.

3.1.3 Cinnamate esters/Cinnamic acid derivatives

The first series of HMT analogues comprised of cinnamate ester derivatives and their corresponding carboxylic acids. Table 3.1 highlights the analogues that were targeted by varying substituents on the *ortho* position to the side chain.

Table 3.1: Cinnamate esters and carboxylic acid derivatives

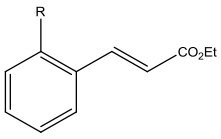

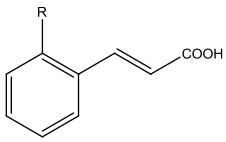

R	R
3.7 CH_3	**3.8** CH_3
3.9 Br	**3.10** Br
3.11 CHO	**3.12** CHO
3.13 CN	**3.14** CN
3.15 $CHCl_2$	**3.16** $CHCl_2$
3.17 H	**3.18** H
3.19 CF_3	**3.20** CF_3

Interaction of HMTs with the target site is unknown, whether it's covalent, electrostatic (dipole-dipole), or hydrogen bonding. Various functionalities were aimed at exploring the nature of the interaction and if the *gem*-chlorines are substitutable. It was also important to retain certain structural features that are present on the natural compounds to determine the effect of introducing the aromatic ring. Therefore -CH_3, -CHO, and -$CHCl_2$ functionalities were included in the series of analogues synthesized. The order of cytotoxicity in the natural products is from -CH_3 < -CHO < -$CHCl_2$ with -CH_3 being considered non-toxic (Antunes et al., 2011). A similar trend in the analogues would signify the aromatic ring is tolerated.

Substituents with similar physicochemical properties to either -CHO or -$CHCl_2$ functionalities were chosen. Polarity had already been assumed to be important in impacting cytotoxic behaviour considering the trends observed in the natural compounds; Plocornulide A (**2.12**) and C (**2.13**). Use of dipole-dipole moments to interact with the target site would suggest that any polar functional group would have a similar cytotoxic effect, hence substitution with -CF_3, or if a halogen is required, then substituents with -Br and -CF_3 should be active. If hydrogen bonding was required, then the similar cytotoxic effect should be noticed when -CN is substituted for -CHO.

The ethyl ester linker results in highly lipophilic analogues which in some cases were similar to the natural compounds; hence absorption issues into cells were averted. However in an effort to improve on water solubility of the analogues, their carboxylic acid counterparts were synthesized and biological activity assessed. This was aimed at satisfying Lipinski's rule of five that tests a compound's suitability to be taken as an oral dosage form.

3.2 Results and discussion

Cinnamate ester derivatives can be prepared by use of various condensation reactions. Commonly adopted methods include the Wittig reaction, Aldol condensation, Perkin condensation and Knoevenagel and Doebner modification reactions (Simonyan, 1999). The synthetic approaches to the preparation of compounds are summarised below (Scheme 3.3).

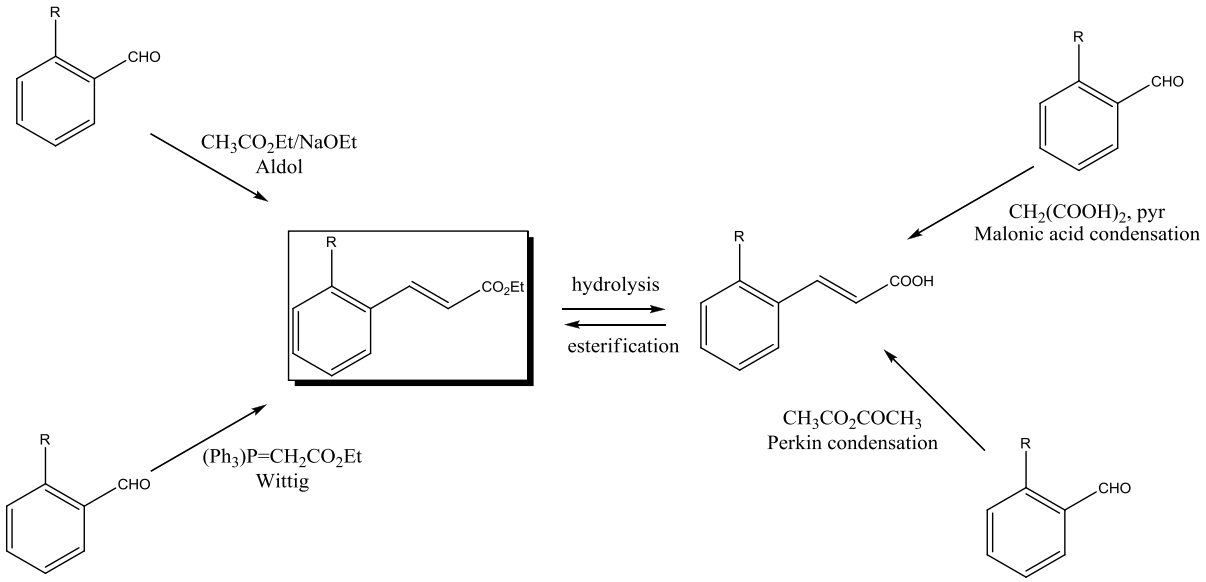

Scheme 3.3: General strategies used in the synthesis of cinnamic acid derivatives

3.2.1. Synthesis of *o*-methyl cinnamate (3.7) and its carboxylic acid derivative (3.8)

O-methyl cinnamate (**3.7**) was synthesized in about 60-70% yield by the condensation of tolualdehyde (**3.21**) with EtOAc using NaOEt as a base (Scheme 3.4) (Srinivasan and Perumal, 2006). Base hydrolysis of **3.7** gave the free acid in good yield (Scheme 3.4). Alternatively, the cinnamic acid (**3.8**) was synthesized *via* a malonic acid condensation reaction, followed by esterification to the cinnamate (**3.7**) (Scheme 3.4).

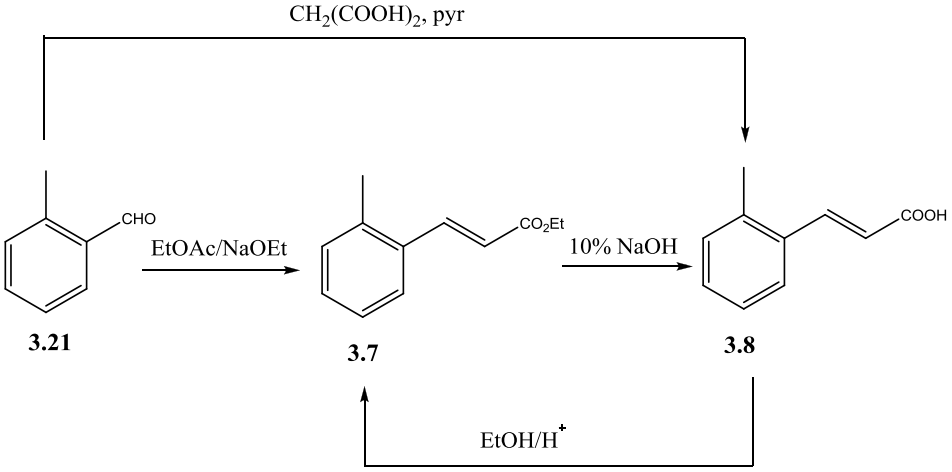

Scheme 3.4: Preparation of *o*-methyl cinnamate (**3.7)** and its free acid (**3.8**)

Distinguishing features of the ^{1}H NMR spectrum of **3.7** include signals at δ 1.38 (3H, t, 7.1 Hz) and δ 4.31 (2H, q, 7.1 Hz) due to the ethyl group; δ 6.46 (1H, d, 16 Hz) and 7.72 (1H, d, 16 Hz) due to the *E*-double bond and an aromatic methyl signal at δ 2.47 (3H, s) (Figure 3.2, Table 3.2). Confirmation of an α, β-unsaturated system was clearly evident from the ^{13}C NMR signals at δ 167.5 (C-3), 119 (C-4) and 142 (C-5) (Figure 3.3). All other ^{1}H and ^{13}C NMR (Table 3.2 & 3.3) chemical shifts are consistent with literature data (Huang et al., 2010).

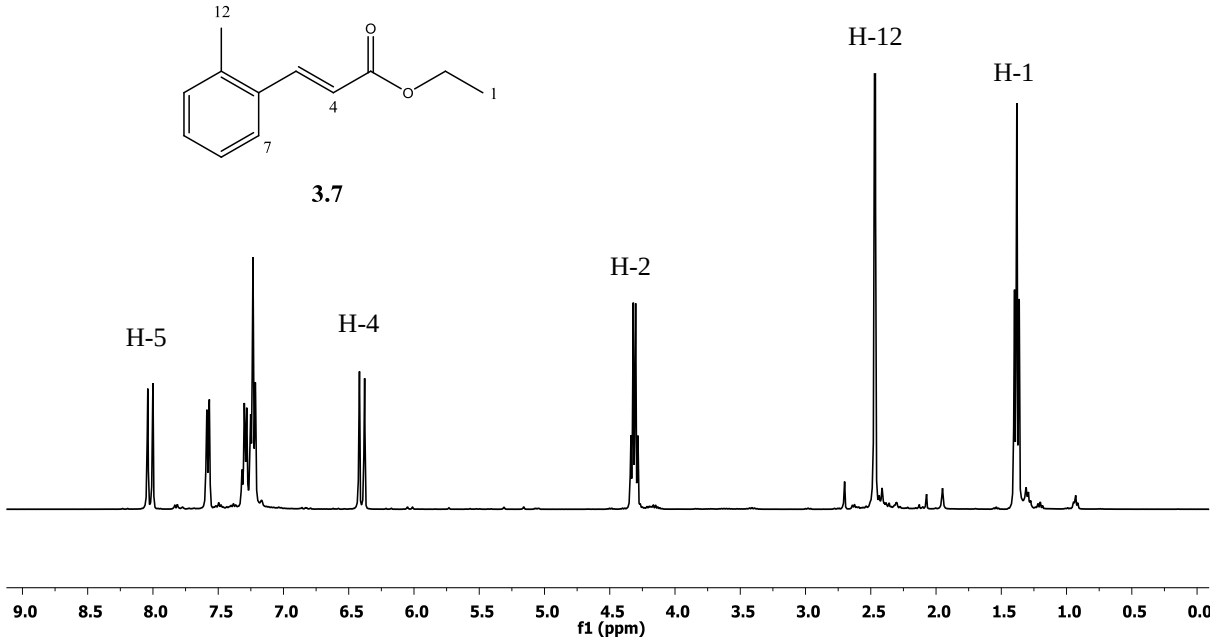

Figure 3.2: ^{1}H NMR (400 MHz, $CDCl_3$) spectrum of *o*-methyl cinnamate (**3.7**)

The ^{1}H and ^{13}C NMR spectra of *o*-methyl cinnamic acid (**3.8**) showed the expected disappearance of the ethyl moiety C-1 and C-2 (Figure 2.4) (Table 3.2 & 3.3). The presence of the carboxylic acid was confirmed by the downfield shift of the carbonyl signal from δ 167.45 to δ 172.48 in the ^{13}C NMR spectrum (Figure 3.3, Table 3.4 & 3.5). The observed chemical shifts for both the proton and carbon spectra are consisted with literature data (Pardin et al., 2008).

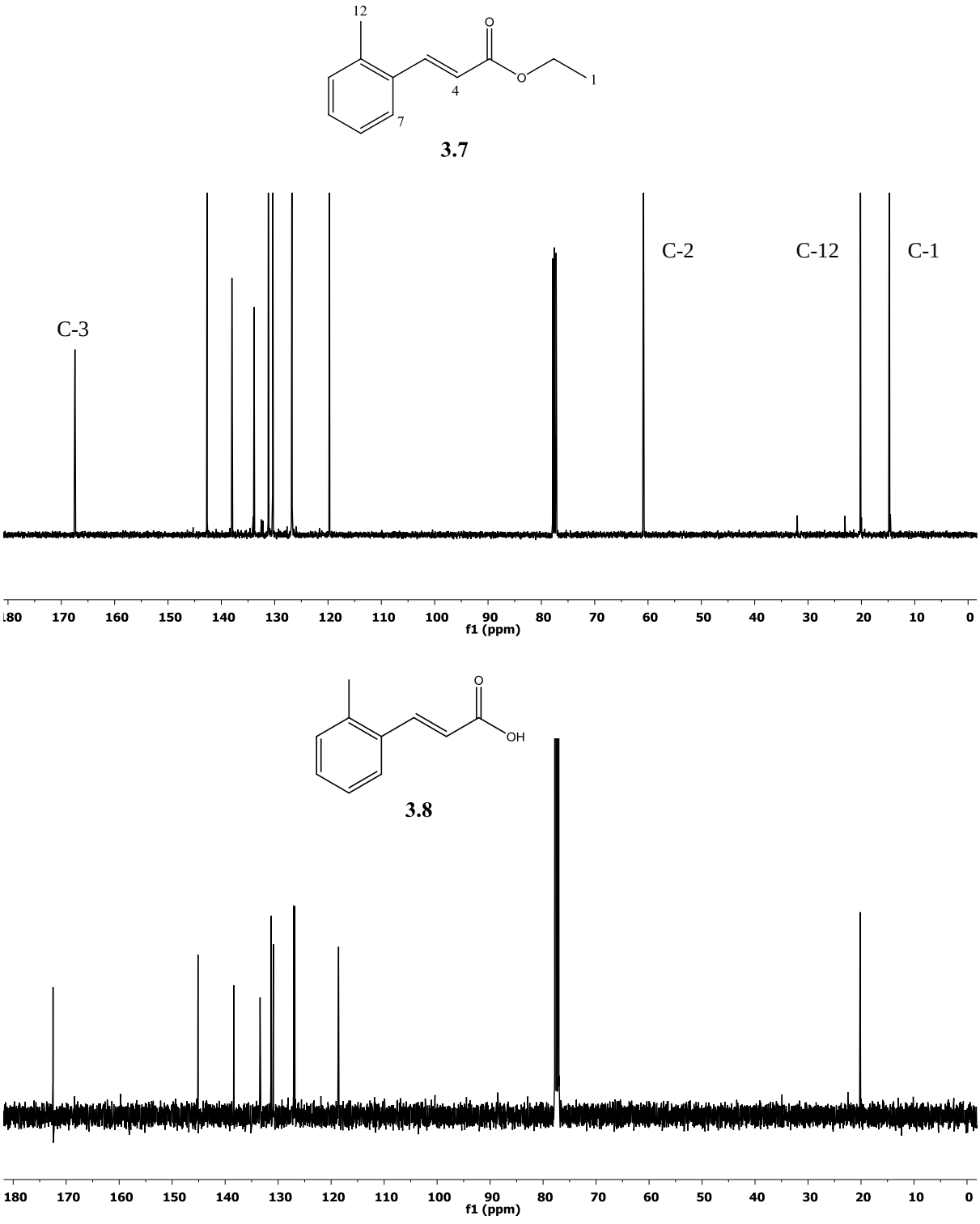

Figure 3.3: Comparison of the ^{13}C (100 MHz, $CDCl_3$) spectra of *o*-methyl cinnamate (**3.7**) and its carboxylic acid derivative (**3.8**)

3.2.2 Synthesis of *o*-bromo cinnamate (3.9) and its carboxylic acid derivative (3.10)

The preparation of *o*-bromo cinnamate (**3.9**) and its carboxylic acid derivative (**3.10**) was conducted in a similar manner to *o*-methyl cinnamate (**3.7**) (Section 3.2.1).

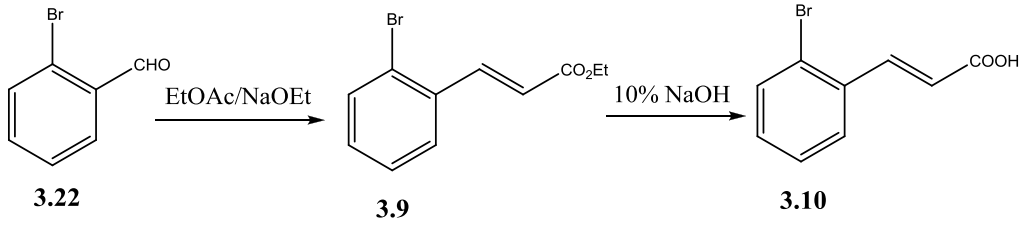

Scheme 3.5: Preparation of o-bromo cinnamate (**3.9**) and its carboxylic acid (**3.10**)

The ^{1}H and ^{13}C NMR data are consistent with data noted in literature (Table 3.2-3.5) (Brittelli, 1981; Lu and Toy, 2011).

3.2.3 Synthesis of *o*-formyl cinnamate (3.11) and its carboxylic derivative (3.12)

Aldol condensation between phthaldialdehyde (**3.23**) and EtOAc did not give the desired *o*-formyl cinnamate (**3.11**). However, *o*-formyl cinnamate (**3.11**) was prepared by a Wittig reaction between phthaldialdehyde (**3.23**) and ethoxycarbonylmethyl-triphenylphosphonium chloride using NaOH as base in 80-85% yields (Scheme 3.6).

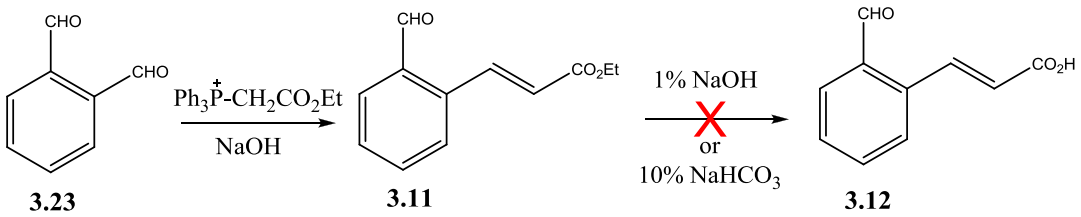

Scheme 3.6: Preparation of o-formyl cinnamate **(3.11)**

The α, β-unsaturated ester moiety was evident from the ^{1}H NMR signals at δ 6.38 (d, 15.9 Hz) and δ 8.52 (d, 15.9 Hz) while the aldehyde proton appeared at δ 10.28 (s). ^{1}H and ^{13}C NMR data for **3.11** is consistent with literature values (Park et al., 2011) (Table 3.2 & 3.3).

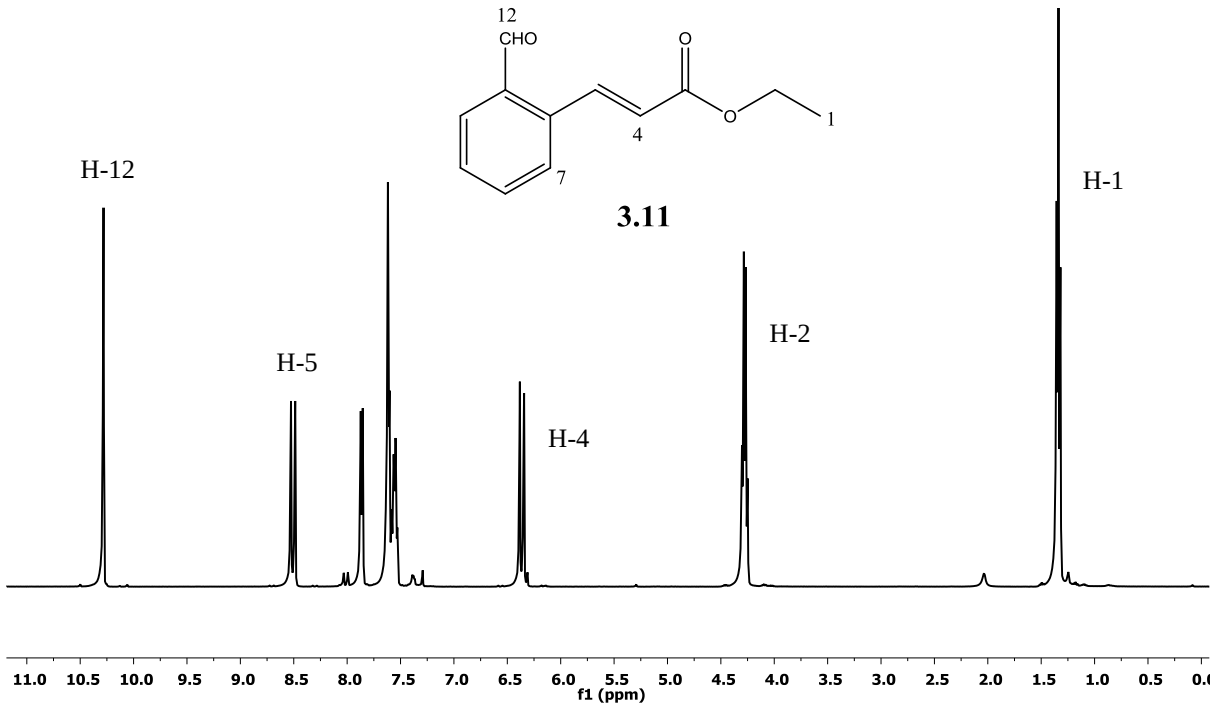

Figure 3.4: ^{1}H NMR (400 MHz, $CDCl_3$) spectrum of *o*-formyl cinnamate (**3.11**)

All attempts at effectively hydrolysing the parent ester (**3.11**) using varying concentrations of NaOH and $NaHCO_3$ were unsuccessful (Scheme 3.6). In order to circumvent problems associated with the hydrolysis of the ester moiety in **3.11** and since we have already demonstrated the formation of the *o*-methyl cinnamic acid (**3.8**) *via* a malonic acid condensation procedure (Doebner modification, Scheme 3.4), we explored the use of this reaction to prepare *o*-formyl cinnamic acid (**3.12**) directly (Scheme 3.7). Thus, phthaldialdehyde (**3.23**) was reacted with malonic acid using pyridine as a base. To our surprise, the ^{1}H NMR spectrum of the crude product showed loss of both aldehyde signals and lack of the expected α, β-unsaturated system in the product. The ^{1}H NMR spectrum (Figure 3.5) of the purified product showed several deshielded aromatic methines and two methylene triplets at δ 2.72 and δ 3.18. In addition, the ^{13}C (Figure 3.6) and DEPT-135 NMR spectra showed the presence of a ketone carbonyl at δ 207.48 while confirming the presence of the two methylene groups at δ 26.24 (C-3) and δ 36.65 (C-2) This information was consistent with the structure of indanone (**3.24**) (Kumar et al., 2011; Sanchez-Larios et al., 2011).

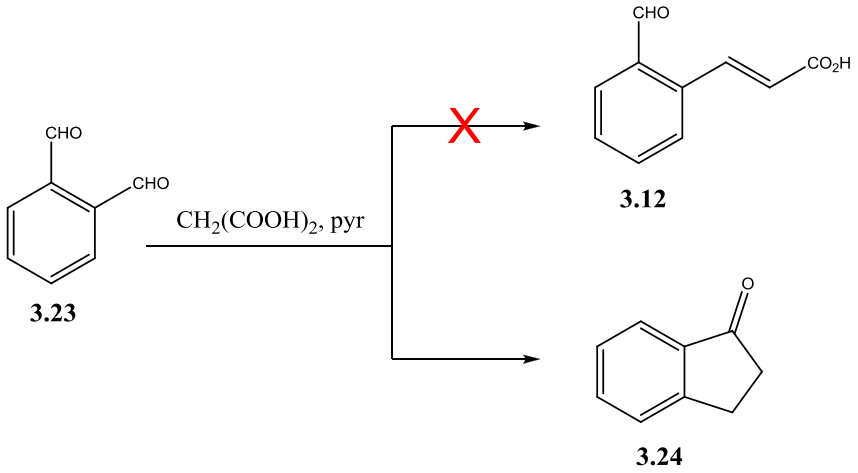

Scheme 3.7: Attempted synthesis of *o*-formyl cinnamic acid (**3.12**) using the Doebner modification of the Knoevenagel reaction

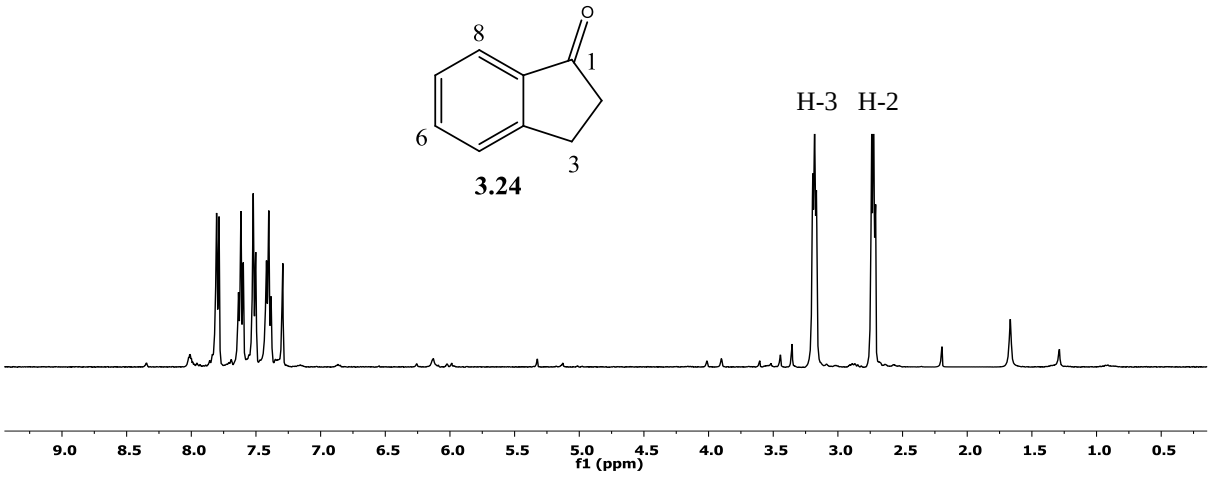

Figure 3.5: ^{1}H NMR (400 MHz, $CDCl_3$) spectrum of indanone (**3.24**)

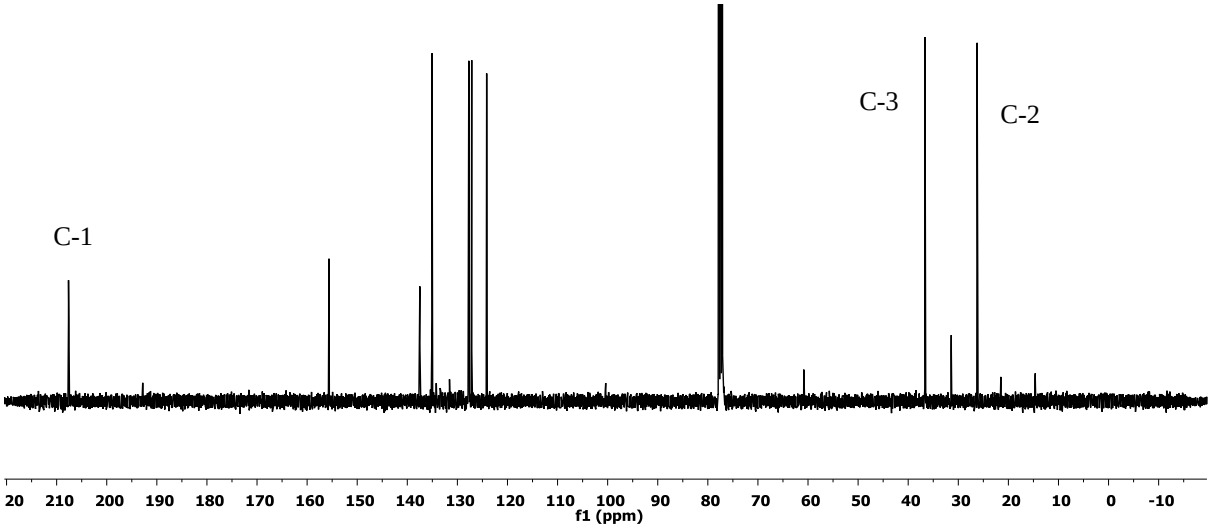

Figure 3.6: ^{13}C NMR (100 MHz, $CDCl_3$) spectrum of indanone (**3.24**)

A literature search found that this reaction had been used in the 1950s in the synthesis of indanone (**3.24**). Wiley and Hobson attempted to synthesise *o*-formyl cinnamic acid by reacting phthaldialdehyde (**3.23**) with malonic acid in the presence of pyridine. They reported a decarboxylation stage that resulted in the formation of indan-l-one (**3.24**). The proposed mechanism for the reaction is shown below (Scheme 3.8).

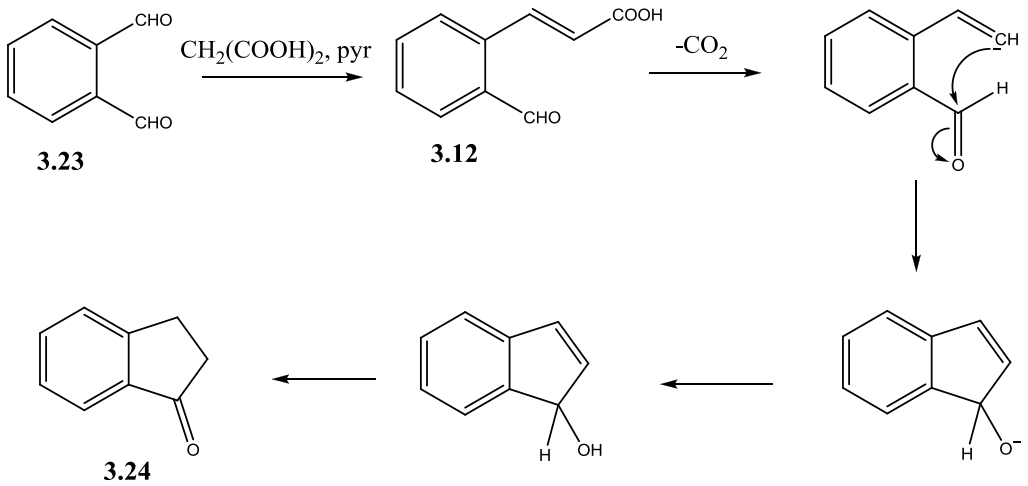

Scheme 3.8: Proposed mechanism for the formation of indanone (**3.24**) from phthaldialdehyde (**3.23**)

In their experiments, they demonstrated that *o*-formyl cinnamic acid (**3.12**) is formed as an intermediate. The cyclization process involves reaction of the ion formed by decarboxylation, with the carbonyl carbon of the neighbouring aldehyde forming 1 hydroxyindene. A prototropic change results in 1 hydroxyindene being converted to indan-1-one (Dijksman and Newbold, 1952).

Isolation of the intermediate *o*-formyl cinnamic acid (**3.12**) presented with challenges of determining at which stage to stop the reaction. Even following the reaction in an NMR tube could not give an indication of the endpoint for the synthesis of the carboxylic acid derivative. Another strategy was therefore formulated, which involved protecting the aldehyde group of *o*-formyl cinnamate (**3.11**) and attempted hydrolysis of the ester.

O-formyl cinnamate (**3.11**) was thus converted to the 1.3-dioxolane (**3.25**) after which the ester was successfully hydrolysed to the carboxylic acid. Treatment of the latter with dilute HCl gave the required *o*-formyl cinnamic acid (**3.12**) in good yield (Scheme 3.9). The ^{1}H NMR spectrum showed the disappearance of the ethyl moiety at signals δ 1.35 (t, 7.1 Hz) and δ 4.29 (q, 7.1 Hz) (Figure 3.7).

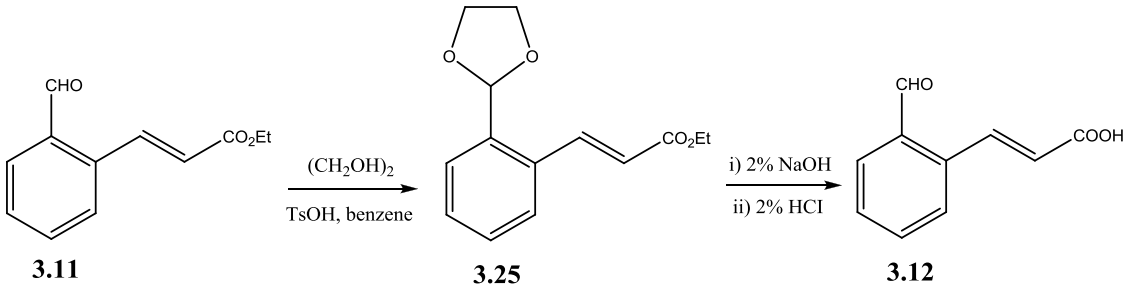

3.11 **3.25** **3.12**

Scheme 3.9: Aldehyde protection of *o*-formyl cinnamate (**3.11**)**,** and its hydrolysis

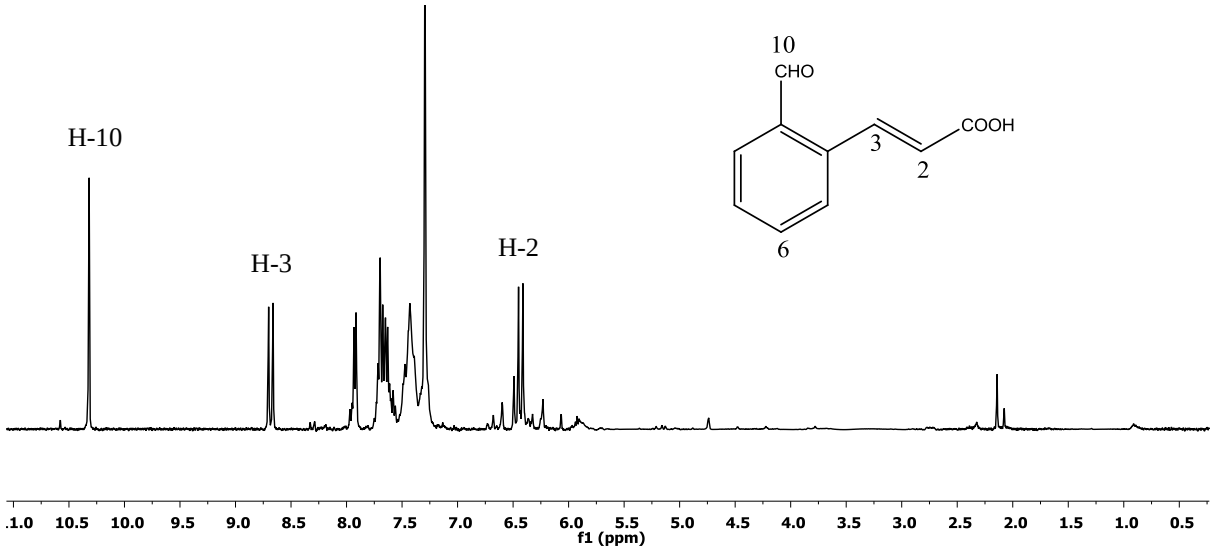

Figure 3.7: ^{1}H NMR (400 MHz, $CDCl_3$) spectrum of *o*-formyl cinnamic acid (**3.12**)

3.2.4 Synthesis of *o*-cyano cinnamate (3.13) and its carboxylic acid derivative (3.14)

A Wittig reaction (section 3.2.3) was also used for the preparation of *o*-cyano cinnamate (**3.13**) (Scheme 3.10) after failure to obtain the desired product *via* the Aldol condensation reaction (Section 3.2.1) between cyanobenzaldehyde (**3.26**) and EtOAc. The ^{1}H and ^{13}C NMR analysis confirmed that product **3.13** had been successfully synthesized. The α, β-unsaturated ester moiety was evident from the ^{1}H NMR signals at δ 6.60 (d, 16.0 Hz) and δ 7.94 (d, 16.0 Hz). The nitrile carbon attached on the aromatic ring could be observed at δ 117.50 in a ^{13}C spectrum. ^{1}H and ^{13}C NMR data for **3.13** are consistent with literature values. (Table 3.2 & 3.3).

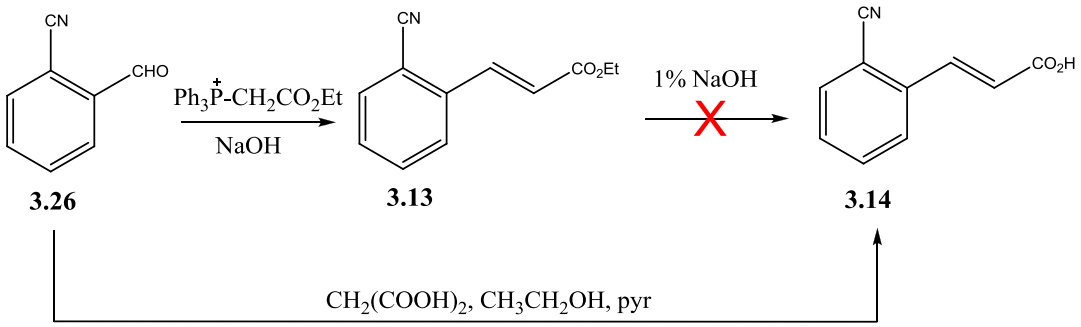

Scheme 3.10: Preparation of *o*-cyano cinnamate (**3.13**) and its carboxylic acid derivative (**3.14**)

The carboxylic acid derivative (**3.14**) could not be obtained by alkaline hydrolysis of the parent ester (**3.13**) as nitriles are also susceptible to base hydrolysis, yielding primary amides and carboxylic acids (Vanderwerff, 1977) (Scheme 3.10). A direct condensation between cyanonbenzaldehyde (**3.26**) and malonic acid was therefore explored using ethanol and a small volume of pyridine yielding **3.14** as an ethanol-insoluble cinnamic acid in good yield (Scheme 3.10). ^{1}H and ^{13}C NMR data obtained are consistent with literature values (Table 3.4 & 3.5).

3.2.5 Synthesis of *o*-dichloromethyl cinnamate (3.15) and its carboxylic acid derivative (3.16)

Several chlorination reagents have been used to generate geminal dichlorides from aldehydes, the most common being PCl_5 (Armstrong and Richardson, 1933). Other reagents include $SOCl_2$/N,N-dimethylformamide (Newman and Sujeeth, 1978), WCl6 (Firouzabadi and Shiriny, 1996), BCl_3 (Kabalka and Wu, 2000) etc. We initially explored the conversion of benzaldehydes to aromatic *gem*-chlorides using BCl_3 and tolualdehyde (**3.21**), as a model reaction (Scheme 3.11). This reaction had previously been employed to convert a number of substituted benzaldehydes to dichlorides (Scheme 3.12). Thus tolualdehyde (**3.21**) was treated with BCl_3 in hexane under anhydrous conditions to give an immediate white precipitate which disappeared on heating for 1.5 h. The reaction was quenched with water and the organic layer separated. The ^{1}H NMR spectrum (Figure 3.8) of the crude reaction mixture showed the presence of both unreacted starting material (aldehyde proton at δ 10.33) and a distinct peak at δ 6.98 which is characteristic of the proton of a dichloromethyl moiety. Integration of the aldehyde peak relative to the dichloromethyl peak suggested 40%

conversion. Increasing the number of equivalents of BCl_3 from one to two resulted in an improved yield of 66%.

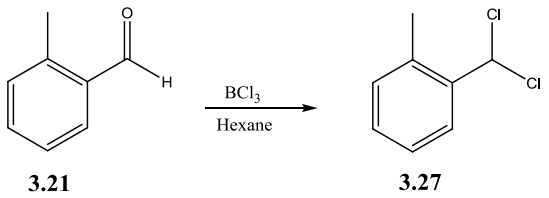

3.21 **3.27**

Scheme 3.11: Conversion of tolualdehyde (**3.21**) to *gem*-dichloromethyltoluene (**3.27**) using BCl_3

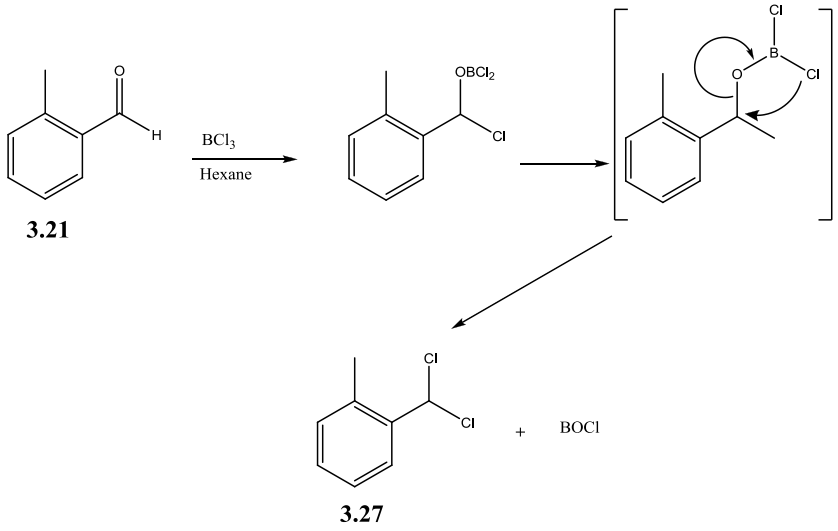

3.21 **3.27**

Scheme 3.12: Proposed mechanism for the conversion of an aldehyde to gem-dichlorines using BCl_3

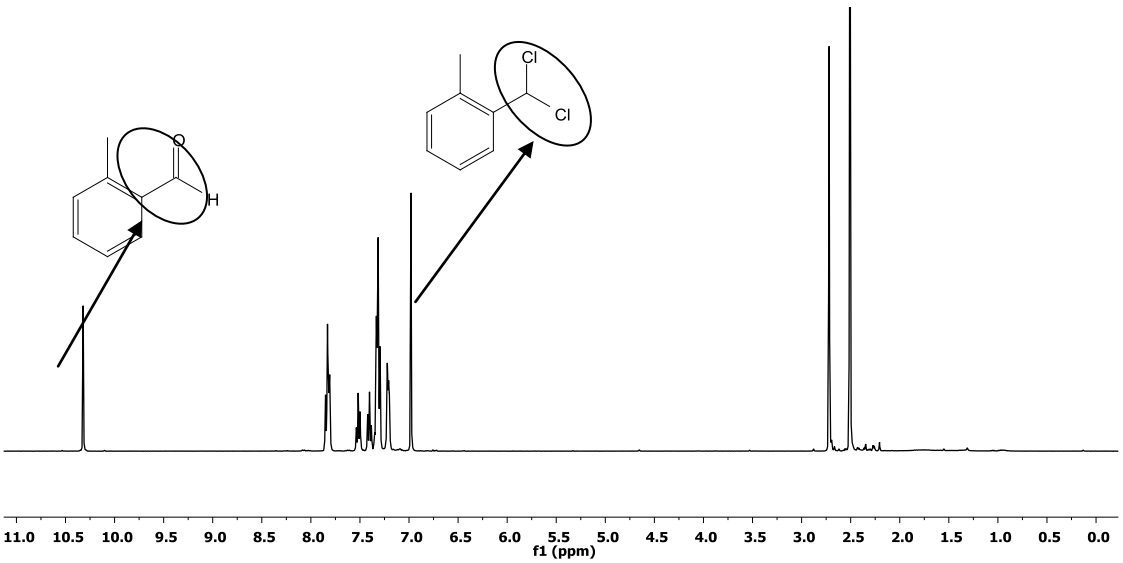

Figure 3.8: ^1H NMR (400 MHz, $CDCl_3$) spectrum of crude reaction mixture of conversion of tolualdehyde (**3.21**) to 1-(dichloromethyl)-2-methylbenzene (**3.27**)

Success of the model reaction encouraged us to use the same protocol to synthesize *o*-dichloromethyl cinnamate (**3.15**) from *o*-formyl cinnamate (**3.11**) (Scheme 3.13). A complex ^{1}H NMR spectrum was obtained with no desired product being formed. An attempt was made in preparing 1-dichloromethyl-benzaldehyde (**3.28**) from phthaldialdehyde (**3.23**) using BCl_3, with the hope of reacting **3.28** with the Wittig reagent to obtain **3.15,** however the reaction was unsuccessful (Scheme 3.13). An attempt to chlorinate a protected phthaldialdehyde (**3.29**) to obtain **3.30** and subsequently to **3.28** by use of an acid was also unsuccessful (Scheme 3.13).

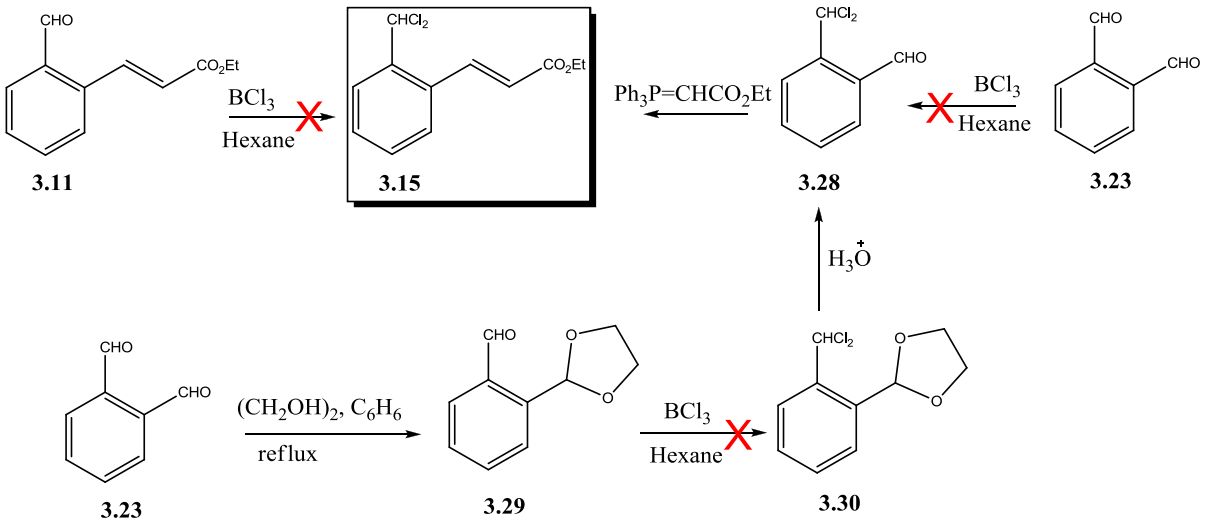

Scheme 3.13: Attempted synthesis of *o*-dichloromethyl cinnamate (**3.15**)

A new chlorinating agent was sought, and thionyl chloride ($SOCl_2$) was selected in the next attempt, also using tolualdehyde as a model reaction (Scheme 3.14).

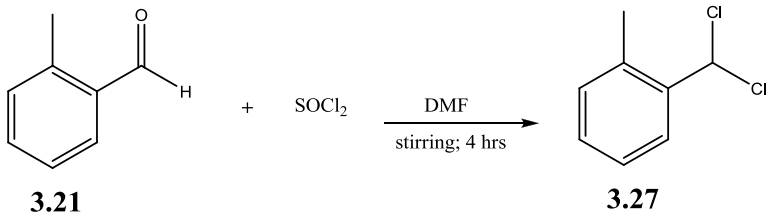

Scheme 3.14: Conversion of tolualdehyde (**3.21**) to *gem*-dichloromethyltoluene (**3.27**) using $SOCl_2$

The ^{1}H NMR spectrum of the product showed the characteristic peak at δ 7.05 suggestive of a dichloromethyl moiety. This reaction showed an improved yield (almost quantitative) compared to the reaction with BCl_3. The successful conversion of tolualdehyde (**3.21**) to

gem-dichloromethyl toluene (**3.27**) gave us confidence that this reaction could be successful in the conversion of *o*-formyl cinnamate (**3.11**) to *o*-dichloromethyl cinnamate (**3.15**) (Scheme 3.15).

3.11 **3.15**

Scheme 3.15: Conversion of *o*-formyl cinnamate (**3.11**) to *o*-dichloromethyl cinnamate (**3.15**)

Reaction of *o*-formyl cinnamate (**3.11**) with $SOCl_2$ in DMF gave a product which lacked the aldehyde signal and showed the expected proton of the dichloromethyl signal at δ 7.06 (s). This latter signal showed HMBC correlation to aromatic carbon signals at δ 128.07 (s) and δ 132.12 (s) confirming its presence on the aromatic ring. The ^{1}H and ^{13}C NMR spectra showed the presence of an intact α, β-unsaturated ester with olefinic methine signals at δ 6.42 (d, 15.7 Hz) (δ 123. 20, s) and δ 8.13 (d, 15.7 Hz) (δ 140.19, s) and ethyl ester signals at δ 1.39 (t, 7.1 Hz (δ 14.70, s), δ 4.33 (q, 7.1 Hz) (δ 61.27, s) and (δ 166.61, s) (Table 3.2 & 3.3).

ESIMS showed a molecular ion at *m/z* 259 and another peak at *m/z* 261 signalling different isotopes of chlorines attached to the molecule. *O*-dichloromethyl cinnamate (**3.15**) was therefore successfully prepared from *o*-formyl cinnamate (**3.11**)**.**

Preparation of *o*-dichloromethyl cinnamic acid (**3.16**) was attempted *via* hydrolysis of its parent ester (**3.15**). ^{1}H NMR of the product showed conversion of the dichloromethyl- moiety to an aldehyde, rather than the ester hydrolysis anticipated (Scheme 3.16). Re-emergence of the aldehyde peak was noted at δ 10.27 (s) with the disappearance of the dichloromethyl proton at δ 7.06 (s) (Table 3.4 & 3.5)

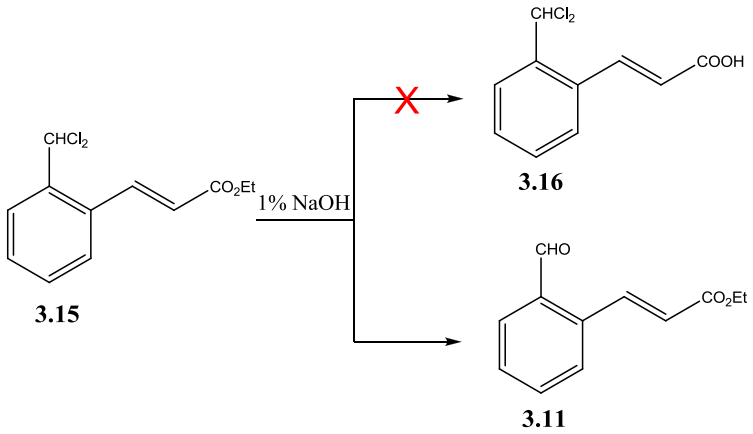

Scheme 3.16: Attempted synthesis of *o*-dichloromethyl cinnamic acid (**3.16**) by hydrolysis of the parent ester (**3.15**)

Successful synthesis of *o*-dichloromethyl cinnamic acid (**3.16**) was achieved by reacting *o*-formyl cinnamic acid (**3.12**) with $SOCl_2$ in dimethylformamide (Scheme 3.17).

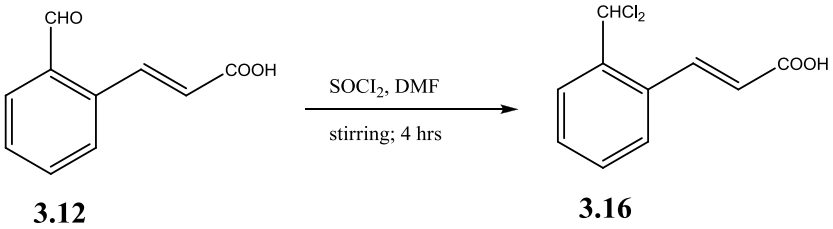

Scheme 3.17: Conversion of *o*-formyl cinnamic acid (**3.12**) to *o*-dichloromethyl cinnamic acid (**3.16**)

The ^{1}H NMR spectrum showed the disappearance of the aldehydic proton at δ 10.32 (s) and the emergence of a signal at δ 7.05 (s) corresponding to the dichloromethyl moeity. The α, β-unsaturated system was still apparent at signals δ 6.52 (d, 15.9 Hz) and δ 8.23 (d, 15.9 Hz)**.** The presence of the carbonyl carbon was observed in the ^{13}C spectrum at δ 170.53 (s) together with a signal at δ 71. 34 (s) corresponding to the dichloromethyl moiety (Table 3.4 & 3.5).

3.2.6 Synthesis of *o*-trifluoromethyl cinnamate (3.19) and its carboxylic acid derivative (3.20)

The preparation of *o*-trifluoromethyl cinnamate (**3.19**) was conducted by esterification of commercially available *o*-trifluoromethyl cinnamic acid (**3.20**) with ethanol.

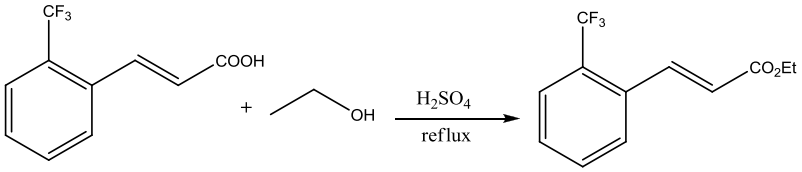

3.20 **3.19**

Scheme 3.18: Esterification of *o*-trifluoromethyl cinnamic acid (**3.20**) to *o*-trifluoromethyl cinnamate (**3.19**)

The ^{1}H and ^{13}C spectroscopic data obtained for the product showed a successful esterification reaction and the formation of *o*-trifluoromethyl cinnamate (**3.19**). The key NMR features highlighted on other ester derivatives' spectra were also noted with an additional peak at δ 123.01 on its ^{13}C spectrum representing the carbon of $-CF_3$. The NMR data are consistent with literature values (Table 3.2 & 3.3) (Liu et al., 2010a).

With the successful synthesis of compounds **3.7** to **3.20**, we were now ready to explore the activity against breast cancer cells (Chapter 4).

Table 3.2: ^{1}H NMR (400 MHz) data for ester derivatives in $CDCl_3$

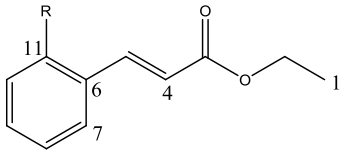

	Compound						
	Chemical shift (δ), mult., *J* (Hz)						
	3.7	**3.9**	**3.11**	**3.13**	**3.15**	**3.17**	**3.19**
	$R=CH_3$	R=Br	R=CHO	R-CN	$R=CHCl_2$	R=H	$R=CF_3$
H-1	1.38, t, 7.1	1.38, t, 7.1	1.35, t, 7.1	1.34, t, 7.1	1.39, t, 7.1	1.35, t, 7.1	1.36, t, 7.1
H-2	4.31, q, 7.1	4.32, q, 7.1	4.29, q, 7.1	4.28, q, 7.1	4.33, q, 7.1	4.29, q, 7.1	4.30, q, 7.1
H-4	6.40, d, 15.9	6.42, d, 15.9	6.38, d, 15.9	6.60, d, 16.0	6.42, d, 15.7	6.46, d, 16.0	6.43, d, 15.8
H-5	8.02, d, 15.9	8.08, d, 15.9	8.52, d, 15.9	7.94, d, 16.0	8.13, d, 15.7	7.72, d, 16.0	8.08, d, 15.8
H-7	7.58, d, 7.7	7.64, d, 7.5	7.56, d, 7.2	7.69, d, 7.7	7.56, d, 7.6	7.53, m	7.71, d, 7.6
H-8	7.23, t, 7.1	7.36, t, 7.4	7.64, t, 7.4	7.63, t, 7.7	7.51, t, 7.6	7.38, m	7.48, t, 7.6
H-9	7.23, t, 7.1	7.26, t, 7.7	7.59, t, 7.2	7.48, t, 7.6	7.44, t, 7.5	7.38, m	7.58, t, 7.6
H-10	7.31, d, 7.2	7.65, d, 7.6	7.86, d, 7.4	7.73, d, 8.0	7.88, d, 7.8	7.38, m	7.71, d, 7.6
H-11	-	-	-	-	-	7.53, m	-
H-12	2.47, s	-	10.28, s	-	7.06, s	-	-

Table 3.3: ^{13}C NMR (100 MHz) data for ester derivatives in $CDCl_3$

Carbon	Compound						
	Chemical shift (δ)						
	3.7	**3.9**	**3.11**	**3.13**	**3.15**	**3.17**	**3.19**
	R=CH_3	R=Br	R=CHO	R=CN	R=$CHCl_2$	R=H	R=CF_3
C-1	14.65	14.64	14.67	14.64	14.70	14.62	14.53
C-2	60.88	61.11	61.09	61.34	61.27	60.82	61.17
C-3	167.45	166.80	166.56	166.19	166.61	167.37	166.49
C-4	119.73	121.59	123.59	123.53	123.20	118.69	122.99
C-5	142.68	143.33	141.29	139.69	140.19	144.99	140.42
C-6	138.02	135.02	136.99	137.74	132.12	134.88	133.83
C-7	130.37	128.18	130.27	133.90	130.75	128.46	129.92
C-8	126.78	131.53	134.25	130.48	130.65	129.30	132.48
C-9	131.19	128.10	128.34	127.42	127.76	130.62	128.27
C-10	133.85	133.84	132.62	138.44	128.07	129.30	132.12
C-11	138.02	125.70	136.99	113.03	138.77	128.46	129.19
C-12	20.18	-	192.14	117.50	69.15	-	122.99

Table 3.4: ^{1}H NMR (400 MHz) data for carboxylic acid derivatives in $CDCl_3$

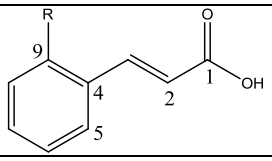

Proton	Compound						
	Chemical shift (δ), mult., *J* (Hz)						
	3.8 R=CH_3	**3.10** R=Br	**3.12** R=CHO	**3.14** R-CN	**3.16** R=$CHCl_2$	**3.18** R=H	**3.20** R=CF_3
H-2	6.42, d, 15.9	6.44, d, 16.0	6.43, d, 15.8	6.74, d, 16.0	6.52, d, 15.9	6.51, d, 16.0	6.55, d, 15.9
H-3	8.13, d, 15.9	8.20, d, 16.0	8.68, d, 15.8	7.97, d, 16.0	8.23, d, 15.9	7.85, d, 16.0	7.93, d, 15.9
H-5	7.63, d, 7.6	7.69, d, 7.4	7.92, d, 7.3	7.81, d, 7.2	7.84, d, 7.3	7.60, d, 7.4	7.62, d, 7.6
H-6	7.33, t, 7.5	7.35, t, 7.6	7.70, t, 7.5	7.74, t, 7.4	7.68, t, 7.4	7.46, m	7.70, t, 7.7
H-7	7.29, t, 7.4	7.40, t, 7.5	7.43, m	7.59, t, 7.4	7.48, t, 7.5	7.46, m	7.52, t, 7.3
H-8	7.25, d, 7.2	7.58, d, 7.5	7.66, d, 7.4	7.63, d, 7.6	7.62, d, 7.4	7.46, m	7.79, d, 7.5
H-9	-	-	-	-	-	7.60, d, 7.3	-
H-10	2.50, s	-	10.28, s	-	7.05, s	-	-

Table 3.5: ^{13}C NMR (100 MHz) data for carboxylic acid derivatives

Carbon	Compound Chemical shift (δ)						
	3.8 R=CH_3	**3.10** R=Br	**3.12** R=CHO	**3.14** R-CN	**3.16** R=$CHCl_2$	**3.18** R=H	**3.20** R=CF_3
C-1	171.97	170.98	173.12	170.82	170.53	172.99	167.74
C-2	118.50	120.09	122.34	123.50	122.85	117.76	124.47
C-3	145.22	145.47	144.82	139.70	145.67	147.55	139.19
C-4	138.48	133.93	135.78	137.48	136.92	134.38	133.87
C-5	131.29	127.61	129.03	133.45	130.56	128.81	129.05
C-6	126.62	128.19	131.23	130.73	131.99	129.40	133.06
C-7	131.29	128.37	128.97	127.10	128.87	131.19	131.00
C-8	130.80	132.02	130.79	131.56	132.01	129.40	126.82
C-9	133.50	125.98	132.34	112.35	134.93	128.81	127.74
C-10	20.03	-	193.42	116.87	71.34	-	124.47

3.3 EXPERIMENTAL

General experimental

Solvents

All solvents (hexane, EtOAc, MeOH) used for chromatography were of Chromasolv grade and acquired from Sigma Aldrich South Africa.

Chromatography

Column chromatography was conducted using silica gel 60 (0.040-0.063 mm), 230-400 mesh (ASTM Merck). Thin layer chromatography experiments were run on silica gel $60F_{254}$ aluminium sheets. TLC plates were visualized using a Syngene UV lamb 230 V, 50 Hz with dual wavelengths 365 nm and 254 nm.

Nuclear magnetic resonance (NMR)

NMR data (1D and 2D experiments) were acquired on a Bruker Avance 400 MHz spectrophotometer. Chemical shifts were recorded in ppm and referenced to residual deuterated solvent ($CDCl_3$ δ_H 7.26, δ_C 77.0). All coupling constants are reported in Hz.

Infrared & Ultra Violet spectrophotometry

Infrared spectra were obtained on a Perkin-Elmer Universal ATR sampling accessory machine as dry films. Ultraviolet measurements were obtained on the GBC UV/ Vis 916 spectrometer in MeOH.

Mass spectrometry

Electrospray ionization mass spectroscopy (ESI-MS) was obtained on a Waters Synapt G2 instrument at Stellenbocsh University, South Africa. Introduction was by direct injections (1 µl) into a stream of 50% acetonitrile, 0.1% formic acid using a Waters UPLC at a flow rate of 0.2 ml/min, capillary voltage 3 kV and Cone voltage 15 V.

(*E*)-ethyl 3-o-tolylacrylate (3.7) and its carboxylic acid derivative (3.8)

(o-methyl cinnamate & o-methyl cinnamic acid)

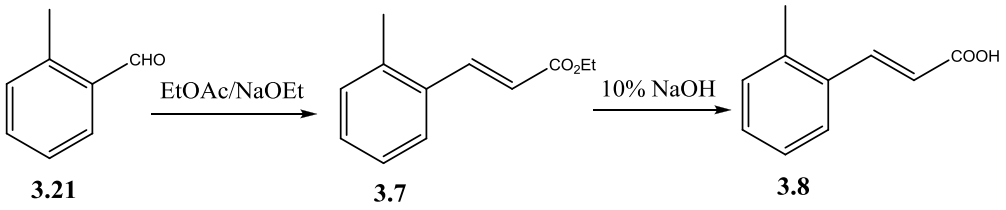

*Preparation of (E)-ethyl 3-o-tolylacrylate (**3.7**)*

An ethanolic solution of EtOAc (5 drops of absolute EtOH in 4.1 ml of EtOAc) was added to freshly prepared sodium slices (0.24 g, 10.4 mmol) placed in a 100 ml round bottomed flask, and the mixture rapidly cooled to 0°C in an ice bath. Dropwise addition of tolualdehyde (**3.21)** (1 g, 8.32 mmol) to the mixture was carried out with constant stirring until all the sodium had reacted. Equal volumes of acetic acid (10 ml) and water (10 ml) were then added in the workup of the reaction. The EtOAc layer was separated and the aqueous layer extracted using EtOAc (2 x 25 ml). Organic layers were combined and washed with brine solution (2 x 10 ml), followed by drying over anhydrous Na_2SO_4. The EtOAc was removed under reduced pressure and the crude material (**3.7**) purified by column chromatography (85:15 hexane/EtOAc) to give 1.15 g (73% yield) of product**.** All spectroscopic data are consistent with those reported in the literature (Huang et al., 2010) for (*E*)-ethyl 3-*o*-tolylacrylate (**3.7**).

^{1}H NMR (400 MHz, $CDCl_3$): see Table 3.2

^{13}C NMR (100 MHz, $CDCl_3$): see Table 3.3

Preparation of (E)-3-o-tolylacrylic acid (**3.8**)

A. Ester Hydrolysis

(E)-ethyl 3-*o*-tolylacrylate (**3.7**) (0.1013 g, 0.532 mmol) was refluxed with 10% NaOH (1.5 ml) at 105-110 ºC for 1 h. The mixture was cooled to room temperature and neutralized with 5 M HCl solution (5.2 ml). The acidified aqueous mixture was then extracted with EtOAc (3 x 10 ml) and the combined EtOAc fractions washed with brine (10 ml) before drying over anhydrous Na_2SO_4. The crude product was concentrated under reduced pressure and purified by column chromatography (hexane – EtOAc 60:40) with a few drops of trifluoroacetic acid (TFA) to give 0.066 g (76.6% yield) of product. All spectroscopic data were consistent with those reported in literature for (*E*)-3-*o*-tolylacrylic acid (**3.8**).

^{1}H NMR (400 MHz, $CDCl_3$): see Table 3.4

^{13}C NMR (100 MHz, $CDCl_3$): see Table 3.5

B. Malonic acid condensation

Tolualdehyde (**3.21**) (1 g, 8.32 mmol) was added to malonic acid (0.95 g, 9.15 mmol) dissolved in pyridine (10 ml) and the mixture stirred at room temperature for 72 h. The mixture was then warmed on a water bath until evolution of CO_2 ceased, and poured into an equal mix of water and EtOAc (10 ml) with a few drops of 5.0 M HCl. The EtOAc layer was collected, dried over anhydrous Na_2SO_4 and evaporated on a rotavap to give a crude product that was purified by column chromatography (hexane – EtOAc 60:40) with a few drops of trifluoroacetic acid (TFA) (25 % yield). All spectroscopic data were consistent with those reported in literature (Huang et al., 2010) for (*E*)-3-*o*-tolylacrylic acid (**3.8**).

^{1}H NMR (400 MHz, $CDCl_3$): see Table 3.4

^{13}C NMR (100 MHz, $CDCl_3$): see Table 3.5

***(E)*-ethyl 3-(2-bromophenyl)acrylate (3.9) and its carboxylic acid derivative (3.10)**

(o-bromo cinnamate & o-bromo cinnamic acid)

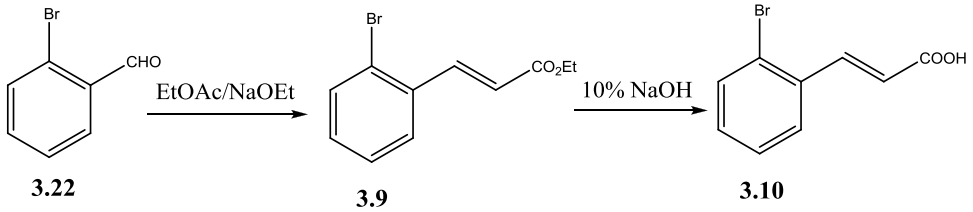

3.22 **3.9** **3.10**

*Preparation of (E)-ethyl- 3-(2-bromophenyl)acrylate (**3.9**)*

The same procedure described for the preparation of *(E)*-ethyl 3-*o*-tolylacrylate (**3.11**) was used for the synthesis of (*E*)-ethyl-3-(2-bromophenyl) acrylate (**3.13**). An ethanolic solution of EtOAc (4 drops of absolute EtOH in 3 ml of EtOAc) was added to freshly prepared sodium slices (0.15 g, 6.81 mmol) in a 100 ml round bottomed flask, and the mixture rapidly cooled to 0 °C in an ice bath. 2-bromobenzaldehyde **(3.22)** (1 g, 5.40 mmol) dissolved in EtOAc (1 ml) was added dropwise to the mixture with constant stirring until all the sodium had reacted. Equal volumes of acetic acid (10 ml) and water (10 ml) were then added to the mixture and the EtOAC layer separated. The aqueous layer was extracted using EtOAc (2 x 25 ml). Organic layers were combined and washed with brine solution (2 x 10 ml), followed

by drying over anhydrous Na_2SO_4. The EtOAc was removed under reduced pressure and the crude material (**3.9**) purified by column chromatography (80:20 hexane/EtOAc) to give 0.97 g (71.0% yield) of product**.** All spectroscopic data are consistent with those reported in the literature for (*E*)-ethyl-3-(2-bromophenyl)acrylate (**3.9**) (Brittelli, 1981).

^{1}H NMR (400 MHz, $CDCl_3$): see Table 3.2
^{13}C NMR (100 MHz, $CDCl_3$): see Table 3.3

Preparation of (E)-3-(2-bromophenyl) acrylic acid (**3.10**)

The same procedure used for the hydrolysis of **3.7** to obtain *(E)*-3-*o*-tolylacrylic acid (**3.8**) was adopted for the synthesis of *(E)*-3-(2-bromophenyl) acrylic acid (**3.10**) from its parent ester (**3.9**). *(E)*-ethyl 3-(2-bromophenyl)acrylate (**3.9**) (0.1019 g, 0.339 mmol) was refluxed with 10% NaOH (1.5 ml) at 105-110 ºC for 1 h. The mixture was cooled to room temperature and neutralized with 5 M HCl solution (5.2 ml). The acidified aqueous mixture was then extracted with EtOAc (3 x 10 ml) and the combined EtOAc fractions washed with brine (10 ml) before drying over anhydrous Na_2SO_4. The crude product was concentrated under reduced pressure and purified by column chromatography (hexane – EtOAc 65:35) with a few drops of trifluoroacetic acid to give 0.064 g (70.3 % yield) of product. All spectroscopic data were consistent with those reported in literature for *(E)*-3-(2-bromophenyl) acrylic acid (**3.10**) (Brittelli, 1981; Lu and Toy, 2011).

^{1}H NMR (400 MHz, $CDCl_3$): see Table 3.4
^{13}C NMR (100 MHz, $CDCl_3$): see Table 3.5

_(E)_-ethyl 3-(2-formylphenyl)acrylate (3.11) and its carboxylic acid derivative (3.12)

(o-formyl cinnamate & o-formyl cinnamic acid)

*Preparation of (E)-ethyl 3-(2-formylphenyl)acrylate (**3.11**)*

A. Aldol condensation procedure

The same method used for the synthesis of compounds **3.7** and **3.9** was attempted whereby an ethanolic solution of EtOAc (2 drops of absolute EtOH in 0.9 ml of EtOAc) with sodium slices (0.02 g, 0.89 mmol) was reacted with phthaldialdehyde (**3.23**, 0.1 g, 0.74 mmol), with constant stirring at 0 ºC until all the sodium had reacted. Equal volumes of acetic acid (5 ml) and water (5 ml) were then added in the workup of the reaction and the mixture extracted using EtOAc (2 x 10 ml). The organic layers were combined and washed with brine solution

(2 x 10 ml), followed by drying over anhydrous Na_2SO_4. The EtOAc was removed under reduced pressure. The ^1H NMR spectrum of the crude product mixture, showed only unreacted material. Changing the reaction temperature and time also did not have a positive effect on the reaction.

B. Wittig reaction

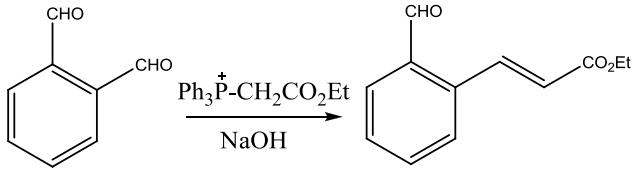

3.23 **3.11**

Dichloromethane (9 ml) was added to a mixture of phthaldialdehyde (**3.23**, 1 g, 7.45 mmol) and 1-ethoxy-carbonyl ethyliden-triphenylphosphorane (2.86 g, 7.45 mmol). The mixture was stirred vigourously for 1 min with the dropwise addition of 50% NaOH (3.8 ml). Stirring was continued for 30 min after which water (2.5 ml) and CH_2Cl_2 (2.5 ml) was added. The organic layer was removed and the aqueous layer extracted with CH_2Cl_2 (2 x 5 ml). Combined organic layers were dried over anhydrous $CaCl_2$ and the CH_2Cl_2 removed under reduced pressure to give a crude mixture of **3.11** (3.55 g) which was purified by column chromatography (85:15 hexane / EtOAc) to give 0.91 g (60.2% yield) of product**.** All spectroscopic data were consistent with those reported in the literature (Sanchez-Larios et al., 2011) for (*E*)-ethyl-3-(2-formylphenyl)acrylate (**3.11**).

^1H NMR (400 MHz, $CDCl_3$): see Table 3.2
^{13}C NMR (100 MHz, $CDCl_3$): see Table 3.3

*Preparation of (E)-ethyl 3-(2-formylphenyl) acrylic acid (**3.12**)*

A. Ester hydrolysis

(*E*)-ethyl-3-(2-formylphenyl)acrylate (**3.11**, 0.034 g, 0.17 mmol) was refluxed with 1% NaOH (1.5 ml) at 95-100 ºC for 1 h. The mixture was cooled to room temperature and neutralized with 5 M HCl solution (1 ml). The acidified aqueous mixture was then extracted with EtOAc (3 x 8 ml) and the combined EtOAc fractions washed with brine (10 ml) before drying over anhydrous Na_2SO_4. The crude product was concentrated under reduced pressure and the ^1H NMR showed a degraded product. All attempts at effectively hydrolysing the parent ester **(3.15)** using 0.5% NaOH and 10% $NaHCO_3$ were unsuccessful.

B. Malonic acid condensation

Phthaldialdehyde (**3.23**) (0.1 g, 0.74 mmol) was added to malonic acid (0.08 g, 0.74 mmol) dissolved in pyridine (5 ml) and the mixture stirred at room temperature for 72 h. The mixture was then warmed on a water bath until evolution of CO_2 ceased, and poured into an equal mix of water and EtOAc (10 ml) with a few drops of 5.0 M HCl. The EtOAc layer was collected, dried over anhydrous Na_2SO_4 and evaporated on a rotavap. The ^{1}H NMR of the product did not show the expected product *(E)*-ethyl 3-(2-formylphenyl) acrylic acid (**3.12**), but however demonstrated the formation of indanone (**3.24**).

^{1}H NMR (400 MHz, $CDCl_3$) δ 7.79 (d, *J* = 7.6 Hz, 1H), 7.62 (t, *J* = 7.4 Hz, 1H), 7.51 (d, *J* = 7.6 Hz, 1H), 7.40 (t, *J* = 7.1 Hz, 1H), 3.18 (m, 2H), 2.72 (m, 2H). ^{13}C NMR (100 MHz, $CDCl_3$) δ 207.63 (s), 155.63 (s), 137.50 (s), 134.05 (s), 127.72 (s), 127.14 (s), 124.15 (s), 36.65 (s), 26.24 (s).

C. Aldehyde protection and ester hydrolysis

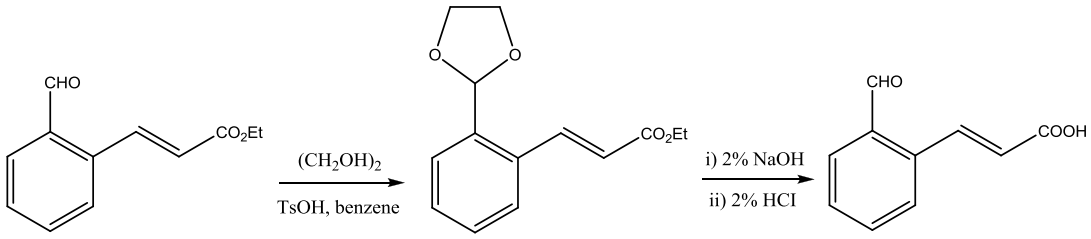

3.11 **3.25** **3.12**

A mixture of *(E)*-ethyl 3-(2-formylphenyl)acrylate (**3.11**, 0.36 g; 1.8 mmol), ethylene glycol (3-4 drops), toluene-p-sulphonic acid (catalytic amount) and benzene (4 ml) was refluxed for 2 h at 80-85 ºC in a round bottomed flask fitted with a Dean and Stark apparatus. Benzene was then evaporated off on a rotavap and the product analysed by ^{1}H NMR, which confirmed a protected *(E)*-ethyl- 3-(2-formylphenyl) acrylate (**3.25**).

Hydrolysis was then conducted by refluxing the protected *(E)*-ethyl-3-(2-formylphenyl) acrylate (**3.25**) with 2% NaOH (3.5 ml) for 1 h at 95-100ºC. 5.0 M HCl (1 ml) was added to neutralize the base and the aqueous layer extracted with EtOAc (2 x 10 ml). Pooled organic fractions were washed with brine solution (2 x 10 ml), dried over anhydrous Na_2SO_4 and the product concentrated on a rotavap. The product was then purified by liquid-liquid extraction of its salt and carboxylic acid using EtOAc and water to give 0.213 g (67.3% yield) of product**.** All spectroscopic data were consistent with those reported in the literature (Kumar et al., 2011) for (*E*)-ethyl 3-(2-formylphenyl) acrylic acid (**3.12**).

^{1}H NMR (400 MHz, $CDCl_3$): see Table 3.4

^{13}C NMR (100 MHz, $CDCl_3$): see Table 3.5

(E)-ethyl 3-(2-cyanophenyl)acrylate (3.13) and its carboxylic acid derivative (3.14)

(o-cyano cinnamate & o-cyano cinnamic acid)

*Preparation of (E)-ethyl 3-(2-cyanophenyl)acrylate (**3.13**)*

A. Aldol condensation

An aldol condensation used for previous analogues was also attempted for the preparation of **3.13**. An ethanolic solution of EtOAc (3 drops of absolute EtOH in 0.5 ml of EtOAc) was added to freshly prepared sodium slices (0.022 g, 0.98 mmol) and the mixture rapidly cooled to 0 °C in an ice bath. Granules of 2-cyanobenzalaldehyde (**3.29**, 0.1 g, 0.77 mmol) were added slowly to the cooled mixture and the mixture stirred until all the sodium had reacted. Equal volumes of acetic acid (5 ml) and water (5 ml) were then added in the workup of the reaction and the mixture extracted using EtOAc (2 x 10 ml). Organic layers were combined and washed with brine solution (2 x 5 ml), followed by drying over anhydrous Na_2SO_4. The EtOAc was removed under reduced pressure and the ^{1}H NMR spectrum showed a complex unrecognised product.

B. Wittig reaction

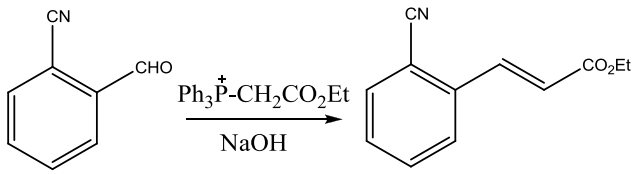

3.26 **3.13**

Dichloromethane (1 ml) was added to a mixture of 2-cyanobenzaldehyde (**3.26**, 0.1 g, 0.76 mmol) and 1-ethoxy-carbonyl ethyliden-triphenylphosphorane (0.29 g, 0.76 mmol). The mixture was stirred vigourously for 1 min with the dropwise addition of 50% NaOH (0.5 ml). Stirring was continued for 30 min after which water (2.5 ml) and CH_2Cl_2 (2.5 ml) was added. The organic layer was removed and the aqueous layer extracted with CH_2Cl_2 (2 x 5 ml). Combined organic layers were dried over anhydrous $CaCl_2$ and the CH_2Cl_2 removed under reduced pressure to give a crude mixture of **3.13** (0.33 g) which was purified by column chromatography (50:50 hexane / EtOAc) to give 0.100 g (65.6% yield) of product**.** All

spectroscopic data were consistent with those reported in the literature for (*E*)-ethyl 3-(2-cyanophenyl) acrylate (**3.13**).

^{1}H NMR (400 MHz, $CDCl_3$): see Table 3.2

^{13}C NMR (100 MHz, $CDCl_3$): see Table 3.3

*Preparation of (E)-ethyl 3-(2-cyanophenyl) acrylic acid (**3.14**)*

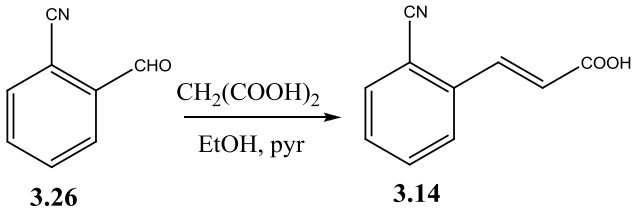

3.26 **3.14**

A mixture of 2-cyanobenzaldehyde (**3.26**, 0.1 g, 0.76 mmol), malonic acid (0.095 g, 0.91 mmol), EtOH (1 ml) and pyridine (0.1 ml) was refluxed for 6 h at a temperature range of 65-80ºC. The off-white crystals were collected, washed with cold EtOH (10 ml), followed by EtOAc (2 x 10 ml) to give a pure yield of 0.09 g (75.8 % yield). All spectroscopic data were consistent with those reported in the literature for (*E*)-ethyl 3-(2-cyanophenyl) acrylic acid (**3.14**).

^{1}H NMR (400 MHz, MeOH): see Table 3.4

^{13}C NMR (100 MHz, MeOH,): see Table 3.5

(E)-ethyl 3-(2-(dichloromethyl) phenyl)acrylate (3.15) and its carboxylic acid derivative (3.16)

(o-dichloromethyl cinnamate & o-dichloromethyl cinnamic acid)

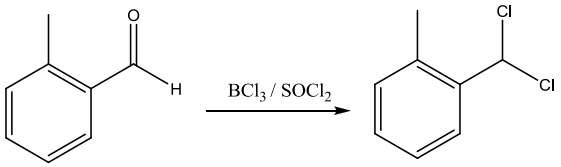

3.21 **3.27**

A. Model reaction using BCl_3 (Kabalka and Wu, 2000)

Tolualdehyde (**3.21**, 0.24 g, 2 mmol) was dissolved in hexane (10 ml) at room temperature under N_2 atmosphere. BCl_3 (0.28 g, 2.4 mmol) was added to the aldehyde solution with formation of an off white precipitate. The mixture was then refluxed for 1.5 h at 80-90ºC, after which it was cooled and water (5 ml) added. The hexane layer was collected and evaporated under reduced pressure. The ^{1}H NMR spectrum of the crude reaction mixture showed the presence of the dichloride (**3.27**) and unreacted aldehyde (**3.21**) in the ratio 1:3 (product: unreacted material).

B. Model reaction using $SOCl_2$ (Newman and Sujeeth, 1978)

Tolualdehyde (**3.21,** 0.5 g, 4.16 mmol) was added drop-wise to a cooled mixture (-10ºC) of $SOCl_2$ (0.5 g, 4.99 mmol) and DMF (10 drops). The mixture was stirred in the cooling bath for 15 min and the temperature allowed to rise slowly to room temperature, after which it was stirred for a further 4 h. The product mixture was then poured onto ice and extracted with EtOAc (10 ml). The EtOAc layer was collected, washed with brine (10 ml) and dried over anhydrous $MgSO_4$. The drying agent was filtered off and the EtOAc removed under reduced pressure. Analysis of the crude product by ^{1}H NMR showed a complete conversion of **3.25** to the product, (dichloromethyl)-2-methylbenzene (**3.27**). ^{1}H NMR (400 MHz, $CDCl_3$) δ 7.87 (m, 1H), 7.36 (m, 1H), 7.35 (m, 2H), 7.24 (m, 1H), 7.02 (s, 1H), 2.53 (s, 1H).

*Preparation of (E)-ethyl 3-(2-(dichloromethyl) phenyl)acrylate (**3.15**)*

3.11 **3.15**

The same method discussed above using $SOCl_2$ as a chlorinating reagent was used to synthesize *(E)*-ethyl-3-(2-(dichloromethyl)phenyl) acrylate (**3.15**). *(E)*-ethyl-3-(2-formylphenyl)acrylate **(3.11)** (0.5 g, 2.4 mmol) was added drop-wise to a cooled mixture (-10ºC) of $SOCl_2$ (0.59 g, 4.9 mmol) and DMF (10 drops). The mixture was stirred in the cooling bath for 15 min and the temperature allowed to rise slowly to room temperature, after which it was stirred for a further 4 h. The product mixture was then poured onto ice and extracted with EtOAc (10 ml). The EtOAc layer was collected, washed with brine (10 ml)

and dried over anhydrous $MgSO_4$. The drying agent was filtered off and the EtOAc removed under reduced pressure. The crude product was purified by thin layer chromatography (80:20 hexane / EtOAc) to give 0.49 g (78.5% yield) of pure **3.15**.

^{1}H NMR (400 MHz, $CDCl_3$): see Table 3.2

^{13}C NMR (100 MHz, $CDCl_3$): see Table 3.3

HRESIMS: *m/z* 259, *m/z* 261

IR (film, cm^{-1}): V_{max} 2982.34, 1709.11, 1636.01, 1572.11, 1479.37, 1446.18, cm^{-1}

UV (MeOH)**:** λ_{max} : 338.45nm

Preparation of (E)-ethyl 3-(2-(dichloromethyl) phenyl)acrylic acid (**3.16**)

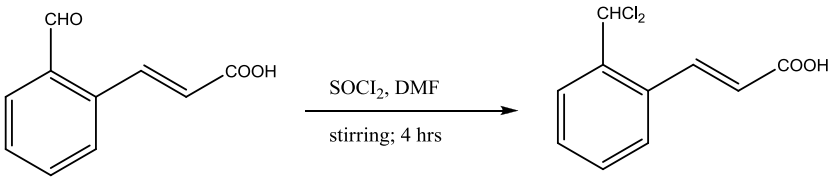

3.12 **3.16**

(E)-ethyl 3-(2-(dichloromethyl) phenyl)acrylic acid (**3.16**) was prepared in a similar way to its parent ester, by chlorinating *(E)*-ethyl-3-(2-formylphenyl)acrylic acid **(3.12).** *(E)*-ethyl-3-(2-formylphenyl)acrylic acid **(3.12)** (0.1 g, 0.56 mmol) was added to a cooled mixture (-10ºC) of $SOCl_2$ (0.14 g, 1.1 mmol) and DMF (3 drops). The mixture was stirred in the cooling bath for 15 min and the temperature allowed to rise slowly to room temperature, after which it was stirred for a further 4 h. The product mixture was then poured onto ice and extracted with EtOAc (5 ml). The EtOAc layer was collected, washed with brine (5 ml) and dried over anhydrous $MgSO_4$. The drying agent was filtered off and the EtOAc removed under reduced pressure. The crude product was purified by thin layer chromatography (50:50 hexane / EtOAc) with a few drops of trifluoroacetic acid (TFA) to give 0.071 g (55.4% yield) of pure compound **3.16**.

^{1}H NMR (400 MHz, $CDCl_3$): see Table 3.4

^{13}C NMR (100 MHz, $CDCl_3$): see Table 3.5

Ethyl cinnamate (3.17)

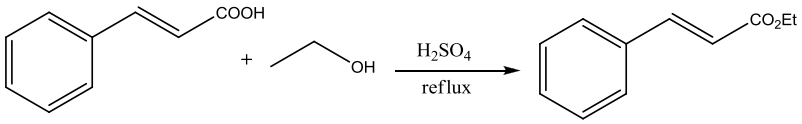

3.18 **3.17**

A mixture of cinnamic acid (**3.18,** 1 g, 6.74 mmol), EtOH (4 ml) and concentrated H_2SO_4 (0.1 ml) was refluxed at 78°C for 4.5 h with stirring. The flask was allowed to cool followed by addition of water (10 ml) and EtOAc (6 ml) to the mixture. The organic layer was collected and washed with brine (2 x 20 ml) and dried over anhydrous Na_2SO_4. The EtOAc was removed under reduced pressure to give 1.06 g of pure material (**3.17**) with 89.2 % yield. All spectroscopic data are consistent with those reported in the literature (Speed et al., 2004) for ethyl cinnamate (**3.17**).

^{1}H NMR (400 MHz, $CDCl_3$): see Table 3.2

^{13}C NMR (100 MHz, $CDCl_3$): see Table 3.3

***(E)*-ethyl 3-(2-(trifluoromethyl)phenyl)acrylate (3.19)**

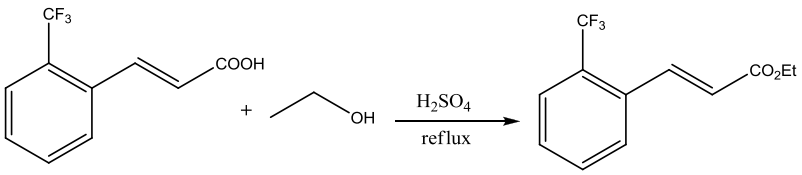

3.20 **3.19**

A similar esterification reaction as above was used to synthesize *(E)*-ethyl 3-(2-(trifluoromethyl)phenyl)acrylate (**3.19**) A mixture of trifluoromethyl cinnamic acid (**3.20,** 1 g, 4.63 mmol), EtOH (3 ml) and concentrated H_2SO_4 (0.1 ml) was refluxed at 80°C for 4.5 h with stirring. The flask was allowed to cool followed by addition of water (10 ml) and EtOAc (6 ml) to the mixture. The organic layer was collected and washed with brine (2 x 20 ml) and dried over anhydrous Na_2SO_4. The EtOAc was removed under reduced pressure to give 0.89 g of pure material (**3.19**) with 78.9 % yield. All spectroscopic data were consistent with those reported in the literature for *(E)*-ethyl 3-(2-(trifluoromethyl)phenyl) acrylate (**3.19**) (Liu et al., 2010b)**.**

^{1}H NMR (400 MHz, $CDCl_3$): see Table 3.2

^{13}C NMR (100 MHz, $CDCl_3$): see Table 3.3

References

Antunes, E.M., Afolayan, A.F., Chiwakata, M.T., Fakee, J., Knott, M.G., Whibley, C.E., Hendricks, D.T., Bolton, J.J., Beukes, D.R., 2011. Identification and in vitro anti-oesophageal cancer activity of a series of halogenated monoterpenes isolated from the South African seaweeds Plocamium suhrii and Plocamium cornutum. Phytochemistry (Elsevier), 72, 769-772.

Armstrong, D.E., Richardson, D.H., 1933. 125. The Reimer-Tiemann reaction. Journal of the Chemical Society, 496-500.

Azzoli, C.G., Baker, J., Temin, S., Pao, W., Aliff, T., Brahmer, J., Johnson, D.H., Laskin, J.L., Masters, G., Milton, D., Nordquist, L., Pfister, D.G., Piantadosi, S., Schiller, J.H., Smith, R., Smith, T.J., Strawn, J.R., Trent, D., Giaccone, G., 2009. American society of clinical oncology clinical practice guideline update on chemotherapy for stage IV non-small-cell lung cancer. Journal of Clinical Oncology, 27, 6251-6266.

Baker, S.D., Sparreboom, A., Verweij, J., 2006. Clinical pharmacokinetics of docetaxel: recent developments. Clinical Pharmacokinetics, 45, 235-252.

Brittelli, D.R., 1981. Phosphite-mediated in situ carboxyvinylation: a new general acrylic acid synthesis. Journal of Organic Chemistry, 46, 2514-2520.

Brown, G., 2006. Artemisinin and a new generation of antimalarial drugs. Journal of Chemical Education, 43, 97-99.

Carr, R.A.E., Congreve, M., Murray, C.W., Rees, D.C., 2005. Fragment-based lead discovery: leads by design. Drug Discovery Today, 10, 987-992.

Da Rocha., Lopes, R.M., Schwartsmann, G., 2001. Natural products in anti-cancer therapy. Current Opinion in Pharmacology., 1, 364-369.

Dijksman, D.J., Newbold, G.T., 1952. 1,2-Dihydro-2-thianaphthalene derivatives. II. Conversion of 1,2-dihydro-1-keto-2-thianaphthalenes into indanones. Journal of the Chemical Society, 13-17.

Firouzabadi, H., Shiriny, F., 1996. New applications of tungsten hexachloride (WCl6) in organic synthesis. Halo-de-hydroxylation and dihalo-de-oxo-bisubstitution. Tetrahedron, 52, 14929-14936.

Foloppe, N., 2011. The benefits of constructing leads from fragment hits. Future Medicinal Chemistry, 3, 1111-1115.

Fuller, R.W., Cardellina, J.H., II, Jurek, J., Scheuer, P.J., Alvarado-Lindner, B., McGuire, M., Gray, G.N., Steiner, J.R., Clardy,J., 1994. Isolation and Structure/Activity Features of Halomon-Related Antitumor Monoterpenes from the Red Alga Portieria hornemannii. Journal of Medicinal Chemistry., 37, 4407-4411.

Fuller, R.W., Cardellina, J.H., II, Kato, Y., Brinen, L.S., Clardy, J., Snader, K.M., Boyd, M.R., 1992. A pentahalogenated monoterpene from the red alga Portieria hornemannii produces a novel cytotoxicity profile against a diverse panel of human tumor cell lines. Journal of Medicinal Chemistry, 35, 3007-3011.

Gloer, J.B., 2000. Biologically Active Natural Products: Pharmaceuticals. Edited by Stephen J. Cutler and Horace G. Cutler (Mercer University, Atlanta, GA). CRC Press, New York, NY. 2000., Journal of Natural Products, 63, 891.

Hajduk, P.J., Greer, J., 2007. A decade of fragment-based drug design: strategic advances and lessons learned. Nature Reviews Drug Discovery, 6, 211-219.

Hofheinz, W., Burgin, H., Gocke, E., Jaquet, C., Masciadri, R., Schmid, G., Stohler, H., Urwyler, H., 1994. Ro 42-1611 (arteflene), a new effective antimalarial: Chemical structure and biological activity. Annals Tropical Medicine and Parasitology, 45, 261-265.

Huang, S.H., Chen, J.R., Tsai, F.Y., 2010. Palladium(II)/cationic 2,2'-bipyridyl system as a highly efficient and reusable catalyst for the Mizoroki-Heck reaction in water. Molecules, 15, 315-330.

Kabalka, G.W., Wu, Z., 2000. Conversion of aromatic aldehydes to gem-dichlorides using boron trichloride. A new highly efficient method for preparing dichloroarylmethanes. Tetrahedron Letters, 41, 579-581.

Kumar, R.A., Maheswari, C.U., Ghantasala, S., Jyothi, C., Reddy, K.R., 2011. Synthesis of 3H-Quinazolin-4-ones and 4H-3,1-Benzoxazin-4-ones via Benzylic Oxidation and Oxidative Dehydrogenation using Potassium Iodide-tert-Butyl Hydroperoxide. Advanced Synthesis and Catalysis, 353, 401-410.

Lanter, J., Zhang, X., Sui, Z., 2011. Medicinal chemistry inspired fragment-based drug discovery. Methods of Enzymology, 493, 421-445.

Liu, J., Liu, H., Wang, L., 2010a. Exploration of amino-functionalized ionic liquids as ligand and base for Heck reaction. Applied Organometallic Chemistry, 24, 386-391.

Liu, J., Liu, H., Wang, L., 2010 b. Exploration of amino-functionalized ionic liquids as ligand and base for Heck reaction. Applied Organometallic Chemistry, 24, 386-391.

Lu, J., Toy, P.H., 2011. Organocatalytic decarboxylative Doebner-Knoevenagel reactions between arylaldehydes and monoethyl malonate mediated by a bifunctional polymeric catalyst. Synlett, 1723-1726.

Newman, M.S., Sujeeth, P.K., 1978. Conversion of aromatic and α, β¦-unsaturated aldehydes to dichlorides by thionyl chloride and dimethylformamide. Journal Organic Chemistry., 43, 4367-4369.

Nicolaou, K.C., Guy, R.K., Potier, P., 1996. Taxoids: new weapons against cancer. Scientific American, 274, 94-98.

Oprea, T.I., 2002. Virtual screening in lead discovery: a viewpoint. Molecules, 7, 51-62.

Pardin, C., Pelletier, J.N., Lubell, W.D., Keillor, J.W., 2008. Cinnamoyl Inhibitors of Tissue Transglutaminase. Journal of Organic Chemistry, 73, 5766-5775.

Park, S.H., Kim, J.Y., Chang, S., 2011. Rhodium-Catalyzed Selective Olefination of Arene Esters via C-H Bond Activation. Organic Letters, 13, 2372-2375.

Rees, D.C., Congreve, M., Murray, C.W., Carr, R., 2004. Fragment-based lead discovery. Nature Reviews Drug Discovery, 3, 660-672.

Sanchez-Larios, E., Holmes, J.M., Daschner, C.L., Gravel, M., 2011. Synthesis of spiro bis-indanes via domino Stetter-aldol-Michael and Stetter-aldol-aldol reactions: scope and limitations. Synthesis, 1896-1904.

Shu, Y.Z., 1998. Recent Natural Products Based Drug Development: A Pharmaceutical Industry Perspective. Journal of Natural Products, 61, 1053-1071.

Simonyan, A., 1999. Phosphorus oxychloride in organic synthesis. Synthesis of cinnamic acid derivatives. Pharmaceutical Chemistry Journal, 33, 158-159.

Speed, T.J., McIntyre, J.P., Thamattoor, D.M., 2004. Wittig reaction using a stabilized phosphorus ylid: An efficient and stereoselective synthesis of ethyl trans-cinnamate. Journal of Chemical Education, 81, 1355-1357.

Srinivasan, M., Perumal, S., 2006. Novel tandem reactions of ethyl acetoacetate with aromatic aldehydes: product- and stereo-selective formation of highly functionalised cyclohexanones. Tetrahedron, 62, 7726-7732.

Titulaer, H.A.C., Zuidema, J., Kager, P.A., Wetsteyn, J.C.F.M., Lugt, C.B., Merkus, F.W.H.M., 1990. The pharmacokinetics of artemisinin after oral, intramuscular and rectal administration to volunteers. Journal of Pharmacy and Pharmacology, 42, 810-813.

Vanderwerff, William Daniel. Hydrolysis of aromatic nitriles to carboxylic acids. [DE2635484A1], 9. 2-24-1977. Sun Ventures, Inc., USA .
Ref Type: Patent

Zartler, E.R., Shapiro, M.J., 2005. Fragonomics: fragment-based drug discovery. Current Opinion in Chemical Biology, 9, 366-370.

CHAPTER FOUR:

Biological activity of halogenated monoterpene inspired analogues

4.1 Introduction

Cytotoxicity studies with cell culture systems provide useful information during the screening of substances with potential anti-cancer properties. Several indicators are used to determine the toxic effect of compounds on cancer cells. The most readily observed effect of cytotoxicity is morphological changes in the cells, which can be done microscopically. Other indicators include altered cell growth/cell reproduction measured by cell count, and determination of cell death by use of vital dyes and cell proliferation reagents to measure cell viability (Gerets et al., 2009). A number of approaches have been developed to rapidly evaluate the cytotoxic activity of test substances (Liu et al., 1997). Principles are based on the idea of basal cytotoxicity, that is how cytotoxic chemicals affect the basic functions of the cell which results in cellular damage (Gerets et al., 2009). Accepted methods used to quantify cell viability in cell-based assays include lactate dehydrogenase (LDH) release assays, trypan blue exclusion, and 3-(4,5-dimethylthiazol-2-yl)-2,5-diphenyl tetrazolium bromide (MTT) reduction assays (Kim et al., 2009).

4.1.1 3-(4,5-dimethylthiazol-2-yl)-2,5-diphenyl tetrazolium bromide (MTT) reduction assays

The above assay measures the conversion of a yellow tetrazolium salt, MTT (**4.1**), into purple formazan crystals (**4.2**) by redox activity of metabolically active cells (Vistica et al., 1991) (Scheme 4.1). The MTT reagent is absorbed *via* endocytosis and reduction occurs in active cellular mitochondria (Burdon et al., 1993). Reduction to formazan is effected by intracellular NAD(P)H oxidoreductases enzymes (Berridge et al., 2005) and the formazan dye formed is quantified by absorbance at 550 nm and 650 nm using a scanning multiwell spectrophotometer (ELISA plate reader). Cell viability is proportional to the increase in formazan product formed. Conversely, a decrease in MTT reduction can be used as a marker for cell damage/death.

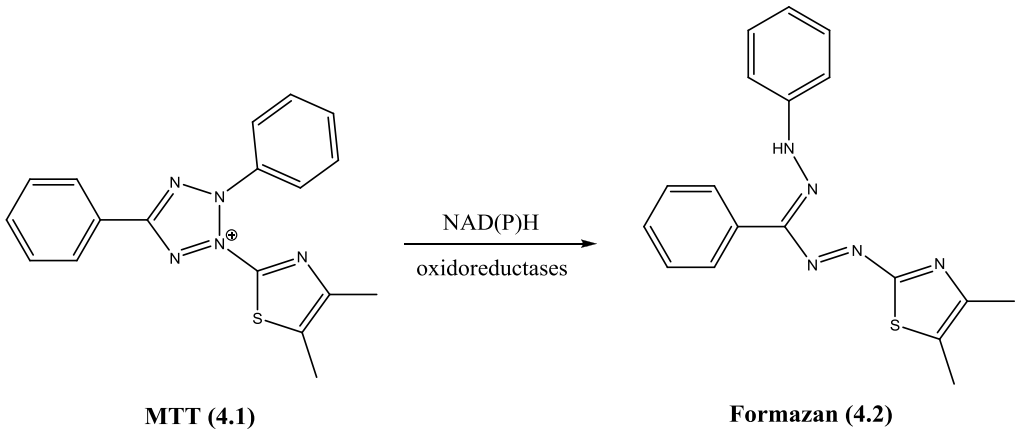

Scheme 4.1: Reduction of MTT to a formazan salt by viable cells

Various different tetrazolium dyes can be used for colorimetric assays similar to the one above. A common alternative to MTT involves the use of disodium mono (4-(3-(-iodophenyl)-2-(4-nitrophenyl)-2H-tetrazol-3-ium-5-yl) benzene-1,3-disulfonate (**4.3**) abbreviated WST-1, as a cell proliferation reagent (Scheme 4.2). It is also a tetrazolium salt and works on similar principles as MTT, namely that it is reduced to formazan dye by active cellular mitochondria, which indicates cell viability (Ngamwongsatit et al., 2008). The WST-1 formazan product is detected by absorbance at 440 nm and a decrease in WST-1 reduction signifies cell damage or death.

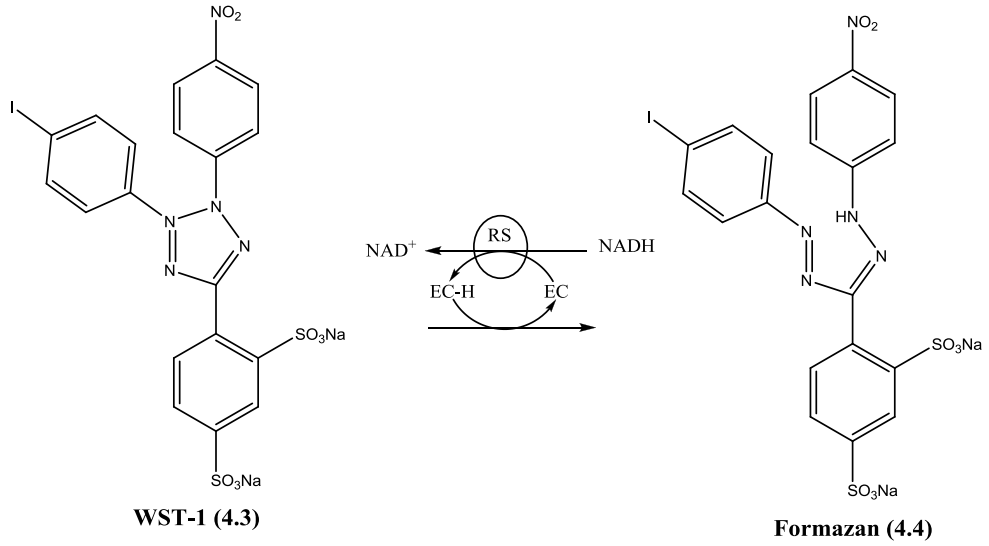

(EC = electron coupling reagent, RS = mitochondrial succinate-tetrazolium-reductase system)

Scheme 4.2: Reduction of WST-1 to a formazan salt by viable cells

Mammalian cell culture is an important component of research in understanding disease profiles and possible treatments especially in the cancer field. The majority of breast cancer research is conducted using established breast cancer cell lines as *in-vitro* models and these include cell lines such as the MCF7 and MDA-MB-231 breast adenocarcinoma and Hs578T breast carcinoma (Burdall et al., 2003). Immortalised cell lines are quite easy to handle, easy to replace from frozen stocks in case of contamination and have the ability to grow to infinite quantities when cultured. However they are susceptible to genotypic and phenotypic changes when continuously cultured. This has been the case with the MCF7 cell line that is commonly used (Osborne et al., 1987). Despite some disadvantages, cell cultures are still commonly used for cancer research. For this study, we used the MDA-MB-231 cell line and its properties are briefly discussed below.

4.1.2 MDA-MB-231 breast cancer cell line

A cell line is defined as a culture that is isolated from a primary culture (culture from the actual cells/tissue/organ removed from an organism) and established as a continuous *in-vitro* culture consisting of successful generations of cells that were originally present in the primary sample (Ekwall et al., 1990). MDA-MB-231 cells were first isolated from pleural effusions from a breast cancer patient in 1973 (Cailleau et al., 1974). They possess epithelial-like characteristics and appear as spindle shaped cells under a microscope. The cells are considered highly invasive/metastatic (Tu et al., 2011) and display relatively high colony forming efficiency. Under the NCI guidelines, MDA-MB-231 cells are categorized as a triple negative form of breast cancer. Their growth is not influenced by the hormones oestrogen and progesterone nor by the presence of human epidermal growth factor receptors 2 (HER 2), therefore cannot be treated by hormonal therapy such as tamoxifen or HER 2 receptor blockers like Herceptin (Otvos et al., 2011). Since this form of cancer is difficult to treat, the MDA-MB-231 cell line is a good choice to use in cytotoxic studies for novel anti-cancer compounds.

The derivatives used for cytotoxic testing against MDA-MB-231 breast cancer cells are shown in Table 4.1.

Table 4.1: Derivatives tested on MDA-MB-231 cells for cytotoxicity

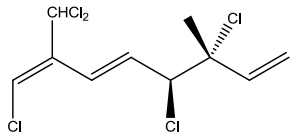	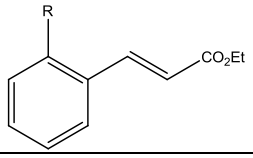	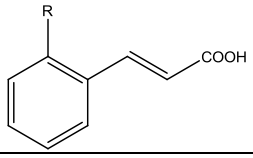
Plocornulide A (**2.12**)	R	R
	3.7 CH_3	**3.8** CH_3
	3.9 Br	**3.10** Br
	3.11 CHO	**3.12** CHO
	3.13 CN	**3.14** CN
	3.15 $CHCl_2$	**3.16** $CHCl_2$
	3.17 H	**3.18** H
	3.19 CF_3	**3.20** CF_3

The aim of the study was to compare the cytotoxicity of the synthesized analogues (**series a** = cinnamate esters; **series b** = carboxylic acid derivatives) with the natural compound plocornulide A. The activity of plocornulide A on WHCO1 oesophageal cancer cells (Antunes et al., 2011) and MCF7 breast cancer cells has been reported but availability and stability issues associated with the natural product have compromised further research. This led to the synthesis of the above mentioned analogues. The rationale for the synthesis of these analogues, as discussed in the previous chapter (Chapter 3), was to have stable entities with retained cytotoxic activity, in order to explore the chemistry and biological activity displayed by halogenated monoterpenes. The series focused on the importance of *gem*-dichlorides in these molecules and whether they can be substituted with other isosteres. Calculated log P values of cinnamate esters are very similar to those of the natural product. Carboxylic acid derivatives were an attempt to increase the water solubility properties of the analogues. The colorimetric cell viability assays (MTT and WST-1 assays) were used to determine the effect of these compounds on the MDA-MB-231 cell line.

4.2 Results and Discussion

4.2.1 Optimization of the cytotoxicity assay on MDA-MB-231 cells using Paclitaxel

Various factors have been identified that can affect MTT specific activity resulting in false positive or negative cell counts (Sylvester, 2011). It is therefore important to optimize assay conditions to obtain accurate results when calculating cell viability. Figure 4.1 represents several parameters that we optimized before the assays were conducted. Paclitaxel is a known anti-cancer agent that was used as a positive control for cytotoxicity in the MDA-MB-231 cell line.

Optimal seeding cell densities are essential to obtain reliable results from these assays. The number of cells seeded should allow cell growth that can yield levels of formazan that are easy to quantify. Inappropriate seeding densities that are either too high or too low can result in either cell over growth in wells or complete cell death due to few cells being present respectively. Figure 4.1A shows the results obtained when the cytotoxicity assay was conducted using different cell densities of 1000, 3000 and 6000 cells per well. The cells were treated with paclitaxel in concentration ranges of 25 nM to 200 nM and the percentage viability determined after 4 days. A 100% cell survival was assigned to absorbance readings of DMEM control wells with all other calculations done relative to this value. Different survival rates observed were influenced by the number of cells seeded in each plate. Plots for 1000 and 3000 cells per well recorded lower percentage survival rates due to fewer numbers of cells seeded initially. The optimal seeding density to use was therefore chosen to be 6000 cells per well for the assays.

The optimal time required for the reduction of tetrazolium to formazan by active cells after addition of cell proliferation reagent to each well, was determined by taking absorbance readings at 1 h, 2 h and 4 h after addition of the tetrazolium reagent. Figure 4.1B shows a plot of absorbance versus time at the various concentrations of paclitaxel used. After the first hour, the amount of formazan product formed increased dramatically, and then there was a more gradual increase in the amount of formazan generated between 2 h and 4 h. Therefore any incubation time after 3 h would have been appropriate. In order to maximize the reduction of MTT to formazan, an incubation period of 4 h was chosen.

Appropriate volumes of cell proliferation reagent should be added to each well such that an accurate linear relationship is obtained between the amount of formazan produced and the

number of viable cells present. Figure 4.1C represents the effect of varying volumes of WST-1 added to each well. The graph showed no obvious difference in adding 5 µl or 10 µl of the WST-1 to the percentage survival of the cells, and therefore 10 µl of proliferation reagent was used in future experiments.

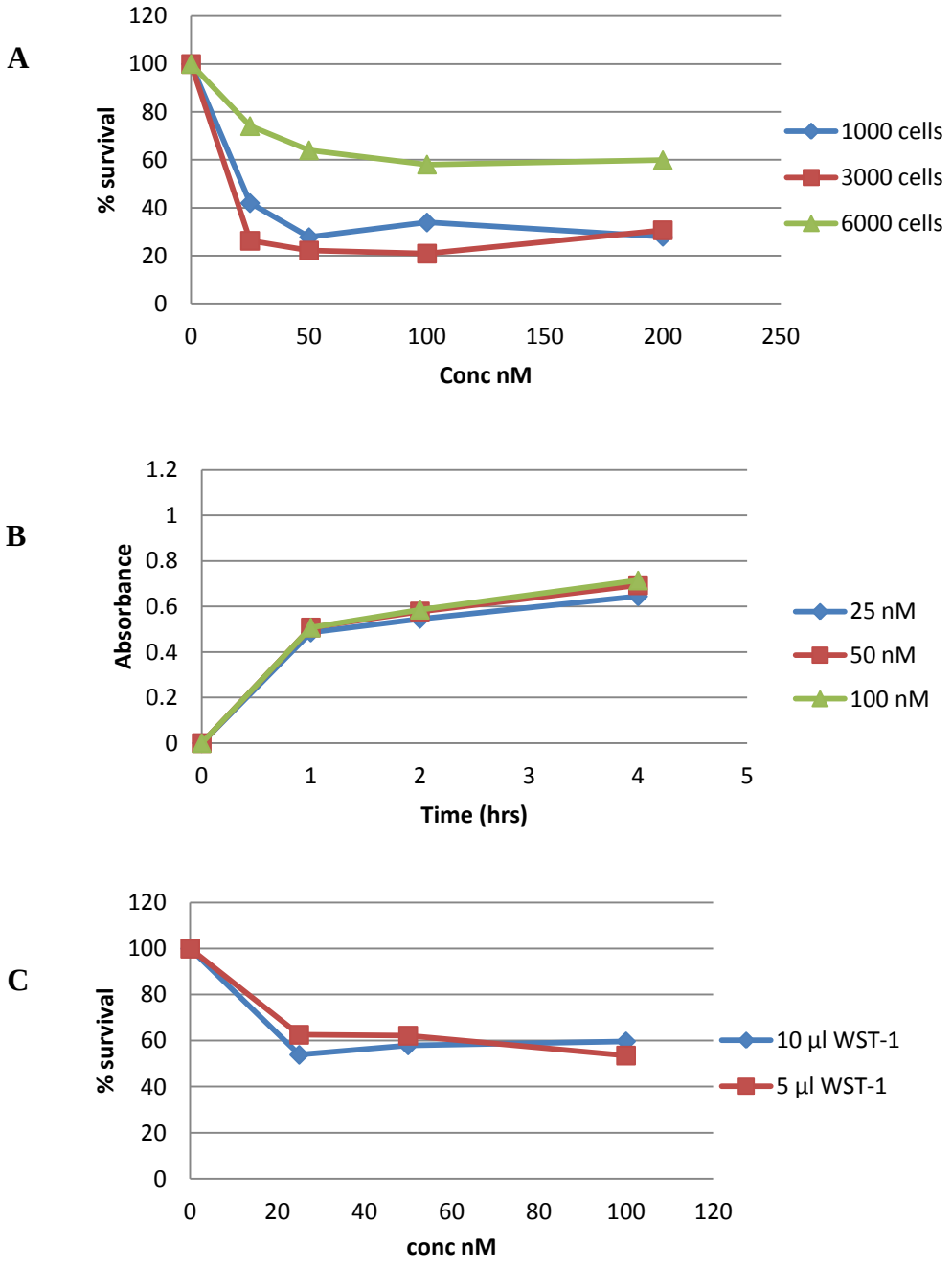

Figure 4.1: Optimization of the cytotoxic assay on MDA-MB-231 cells using paclitaxel
A. Percentage survival plot of MDA-MB-231 cells seeded at 1000 cells (blue), 3000 cells (red) and 6000 cells (green) per well after treating with Paclitaxel **B.** Absorbance versus time graph at different intervals, 1 h, 2 h and 4 h after adding WST-1 reagent to MDA-MB-231 cells treated with paclitaxel. **C.** Percentage survival plot of MDA-MB-231 cells after treating with Paclitaxel and adding different volumes of WST-1 reagent, 10 µl (blue) and 5 µl (red).

4.2.2 Validation of cytotoxicity assay on MDA-MB-231 cells using Paclitaxel

The assay was conducted with a known cytotoxic compound to validate that the optimized conditions described previously could be used to determine the cytotoxicity to MDA-MB-231 cells. This assay was conducted by treating MDA-MB-231 cells with paclitaxel, at concentrations ranging from 0.05 μM to 10 μM. Figure 4.2 represents the dose response curve obtained by plotting percentage survival versus the drug concentration. The IC_{50} value of paclitaxel was calculated to be 0.0959 μM (95.9 nM) which is consistent with literature values of 100 nM in the MCF7 breast cancer cell line (Munster et al., 2002) and with the unpublished observations of other researchers in our group (Jo-anne de la Mare, personal communication). The profile of the survival curve and the IC_{50} values obtained suggested that the cytotoxicity assay was performed as expected. Paclitaxel was therefore included in the assays of novel derivatives as a positive control. A more accurate determination of the IC_{50} value of paclitaxel would involve narrowing the concentration range to the 0.05 μM – 0.5 μM.

4.2.3 Investigation into possible interaction between derivatives and cell proliferation reagent

Possible interfering chemical interactions between the test analogues and WST-1 reagent were investigated. A blank assay was conducted in a 96 well microplate that lacked cells. Respective wells contained media, WST-1 reagent and analogues at concentrations ranging from 10 μM to 100 μM. Control wells contained only media and WST-1 solution. The culture was incubated for 4 h and absorbance readings taken. Figure 4.3 shows the absorbance values of the various wells relative to the control. No noticeable changes were observed in the absorbance values of the analogues in comparison to the control assigned a concentration of 0 μM. A dose dependent increase in the concentration of the analogues did not result in any obvious change in the absorbance values. This indicated that no chemical interactions occurred between the 2 components. The data also demonstrated that the series of analogues used do not absorb energy at the wavelengths set on the ELISA reader; hence do not contribute to the absorbance values noted during the assays.

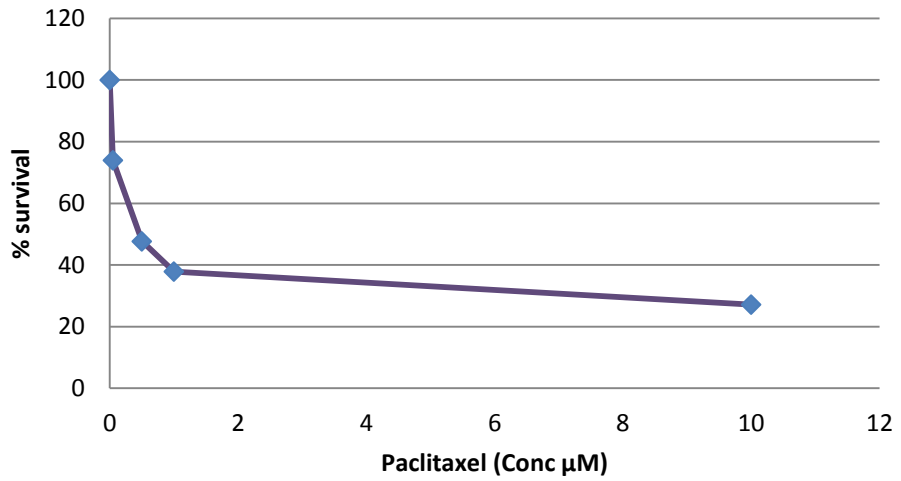

Figure 4.2: Validation of cytotoxic assay on MDA-MB-231 cells using Paclitaxel
Percentage survival plot of MDA-MB-231 cells treated with paclitaxel at concentrations ranging from 0.05 µM to 10 µM for 96 h. Percentage survivals were calculated relative to the DMEM control which was assigned 100% survival.

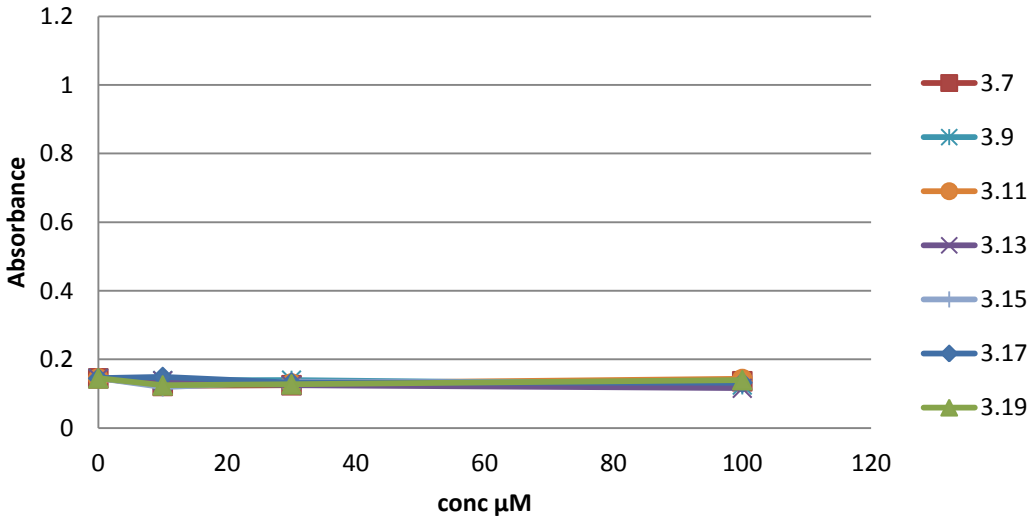

Figure 4.3: Determination of possible interaction between cell proliferation reagent and derivatives
Absorbance versus concentration plot of blank wells (with media only and no cells) dosed with analogues in concentrations ranging from 10 µM to 100 µM with WST-1 reagent for 4 hours. WST-1 and media only wells served as controls for this assay.

WST-1 and MTT reagents function on similar principles as indicated above. The only difference between these 2 reagents is the nature of formazan dye formed. WST-1 reagent gives rise to soluble formazan whereby with MTT, insoluble formazan crystals are formed. An MTT assay therefore requires an additional solubilizing step of formazan before the plates are read (Ngamwongsatit et al., 2008). Therefore it should be noted that though the assay was optimized using the WST-1 cell proliferation reagent, the same parameters (optimal seeding densities, optimal incubation period and optimal amount of proliferation reagent to add) determined were then used for MTT assays conducted with test compounds.

4.2.4 Cytotoxicity of cinnamate esters derivatives

The percentage survival of MDA-MB-231 cells was determined at 3 different concentrations; 10 µM, 30 µM and 100 µM after a dosing incubation period of 96 h. The DMEM treated wells were taken as 100% cell survival and acted as the negative control for the assay. All calculations were therefore relative to DMEM control. The results obtained from the MTT assay are shown in Figure 4.4. Dose response curves were drawn for the 7 ester derivatives tested and error bars included on the graphs. Derivatives **3.11** and **3.15** had noticeable cytotoxic effect on MDA-MB-231 cells, reducing the percentage survival relative to the untreated cells to approximately 50% and 40% respectively at the highest concentration tested, with **3.11** being the most toxic. The other analogues appeared to have a minor effect on the cells, leading to a cell viability of between 70% and 90% at the highest concentration tested.

IC_{50} values were estimated from the dose response curves constructed, and the results are displayed in Table 4.2. It is important to note that the values obtained were approximations from the screening process conducted with a 3 point assay. Analogues **3.11** and **3.15** had approximate IC_{50} values of 43.45 µM and 100.01 µM respectively. IC_{50} determinations for the other derivatives were done by extrapolating the data beyond the concentration range tested; hence the degree of accuracy is limited. To obtain more accurate figures, the concentration range could be widened; however these higher concentrations are likely to fall outside the druggable range. A maximum concentration of 100 µM was chosen as a cutoff point to determine which derivatives to pursue for further optimization. Considering that most of the cancer drugs on the market have IC_{50} values in the nanomolar range, for example paclitaxel has an IC_{50} value of 100 nM in MCF7 cells (Munster et al., 2002), it was

considered appropriate to start at the lower end of the micromolar range and attempt structural modifications to increase cytotoxic activity.

The data obtained demonstrated the importance of having -$CHCl_2$ or -CHO on the molecule, a similar characteristic observed in natural compounds isolated from *P. cornutum.* Natural extracts containing -CH_3 on the same position (Plocornulide C, **2.13**) had minimal to no effect on a breast cancer cell line, whilst cartilageneal (**2.11**) and plocornulide A (**2.12**), with -CHO and -$CHCl_2$ functionalities respectively were cytotoxic (de la Mare et al., 2012; Lawson J., 2009).

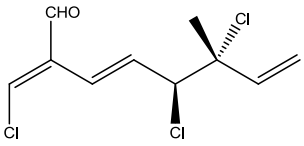

2.11

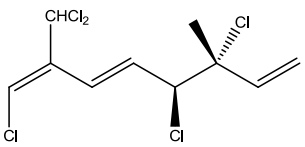

2.12

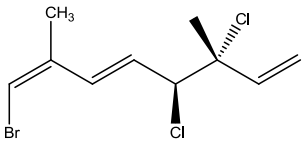

2.13

The IC_{50} value of plocornulide A (**2.12**) was determined to be 3.5 μM and 3.0 μM in MCF12A and MCF7 cells lines respectively whilst Plocornulide C (**2.13**) was non-toxic. The same trend was observed with analogue **3.15** which possessed cytotoxic properties and **3.7** being non-toxic. It was however interesting to note that **3.11** was more cytotoxic than **3.15** whilst in the natural compounds the trend is reversed. Several reactions have demonstrated the tendency of -$CHCl_2$ to be oxidized to -CHO, hence the 2 groups can interchange. We assume this also occurs on a cellular level.

The cytotoxic trends observed with ester derivatives confirmed that introduction of a terminal aromatic ring to the natural product's structure did not compromise the chemistry of halogenated monoterpenes although the cytotoxic effect was reduced. Plocornulide A (**2.12**) has an IC_{50} of 6.15 μM (de la Mare et al., 2012) compared to 100.01 μM for compound **3.15.** In comparison to halomon (Chapter 1, Section 1.3.2), moderate activity was observed (Davies-Coleman and Beukes, 2005) with less differential cytoxicity as plocornulide A was toxic to both the MCF12A and MCF7 breast cancer cell lines.

The nature of interaction between halogenated monoterpenes and the biological target site was somehow related to having an aldehyde (-CHO) or *gem*-dichlorides (-$CHCl_2$) on the molecule as observed in the MTT assay results. Substituents with similar physicochemical properties to -CHO or -$CHCl_2$ moieties had been selected. Polarity was assumed to be

important in impacting cytotoxic behaviour, considering the trends observed in the natural compounds; Plocornulide A (**2.12**) and C (**2.13**). The use of dipole-dipole moments to interact with the target site would suggest any polar functional group to have the same cytotoxic effect, hence substitution with $-CF_3$, or if a halogen is required, then substituents with -Br and $-CF_3$ should be toxic. If hydrogen bonding was required, then the same cytotoxic effect should be noticed when -CN is substituted for -CHO. The activities displayed by the MTT assay suggest that none of the mentioned interactions are responsible for cytotoxic activity observed. It can be concluded that -CHO or $-CHCl_2$ were specifically required for the compounds to show biological activity. The nature of interaction with the target site may be assumed to be covalent. Any structural modifications to be made should retain these functional groups for any activity to be observed.

Reduced activity of the analogues in comparison to Plocornulide A (**2.12**) might be related to the lack of vicinal chlorines on the molecule i.e., chlorines across the double bond of the side chain. It is assumed that a synergistic effect will be observed when both sets of chlorines are present. Vicinal chlorines alone have no impact on cytotoxicity. This is extrapolated from the natural compounds, in which Plocornulide C has vicinal chlorines but yet inactive. The next step of the study therefore would involve adding a set of halogens across the double bond and conduct cytotoxicity studies to determine their effect on biological activity.

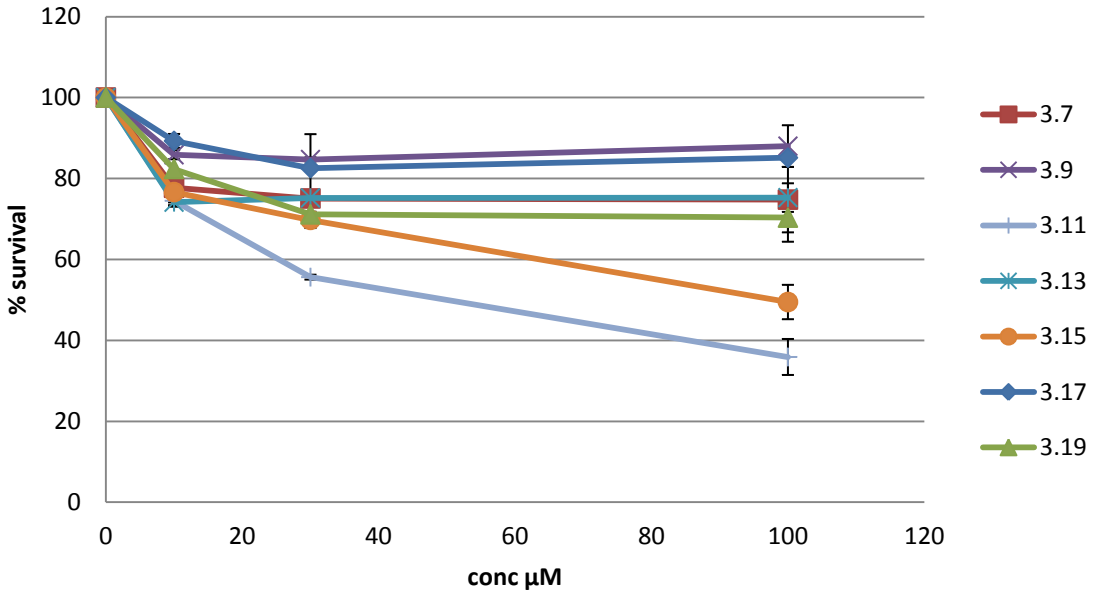

Figure 4.4: Comparison of the cytotoxic activity of cinnamate ester derivative in MDA-MB-231 cells

MDA-MB-231 cells were treated with 7 ester derivatives at 3 different concentrations, 10 µM, 30 µM and 100 µM for 96 h. An MTT assay was conducted to determine percentage survival of the cells and all calculations were relative to the DMEM control which was assigned 100% cell survival

Table 4.2: Estimated IC_{50} values in micromolar concentrations from dose response curves in Figure 4.4

Derivative	Estimated IC_{50} values (µM)
(**3.7**) CH_3	573 ± 15.56
(**3.9**) Br	≥ 1000
(**3.11**) CHO	43.45 ± 5.85
(**3.13**) CN	552.52 ± 17.47
(**3.15**) $CHCl_2$	100.01 ± 2.56
(**3.17**) H	≥ 1000
(**3.19**) CF_3	442.5 ± 17.39

4.2.5 Cytotoxicity of Carboxylic Acid Derivatives

The percentage survival of MDA-MB-231 cells was determined after dosing respective wells with carboxylic acid derivatives for 96 h. The calculations were done in a similar way to the ester derivatives at the 3 different concentrations used; 10 µM, 30 µM and 100 µM. Figure 4.5 below represents dose response curves obtained from the MTT assay conducted. All calculations were done relative to the DMEM control, which was assigned 100% cell survival.

Dose response curves indicated the non-toxic nature of carboxylic acid derivatives. No effect was observed on MDA-MB-231 cell survival as the concentration of the analogues was increased. Derivatives **3.11** and **3.15** had displayed cytotoxic tendencies and it was hoped **3.12** and **3.16** would also show a similar trend but however that wasn't the case. Determination of IC_{50} values was not possible, given the flat trendlines seen in Figure 4.5**.** Estimates will also be most likely inaccurate as they will be based on extrapolated concentration ranges that were not tested in the study.

This series was derived from ester derivatives of **series a** by hydrolysis of the parent analogues. The aim was to improve water solubility properties of the analogues to enable oral route administration into a biological system for *in-vivo* work when required. In drug design, a balance between hydrophobic and hydrophilic properties of a molecule should be attained to facilitate easy administration *via* oral route (bioavailability), absorption into the transport system and eventually into the cells (Bowe et al., 1997). Observed trends for carboxylic acid derivatives especially focusing on **3.12** and **3.16** which were active as esters, could suggest failure of these compounds to enter the cells and effect changes on cell survival. An ester linkage masks the polar nature of $-COO^-$ functional groups imparting some hydrophobic nature to the molecule. Such molecules can therefore cross the lipid bilayer of cells which is predominately hydrophobic due to the presence of phospholipids. A free $-COO^-$ moiety has hydrophilic properties and it could be assumed that **3.12** and **3.16** showed no cytotoxic effect due to failure to cross the lipid bilayer of MDA-MB-231 cells and reach the target site. The other derivatives were not expected to show cytotoxic behaviour since their ester counterparts were inactive in the previous studies.

Attempts to increase water solubility of the analogues by other means will be explored. Substituting the ester linker with an amide bond might result in better polarity properties that still favour absorption of the molecules into cancer cells.

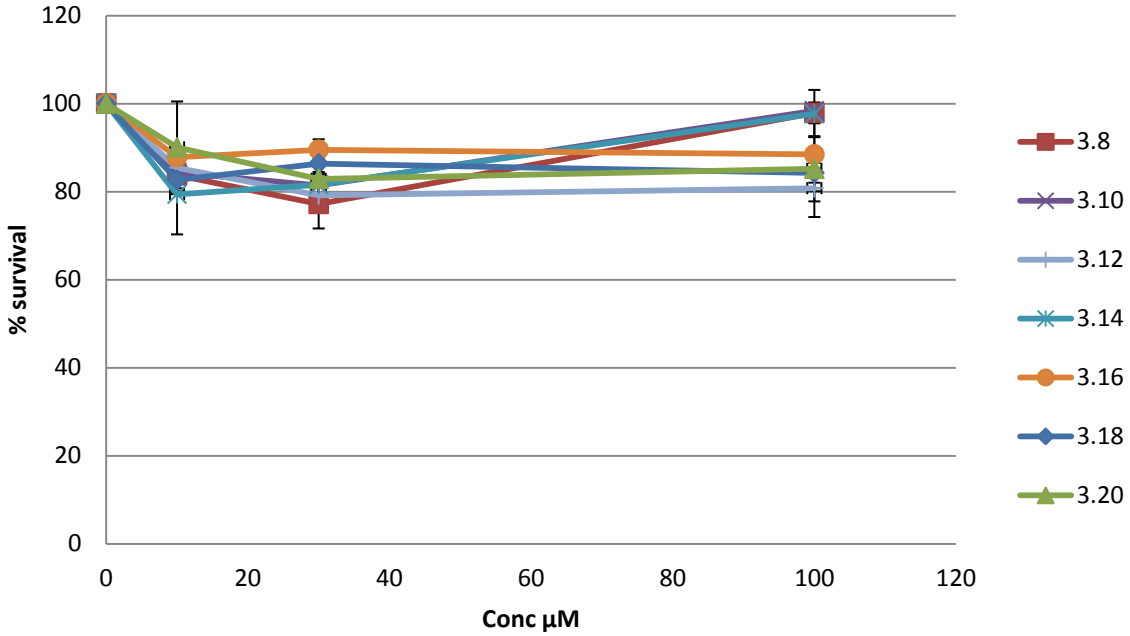

Figure 4.5: Comparison of cytotoxic activity of carboxylic acid derivatives in MDA-MB-231 cells

MDA-MB-231 cells were treated with 7 carboxylic acid derivatives at 3 different concentrations, 10 µM, 30 µM and 100 µM for 96 h. An MTT assay was conducted to determine percentage survival of the cells and all calculations were relative to the DMEM control which was assigned 100% cell survival.

4.3 Conclusion

Derivatives **3.11** and **3.15** containing -CHO and -$CHCl_2$ moieties had estimated IC_{50} values of 43.45 µM and 100.01 µM respectively, whilst the rest of the analogues in that series were inactive. Activity was therefore related to having either a -$CHCl_2$ or -CHO on the molecule, making these groups unsubstitutable. The carboxylic acid counterparts showed little to no cytotoxic activity, which could be attributed to failure of the molecules to be absorbed into MDA-MB-231 cells especially when considering **3.12** and **3.16** that also contained the -CHO and -$CHCl_2$ functional groups respectively. Priority is therefore focused on derivatives **3.11** and **3.15;** more structural modification will be done on the analogues to increase their cytotoxic nature to fall within the nanomolar region.

4.4 EXPERIMENTAL

4.4.1 Cell culture

MDA-MB-231 cells were cultured in Dulbecco's Modified Eagle Medium (DMEM) (Gibco) supplemented with 10% (v/v) heat inactivated fetal bovine serum (FBS), 100 U/ml penicillin, 100 µg/ml streptomycin and 2.5 µg/ml amphotericin (Lonza) in T75 culture flasks (Corning). The flasks were incubated at 10% CO_2, 37ºC until cell confluency was observed under the microscope. The cells were harvested by aspirating the media from the flask, washing the cells with a phosphate buffered saline solution (PBS) and adding 0.5 ml of trypsin/ethylenediaminetetra acetic acid (EDTA) (Gibco) to facilitate dislodging of adherent cells. The trypsinized flask was incubated at 10% CO_2, 37ºC for 5-7 minutes for the cells to be lifted. Once cells had been dislodged, trypsin was quenched by addition of 10 ml of DMEM supplemented with FCS. The cells were transferred to a 15 ml centrifuge tube and centrifuged (Eppendorf centrifuge 5804R instrument) at 2000 rpm for 2 minutes, and resuspended in 10 ml of growth medium. A cell count was then carried out as below.

4.4.2 Microscopic count of viable cells

Viable cells were counted using a haemocytometer. A 20 µl sample of cells in DMEM was mixed with 20 µl of trypan blue dye in an Eppendorf tube. Trypan blue is excluded from intact cells but stains cells with a permeable membrane a dark blue colour. This step therefore serves both to count cells and to determine cell viability before commencing an assay.

The haemocytometer was placed under a microscope and the grids located during which cells in any one of the 1 mm square areas were counted on both chambers. Counting was repeated 3 times rinsing the cover slip and slide with 70% ethanol in between each count. The average number of cells was calculated and the number of cells harvested from the flask determined by the following formula:

Number of cells = 1 x 10^4 x 2 (dilution of sample) x 10 (total volume of cell suspension) x average number of cells/1 mm square

Volume of media was adjusted so as to obtain a cell density of 1.2 x 10^5 (120 000) cells per ml.

4.4.3 Cytotoxicity assay

MDA-MB-231 cells were seeded in 96 well microplates at a concentration of 6000 cells per well (i.e. 50 µl of 1.2 x 10^5 cells/ml cell suspension was added to each well). The optimum number of cells to seed had been determined by conducting WST-1 assays (Figure 4.1A). The plates that were seeded with MDA-MB-231 cells were incubated overnight at 37ºC, 10% CO_2. Thereafter, a three point assay was carried out using cinnamate ester analogues and their corresponding carboxylic acids with varying concentrations of 10 µM, 30 µM and 100 µM. Sample analogues were first dissolved in sterile DMSO (Sigma). The assay was validated by including paclitaxel as a positive control on each 96 well microplate, at concentrations ranging from 50 nM to 10 µM. Duplicate wells were left blank with only cells and media with no dosing, and another set dosed with DMSO only. These acted as negative controls of the assay. Dosed plates were then incubated at 37ºC, 10% CO_2 for 96 hours. Cytotoxicity testing for the individual analogues was carried out in duplicate.

A qualitative analysis of the cells was done by viewing respective wells under a microscope after 96 h. The morphology and density of cells were noted as additional indicators of cytotoxicity. Quantitative analysis was done using a Cell Proliferation Kit 1 (MTT) (Roche) whereby 10 µl of MTT cell proliferation reagent was added to each well, followed by an incubation period of 4 hours at 37ºC and 10% CO_2. The volume of reagent to use had been optimized by conducting WST-1 assays on MDA-MB-231 cells treated with paclitaxel using 5 µl and 10 µl volumes of WST-1 cell proliferation reagent (Figure 4.1B). A 100 µl volume of solubilization solution was added to all the wells and overnight incubation done at 37ºC and 10 % CO_2. The colour change from yellow to purple for each well was measured using a multi-well spectrophotometer (PowerWave) set at dual wavelengths, 550 nm and 650 nm. The average absorbance for each analogue at different concentrations was calculated and wells with cells and media only, assigned a 100% cell survival. DMSO alone had little to no effect on cell viability. Percentage survival of cells at each concentration for all the analogues was then calculated relative to the DMEM control. Dose response curves of percentage survival against concentration were plotted. The calculation of the IC_{50} value (which represents the concentration of compound resulting in 50% growth inhibition) was determined by taking the $\log_{10}$ of the concentrations and plotting percentage survival against $\log_{10}$ concentration, to which a trendline was added and IC_{50} values calculated using the equation of the line $y = mx + c$.

References

Antunes, E.M., Afolayan, A.F., Chiwakata, M.T., Fakee, J., Knott, M.G., Whibley, C.E., Hendricks, D.T., Bolton, J.J., Beukes, D.R., 2011. Identification and in vitro anti-oesophageal cancer activity of a series of halogenated monoterpenes isolated from the South African seaweeds Plocamium suhrii and Plocamium cornutum. Phytochemistry (Elsevier), 72, 769-772.

Berridge, M.V., Herst, P.M., Tan, A.S., 2005. Tetrazolium dyes as tools in cell biology: new insights into their cellular reduction. Biotechnology Annual. Review, 11, 127-152.

Bowe, C.L., Mokhtarzadeh, L., Venkatesan, P., Babu, S., Axelrod, H.R., Sofia, M.J., Kakarla, R., Chan, T.Y., Kim, J.S., Lee, H.J., Amidon, G.L., Choe, S.Y., Walker, S., Kahne, D., 1997. Design of compounds that increase the absorption of polar molecules. Proceeding of the National Academy of. Sciences. U. S. A., 94, 12218-12223.

Burdall, S.E., Hanby, A.M., Lansdown, M.R.J., Speirs, V., 2003. Breast cancer cell lines: friend or foe? Breast Cancer Research, 5, 89-95.

Burdon, R.H., Gill, V., Rice-Evans, C., 1993. Reduction of a tetrazolium salt and superoxide generation in human tumor cells (HeLa). Free Radical Research Community, 18, 369-380.

Cailleau, R., Young, R., Olive, M., Reeves Jr, W.J., 1974. Breast tumor cell lines from pleural effusions. Journal of the National Cancer Institute, 53, 661-674.

Davies-Coleman, M.T., Beukes, D.R., 2004., Ten Years of Marine Natural Products Research at Rhodes University., South African Journal of Science, 100 (11 & 12). pp. 539-544. ISSN 0038-2353

de la Mare, J., Lawson, J.C., Chiwakata, M.T., Beukes, D.R., Edkins, A.L., Blatch, G.L.,2012 – Quinones and halogenated monoterpenes of algal origin show anti-proliferative effects against breast cancer cells in vitro. Accepted in Investigational New Drugs. Doi:10.1007/s10637-011-9788-0

Ekwall, B., Silano, V., Paganuzzi-Stammati, A., Zucco,F., 1990. Toxicity tests with mammalian cell cultures. SCOPE, 41, 75-97.

Gerets, H.H.J., Hanon, E., Cornet, M., Dhalluin, S., Depelchin, O., Canning, M., Atienzar, F.A., 2009. Selection of cytotoxicity markers for the screening of new chemical entities in a pharmaceutical context: A preliminary study using a multiplexing approach. Toxicology in Vitro, 23, 319-332.

Kim, H., Yoon, S.C., Lee, T.Y., Jeong, D., 2009. Discriminative cytotoxicity assessment based on various cellular damages. Toxicology Letters, 184, 13-17.

Lawson, J., 2009. Analysis of the anti-cancer activity of novel indigenous algal compounds in breast cancer: Towards the development of a model for screening anti-cancer stem cell activity (MSc thesis). Rhodes University, Grahamstown, South Africa.

Liu, Y., Peterson, D.A., Kimura, H., Schubert, D., 1997. Mechanism of cellular 3-(4,5-dimethylthiazol-2-yl)-2,5-diphenyltetrazolium bromide (MTT) reduction. Journal of Neurochemistry, 69, 581-593.

Munster, P.N., Marchion, D.C., Basso, A.D., Rosen, N., 2002. Degradation of HER2 by ansamycins induces growth arrest and apoptosis in cells with HER2 overexpression via a HER3, phosphatidylinositol 3'-kinase-AKT-dependent pathway. Cancer Research, 62, 3132-3137.

Ngamwongsatit, P., Banada, P.P., Panbangred, W., Bhunia, A.K., 2008. WST-1-based cell cytotoxicity assay as a substitute for MTT-based assay for rapid detection of toxigenic Bacillus species using CHO cell line. Journal of Microbiology. Methods, 73, 211-215.

Osborne, C.K., Hobbs, K., Trent, J.M., 1987. Biological differences among MCF-7 human breast cancer cell lines from different laboratories. Breast Cancer Research and Treatment, 9, 111-121.

Otvos, L.J., Kovalszky, I., Riolfi, M., Ferla, R., Olah, J., Sztodola, A., Nama, K., Molino, A., Piubello, Q., Wade, J.D., Surmacz, E., 2011. Efficacy of a leptin receptor antagonist peptide in a mouse model of triple-negative breast cancer. European Journal of Cancer, 47, 1578-1584.

Sylvester, P.W., 2011. Optimization of the tetrazolium dye (MTT) colorimetric assay for cellular growth and viability. Methods in Molecular Biology (Clifton, N. J.), 716, 157-168.

Tu, Y.F., Kaipparettu, B.A., Ma, Y., Wong, L.J., 2011. Mitochondria of highly metastatic breast cancer cell line MDA-MB-231 exhibits increased autophagic properties. Biochim. Biophys. Acta, Bioenerg., 1807, 1125-1132.

Vistica, D.T., Skehan, P., Scudiero, D., Monks, A., Pittman, A., Boyd, M.R., 1991. Tetrazolium-based assays for cellular viability: a critical examination of selected parameters affecting formazan production. Cancer Research, 51, 2515-2520.

Chapter Five

5.1 Summary and Conclusion

(1E,3E,5S,6R)-1,5,6-trichloro-2-(dichloromethyl)-6-methylocta-1,3,7-triene (**2.12**) isolated from *P. cornutum* has been demonstrated to show cytotoxicity in the micromolar range against MCF7 and MDA-MB-231 breast cancer cell lines. Stability and availability issues of the natural product always impede progress in drug development and prompts for continuous extraction and isolation of the metabolite for further work to be done. In this project, sites to be visited for re-isolation of target compounds were determined by conducting geographical variation studies, of which (1E,3E,5S,6R)-1,5,6-trichloro-2-(dichloromethyl)-6-methylocta-1,3,7-triene (**2.12**) is abundant in samples collected from Noordhoek, Port Elizabeth and Kenton-on-Sea.

Structural activity relationships indicated that a -$CHCl_2$ or -CHO is required on position 7 of the molecule for cytotoxic properties to be noted. The same trend was noted in the cinnamate ester derivatives synthesized in an attempt to have stable analogues. *O*-formyl cinnamate (**3.11**) and *o*-dichloromethyl cinnamate (**3.15**) had IC_{50} values of 43.45 µM and 100.01 µM respectively compared to the 6.15 µM of **(**1E,3E,5S,6R)-1,5,6-trichloro-2-(dichloromethyl)-6-methylocta-1,3,7-triene (**2.12**). Cytotoxicity observed for *o*-formyl cinnamate (**3.11**) and *o*-dichloromethyl cinnamate (**3.15**) indicated that introduction of a terminal aromatic ring does not abolish activity although it was reduced. It however enabled us to have a better handle on the molecule and allows for further structural activity modifications to be conducted.

Since it has been determined that the -$CHCl_2$ or -CHO functionality is necessary on the molecule, a shift of focus will be on the vicinal chlorines and their influence on cytotoxicity, although it can be assumed that they have no effect since in the natural compounds (1Z,3E,5S,6R)-1-bromo-5,6-dichloro-2,6-dimethylocta-1,3,7-triene (**2.13**) is inactive. However, the effect of the vinyl chlorine at position 8 on cytotoxicity could be determined. Other attempts can be made to improve on the water solubilities of the cinnamate analogues by introducing an amide linkage at position 1 instead of having a free carboxylic moiety that results in the molecule being too polar. Further structural modifications would indeed be required for potency of these molecules to be increased to fall in the nanomolar range.